Universidad de Concepción
Dirección de Postgrado
Facultad de Ciencias Físicas y Matemáticas
Programa de Doctorado en Ciencias Aplicadas
con Mención en Ingeniería Matemática

Métodos Numéricos para dos tipos de Ecuaciones Diferenciales Estocásticas con coeficientes no globalmente Lipschitz

Numerical Methods for two types of Stochastic Differential Equations with Nonglobally Lipschitz Coefficients

Tesis para optar al grado de Doctor en Ciencias Aplicadas
con mención en Ingeniería Matemática

Mario Alejandro Muñoz Muñoz
Concepción - Chile
2023

Profesor Guia: Carlos Mora
CI²MA y Departamento de Ingeniería Matemática
Concepción, Chile

Cotutor: Hugo de la Cruz
School of Applied Mathematics, Fundação Getulio Vargas
Rio de Janeiro, Brazil

Abstract

This doctoral thesis focuses on the numerical solution of Stochastic Differential Equations (SDEs) with non-globally Lipschitz coefficients. It involves two independent investigations that propose different procedures for the effective numerical simulation of these models.

The first investigation centers on the numerical solution of the non-linear stochastic Schrödinger equation, which is a stochastic differential equation with locally Lipschitz continuous coefficients commonly used to model quantum measurement processes. We analyze the rate of weak convergence of an exponential scheme that reproduces the norm of the desired solution by using a projection onto the unit sphere. In particular, we prove that the exponential scheme converges with weak-order one, and obtain the leading order term of its weak error expansion. This justifies using the Talay-Tubaro extrapolation procedure in the numerical simulation of open quantum systems. By employing this procedure, a second-order method for computing mean values of smooth functions of the solution is obtained. Furthermore, we prove that the exponential scheme under study has order of strong convergence 1/2, validating its application in the Multilevel Monte Carlo method. Numerical experiments involving a quantized electromagnetic field interacting with a reservoir showcase the effectiveness of the proposed methods.

The second investigation introduces a new methodology for the effective pathwise numerical simulation of stochastic differential equations with non-globally Lipschitz continuous coefficients. Specifically, we focus on SDEs with linear multiplicative noise. We employ a suitable invertible continuous transformation to establish a connection between the original SDE and an auxiliary Random Differential Equation (RDE). This explicit conjugacy enables the development of new pathwise numerical schemes for the studied SDE, utilizing numerical approximations of the auxiliary RDE. In particular, we introduce two numerical methods: one based on an exponential scheme and the other based on the Heun scheme. In order to showcase the practical applicability of our approach, we implement it within a

compartmental epidemic model, specifically the stochastic SVIR model. This SDE captures the dynamics of a continuous vaccination strategy in the presence of environmental noise effects. Through comparative analysis with commonly used numerical approximations, we validate the effectiveness of our proposed numerical methods for simulating epidemiological models.

Resumen

Esta tesis doctoral se centra en la solución numérica de Ecuaciones Diferenciales Estocásticas (EDE) con coeficientes no globalmente Lipschitz continuos. En esta se desarrollaron dos investigaciones independientes que proponen procedimientos distintos para la simulación numérica efectiva de cada uno de estos modelos.

La primera investigación se centra en la solución numérica de la ecuación estocástica no lineal de Schrödinger, que es una ecuación diferencial estocástica con coeficientes localmente Lipschitz continuos, que es utilizada para modelar procesos de medida cuántica. Analizamos la tasa de convergencia débil de un esquema exponencial que reproduce la norma de la solución deseada utilizando una proyeccción sobre la esfera unitaria. En particular, probamos que el esquema exponencial converge con orden débil uno, y obtenemos el término de orden principal de su expansión de error débil. Esto justifica el uso del procedimiento de extrapolación de Talay-Tubaro en la simulación numérica de sistemas cuánticos abiertos. Empleando este procedimiento, se obtiene un método de segundo orden para calcular valores esperados de funciones suaves de la solución. Además, probamos que el esquema exponencial tiene orden de convergencia fuerte 1/2, validando su aplicación en el método Multilevel Monte Carlo. Experimentos numéricos que involucran un campo electromagnético cuantizado interactuando con un reservorio muestran la efectividad de los métodos propuestos.

La segunda investigación introduce una nueva metodología para la simulación numérica trayectorial de ecuaciones diferenciales estocásticas con coeficientes no globalmente Lipschitz continuos. En concreto, nos centramos en las EDE con ruido multiplicativo lineal. Empleamos una transformación continua invertible adecuada para establecer una conexión entre la EDE original y una Ecuación Diferencial Aleatoria (EDA) auxiliar. Esta conjugación explícita permite el desarrollo de nuevos esquemas numéricos para la EDE estudiada, utilizando aproximaciones numéricas de la EDA auxiliar. En particular, introducimos dos métodos numéricos: uno basado en un esquema exponencial y otro basado en el esquema de

Heun. Para demostrar la efectividad práctica de nuestro enfoque, lo aplicamos a un modelo epidémico compartimental, en concreto a un modelo estocástico SVIR. Este modelo captura la dinámica de una estrategia de vacunación continua en presencia de efectos de ruido ambiental. Mediante un análisis comparativo con aproximaciones numéricas comunmente utulizadas, validamos la eficacia de nuestros métodos numéricos propuestos para simular modelos epidemiológicos.

Acknowledgments

I would like to express my deepest gratitude to my partner, family, and friends for their unconditional support. I am very grateful to my thesis directors, Carlos Mora Gonzales and Hugo de la Cruz, for their invaluable guidance and friendship. I would also like to thank the professors of the Ph.D. program and their directors, who always gave me their help with great willingness. My gratitude is extended to the Centro de Investigación en Ingeniería Matemática (CI2MA) of the Universidad de Concepción and its directors for providing me with a favorable and comfortable space to carry out this research. I thank the Millennium Institute for Research in Optics (MIRO) and its director, Aldo Delgado, with whom I have shared rewarding research and forged great friendships. Finally, I thank the Universidad de Concepción and the Agencia Nacional de Investigación y Desarrollo (ANID) of Chile for supporting my Ph.D. studies through their scholarship programs. To each of you, thank you from the bottom of my heart!

Agradecimientos

Quiero expresar mi más profundo agradecimiento a mi pareja, familia y amigos por su apoyo incondicional. Agradezco enormemente a mis directores de tesis, Carlos Mora Gonzales y Hugo de la Cruz, por su valiosa orientación y amistad. También quiero agradecer a los profesores del programa de doctorado y a sus directores, quienes siempre me brindaron su ayuda con la mejor disposición. Mi gratitud se extiende al Centro de Investigación en Ingeniería Matemática (CI2MA) de la Universidad de Concepción y a sus directores, por proporcionarme un espacio propicio y cómodo para llevar a cabo esta investigación. Agradezco al Instituto Milenio de Investigación en Óptica (MIRO) y a su director, Aldo Delgado, con quienes he compartido una enriquecedora investigación y forjado grandes amistades. Finalmente, doy las gracias a la Universidad de Concepción y a la Agencia Nacional de Investigación y Desarrollo (ANID) de Chile por permitir mi estudio de doctorado a través de sus programas de becas. A cada uno de ustedes, ¡gracias de corazón!

Contents

List of Figures

List of Tables

Introduction

Motivation

Including random effects in mathematical modeling is a growing trend in scientific research. This consideration arises when deterministic models need to be more efficient and relevant. Such situations typically occur when the phenomenon under investigation is influenced by numerous uncontrollable factors, when measurements exhibit erratic behavior, or when the phenomenon is inherently random. Regardless of their source of randomness, these random systems are frequently modeled by Stochastic Differential Equations (SDEs).

Stochastic Differential Equations investigate random systems as diffusion processes by utilizing stochastic calculus. The foundation of stochastic calculus can be traced back to the pioneering work of Kiyosi Itô in the 1940s. Itô introduced the concept of the stochastic integral, a generalization of the Riemann–Stieltjes integral in stochastic analysis. Specifically, the integrands and integrators of this new integral are stochastic processes that often exhibit unbounded variation. These contributions provide a solid mathematical foundation for studying SDEs, enabling researchers to rigorously investigate a wide range of problems in various fields, including physics, finance, engineering, and biology.

In general, analytical solutions for stochastic differential equations are not available, and even when they exist, their efficient computation is not always feasible. Therefore, numerical approximations are necessary to investigate these systems. Traditional numerical methods [13, 56, 65, 68] rely on convergence assumptions often unmet in practice. One of the most restrictive requirements among these assumptions is the condition of global Lipschitz continuity. When this condition is not met, the SDE may become stiff, leading to divergence and instability in standard numerical approximations (see, e.g., [49, 66, 70]). To address these issues, alternative approaches have been proposed, including semi-implicit methods [55, 86], balanced methods [2, 64, 69], tamed methods [41, 49, 96], and truncated methods [33, 34, 63].

However, these procedures still lack generality, leaving many equations unaddressed.

Related Work

A stochastic differential equation is considered stiff when its numerical integration becomes challenging, and standard numerical methods (see, e.g., [13, 56, 65, 68]) fail to maintain stability unless substantial computational effort is applied. The stability issues may arise when one of the coefficients of the SDE exhibits oscillatory behavior or changes abruptly fast to respect the other. In particular, SDE with non globally Lipschitz coefficient and multiplicative noise SDE are often stiff (see, e.g., [70]). Examples include non-linear SDEs and SDEs with linear multiplicative noise.

Explicit methods have been shown to diverge when applied to non-globally Lipschitz SDE. In particular, the Euler-Maruyama method diverges for SDEs with super-linear growth coefficients [40]. Even if the SDE satisfies the linear growth condition, the Euler-Maruyama method necessitates small step-sizes to ensure almost sure exponential stability [38]. As an alternative, semi-implicit methods (implicit only in the drift term) are well-suited for stiff systems with small stochastic noise intensity or additive noise [24, 55]. In particular, the stochastic Theta method guarantees almost sure exponential stability for non-linear SDEs, provided that the drift coefficient satisfies a one-sided Lipschitz condition, and the diffusion coefficient satisfies a linear growth condition [37, 38]. However, in cases where the stochastic component plays a significant role in the dynamics, such as with large multiplicative noise, the application of fully implicit methods, like balanced methods, becomes necessary [2, 69]. Although less restrictive in their assumptions, implicit methods (semi-implicit and fully implicit) require higher computational effort due to their increased complexity. Alternative numerical approximations are presented in [1, 16, 63, 78]. Nonetheless, these methods still involve a trade-off between restrictive Lipschitz-type conditions and computational effort.

In summary, the numerical simulation of SDEs relies on assumptions regarding the Lipschitz continuity of the coefficients. By relaxing these assumptions, the numerical complexity of the integrators increases, thus limiting their applicability. As a result, many non-linear and multiplicative noise stochastic systems have not been adequately addressed. Two examples worth mentioning are the non-linear stochastic Schrödinger equation (see, e.g., [11, 73]) and a stochastic SVIR model presented in [99].

The non-linear stochastic Schrödinger equation describes the evolution of open quantum

systems and is used, for instance, to describe the evolution of quantum measurement processes. It is a stochastic differential equation with locally Lipschitz continuous coefficients, and its main focus lies in the distribution of its solution. In a previous work [73], an exponential scheme was proposed to compute expected values for quantum observables of the non-linear stochastic Schrödinger equation. Specifically, the exponential scheme is employed to approximate the mean value of the function $x \to \langle x, Ax \rangle$ applied to the solution, where A represents an observable of the system. Here, the exponential scheme exhibits linear convergence whenever random variables with compact support simulate the increments of the Brownian motion.

On the other hand, the stochastic SVIR model presented in [99] is a SDE with non-globally Lipschitz continuous coefficients and linear multiplicative noise. This compartmental model incorporates a continuous vaccination strategy and ambient white noise perturbations to the classical SIR model formulated by Kermack and McKendrick [50]. Specifically, several probabilistic properties of the continuous system have been proved, including ergodicity and the existence of a stationary distribution. These remarkable properties, combined with the lack of global Lipschitz continuity in the system, make the effective numerical simulation of the stochastic SVIR model challenging.

Objectives and outline

The main objective of this PhD thesis is to develop efficient numerical methods for solving stochastic differential equations with nonglobally Lipschitz continuous coefficients. The research focuses on two models: the non-linear stochastic Schrödinger equation and SDEs with linear multiplicative noise. In particular, a stochastic SVIR model is considered for the second model.

The main contents of this thesis are structured as follows:

- Chapter 1 provides a brief overview of the fundamental concepts necessary for developing this thesis. This review focuses on stochastic analysis, stochastic differential equations, and their numerical approximation.

- Chapter 2 focuses on the numerical simulation of the non-linear stochastic Schrödinger equation. The main goal of this investigation is to develop weak numerical solutions for this equation. We specifically investigate an exponential scheme proposed in [73], which

incorporates a projection onto the unit ball. To extend the numerical analysis provided in [73], we consider a general class of smooth functions and remove the restrictions of compact support on simulating the increment of the Brownian Motion. Two main challenges arise in this error analysis. Firstly, due to the absence of a global Lipschitz condition, We employ a localization procedure that enables us to address the non-linear stochastic Schrödinger equation through the use of a globally Lipschitz SDE. In this SDE, the drift and diffusion coefficients correspond to those of the nonlinear stochastic Schrödinger equation within the unit ball. Secondly, the projection on the unit sphere exhibits a singularity at 0. Consequently, we derive a short-time asymptotic expansion for the projection concerning the step-size. Numerical simulations were conducted while employing two numerical refinements of the method: the utilization of the Talay-Tubaro extrapolation procedure and the application of the Multilevel Monte Carlo method to the Exponential scheme.

The contents of this chapter originally appeared in the following paper:

[79] Carlos M Mora and Mario Muñoz, *On the rate of convergence of an exponential scheme for the non-linear stochastic Schrödinger equation with finite-dimensional state space*. Physica Scripta, vol. 98, pp. 87–94, (2023).

- Chapter 3 is dedicated to the numerical simulation of non-globally Lipschitz SDEs with linear multiplicative noise. The primary objective of this investigation is to compute sample paths of the solution, which entails developing pathwise solutions for this specific class of SDEs. To accomplish this, we establish a connection between the original SDE and an auxiliary random differential equation incorporating an Ornstein-Uhlenbeck process as the sole input parameter. This explicit conjugacy is established by utilizing a suitable invertible continuous transformation. Subsequently, we introduce new pathwise numerical methods for the original SDE, relying on numerical approximations of the auxiliary RDE. Specifically, we formulate a conjugated exponential method and a conjugated Heun method. These numerical approximations are then employed to simulate a stochastic SVIR model. Comparative analysis with commonly used numerical approximations shows the practical applicability of the proposed numerical methods.

  The contents of this chapter gave rise to the following paper:

[81] M. Muñoz, H. de la Cruz, and C. M. Mora, *Pathwise methods for the integration of a stochastic SVIR model*. Mathematical Methods in the Applied Sciences, (2023), pp. 1-15.

- Chapter 4 is dedicated to presenting the conclusions of this PhD thesis. Furthermore, it outlines ongoing and future projects.

Introducción

Motivación

La inclusión de efectos aleatorios en la modelación matemática es una tendencia creciente en la investigación científica. Esta consideración surge cuando los modelos deterministas necesitan ser más eficaces y pertinentes. Estas situaciones suelen darse cuando el fenómeno investigado se ve influido por numerosos factores incontrolables, cuando las mediciones muestran un comportamiento errático o cuando el fenómeno es intrínsecamente aleatorio. Independientemente de su fuente de aleatoriedad, estos sistemas aleatorios se modelan frecuentemente mediante ecuaciones diferenciales estocásticas (EDE).

Las ecuaciones diferenciales estocásticas investigan los sistemas aleatorios como procesos de difusión utilizando el cálculo estocástico. Los orígenes del cálculo estocástico se remontan a los trabajos pioneros de Kiyosi Itô en la década de 1940. Itô introdujo el concepto de integral estocástica, una generalización de la integral de Riemann-Stieltjes en el análisis estocástico. En concreto, los integrandos e integradores de esta nueva integral son procesos estocásticos que, en general, presentan una variación no acotada. Estas aportaciones proporcionaron una sólida base matemática para el estudio de las EDE, lo que permite a los investigadores estudiar con rigor una amplia gama de problemas en diversos campos, como la física, las finanzas, la ingeniería y la biología.

En general, no se dispone de soluciones analíticas para las ecuaciones diferenciales estocásticas, e incluso cuando existen, su cálculo eficiente no siempre es factible. Por lo tanto, se necesitan aproximaciones numéricas para investigar estos sistemas. Los métodos numéricos tradicionales [13, 56, 65, 68] se basan en supuestos de convergencia que a menudo no se cumplen en la práctica. Uno de los requisitos más restrictivos entre estos supuestos es la condición de continuidad global de Lipschitz. Cuando esta condición no se cumple, la SDE puede volverse rígida, lo que conduce a divergencia e inestabilidad en las aproximaciones

numéricas estándar (véase, por ejemplo, [49, 66, 70]). Para hacer frente a estos problemas, se han propuesto enfoques alternativos, incluyendo métodos semi-implícitos [55, 86], métodos balanced [2, 64, 69], métodos tamed [41, 49, 96], y métodos truncados [33, 34, 63]. Sin embargo, estos procedimientos aún carecen de generalidad, dejando muchas ecuaciones sin abordar.

Trabajos Previos

Una ecuación diferencial estocástica se considera rígida cuando su integración numérica se convierte en un reto, y los métodos numéricos estándar (véase, por ejemplo, [13, 56, 65, 68]) no consiguen mantener la estabilidad a menos que se aplique un esfuerzo computacional considerable. Los problemas de estabilidad pueden surgir cuando uno de los coeficientes de la SDE exhibe un comportamiento oscilatorio o cambia abruptamente rápido con respecto al otro. En particular, las EDE con coeficiente no globalmente Lipschitz y las EDE con ruido multiplicativo suelen ser rígidas (véase, por ejemplo, [70]). Los ejemplos incluyen EDEs no lineales y EDEs con ruido multiplicativo lineal.

Se ha demostrado que los métodos explícitos divergen cuando se aplican a EDE no globalmente Lipschitz. En particular, el método de Euler-Maruyama diverge para EDEs con coeficientes de crecimiento super-lineal [40]. Incluso si la EDE satisface la condición de crecimiento lineal, el método de Euler-Maruyama requiere pequeños tamaños de paso para garantizar la estabilidad exponencial casi segura [38]. Como alternativa, los métodos semi-implícitos (implícitos sólo en el término de deriva) son adecuados para sistemas rígidos con pequeña intensidad de ruido estocástico o ruido aditivo [24, 55]. En particular, el método theta estocástico garantiza estabilidad exponencial casi segura para EDEs no lineales, siempre que el coeficiente de deriva satisfaga una condición de Lipschitz unilateral, y el coeficiente de difusión satisfaga una condición de crecimiento lineal [37, 38]. Sin embargo, en los casos en que el componente estocástico desempeña un papel significativo en la dinámica, como con ruido multiplicativo grande, se hace necesaria la aplicación de métodos totalmente implícitos, como los métodos balanced [2, 69]. Aunque son menos restrictivos en sus supuestos, los métodos implícitos (semi implícitos y totalmente implícitos) requieren un mayor esfuerzo computacional debido a su mayor complejidad. En [1, 16, 63, 78] se presentan aproximaciones numéricas alternativas. No obstante, estos métodos siguen implicando una concesión entre las condiciones restrictivas de tipo Lipschitz y el esfuerzo computacional.

En resumen, la simulación numérica de las EDE se basa en supuestos relativos a la continuidad de Lipschitz de los coeficientes. Al relajar estos supuestos, aumenta la complejidad numérica de los integradores, lo que limita su aplicabilidad. En consecuencia, muchos sistemas estocásticos no lineales y con ruido multiplicativo no se han abordado adecuadamente. Dos ejemplos dignos de mención son la ecuación estocástica no lineal de Schrödinger (véase, por ejemplo, [11, 73]) y un modelo estocástico SVIR presentado en [99].

La ecuación estocástica no lineal de Schrödinger describe la evolución de los sistemas cuánticos abiertos y se utiliza, por ejemplo, para describir la evolución de los procesos de medición cuántica. Se trata de una ecuación diferencial estocástica con coeficientes localmente Lipschitz continuos, y su principal interés radica en la distribución de su solución. En un trabajo anterior [73], se propuso un esquema exponencial para calcular los valores esperados de los observables cuánticos de la ecuación estocástica no lineal de Schrödinger. En concreto, un esquema exponencial se emplea para aproximar el valor medio de la función $x \to \langle x, Ax \rangle$ aplicada a la solución, donde A representa un observable del sistema. En este caso, el esquema exponencial muestra una convergencia lineal siempre que variables aleatorias con soporte compacto simulen los incrementos del movimiento browniano.

Por otro lado, el modelo estocástico SVIR presentado en [99] es una SDE con coeficientes no globalmente Lipschitz continuos y ruido multiplicativo lineal. Este modelo compartimental incorpora una estrategia de vacunación continua y perturbaciones de ruido blanco ambiental al modelo SIR clásico formulado por Kermack y McKendrick [50]. En concreto, se han demostrado varias propiedades probabilísticas del sistema continuo, incluida su ergodicidad y la existencia de una distribución estacionaria. Estas notables propiedades, combinadas con la falta de continuidad Lipschitz global en el sistema, hacen que la simulación numérica efectiva del modelo estocástico SVIR sea todo un reto.

Objetivos y estructura

El objetivo principal de esta tesis doctoral es desarrollar métodos numéricos eficientes para resolver ecuaciones diferenciales estocásticas con coeficientes que no son globalmente Lipschitz continuos. La investigación se centra en dos modelos: la ecuación estocástica no lineal de Schrödinger y las EDEs con ruido multiplicativo lineal. En particular, para el segundo modelo se considera un modelo estocástico SVIR.

Los principales contenidos de esta tesis se estructuran de la siguiente manera:

- El capítulo 1 proporciona una breve visión general de los conceptos fundamentales necesarios para el desarrollo de esta tesis. Esta revisión se centra en el análisis estocástico, las ecuaciones diferenciales estocásticas y su aproximación numérica.

- El capítulo 2 se centra en la simulación numérica de la ecuación estocástica no lineal de Schrödinger. El objetivo principal de esta investigación es desarrollar soluciones numéricas débiles para esta ecuación. En concreto, investigamos un esquema exponencial propuesto en [73], que incorpora una proyección sobre la bola unitaria. Para ampliar el análisis numérico proporcionado en [73], consideramos una clase general de funciones suaves y eliminamos las restricciones de soporte compacto al simular el incremento del movimiento browniano. En este análisis de errores surgen dos principales retos. En primer lugar, debido a la ausencia de una condición global de Lipschitz, empleamos un procedimiento de localización que nos permite abordar la ecuación estocástica no lineal de Schrödinger mediante el uso de una SDE globalmente Lipschitz. En esta EDE, los coeficientes de deriva y difusión corresponden a los de la ecuación estocástica no lineal de Schrödinger dentro de la bola unidad. En segundo lugar, la proyección sobre la esfera unitaria presenta una singularidad en 0. En consecuencia, derivamos una expansión asintótica de corto plazo para la proyección relativa al tamaño del paso. Se realizaron simulaciones numéricas empleando dos refinamientos numéricos del método: la utilización del procedimiento de extrapolación de Talay-Tubaro y la aplicación del método de Multilevel Monte Carlo al esquema exponencial.

  El contenido de este capítulo apareció originalmente en el siguiente artículo:

  [79] Carlos M Mora and Mario Muñoz, *On the rate of convergence of an exponential scheme for the non-linear stochastic Schrödinger equation with finite-dimensional state space*. Physica Scripta, vol. 98, pp. 87–94, (2023).

- El capítulo 3 está dedicado a la simulación numérica de EDEs no globalmente Lipschitz con ruido multiplicativo lineal. El objetivo principal de esta investigación es investigar trayectorias de la solución, lo que implica el desarrollo de soluciones trayectoriales para esta clase específica de EDEs. Para ello, establecemos una conexión entre la EDE original y una ecuación diferencial aleatoria (EDA) auxiliar que incorpora un proceso de Ornstein-Uhlenbeck como único parámetro de entrada. Esta conjugación explícita se establece utilizando una transformación continua invertible adecuada. Posteriormente,

introducimos nuevos métodos numéricos para la EDE original, basados en aproximaciones numéricas de la EDA auxiliar. En concreto, formulamos un método exponencial conjugado y un método de Heun conjugado. Estas aproximaciones numéricas se emplean después para simular un modelo SVIR estocástico. la aplicabilidad práctica de los métodos numéricos propuestos se muestran a través de un análisis comparativo con aproximaciones numéricas comunmente utilizadas.

El contenido de este capítulo dio lugar al siguiente artículo:

[81] M. Muñoz, H. de la Cruz, and C. M. Mora, *Pathwise methods for the integration of a stochastic SVIR model*. Mathematical Methods in the Applied Sciences, n/a.

- El Capítulo 4 está dedicado a presentar las conclusiones de esta tesis doctoral. Además, se mencionan los proyectos en curso y futuros.

Chapter 1

Preliminaries

This chapter provides a brief overview of the fundamental concepts necessary for developing this thesis. For a more comprehensive review, we recommend consulting [6, 83, 104] for a detailed understanding of stochastic analysis and [56, 70] for numerical approximations of SDEs.

1.1 Stochastic Analysis and Stochastic Differential Equations

A probability space is a tuple $(\Omega, \mathcal{F}, \mathbb{P})$ consisting of a set Ω, a σ-field $\mathcal{F}$ of Ω and a probability measure $\mathbb{P}$ defined on $(\Omega, \mathcal{F})$. A filtration on $(\Omega, \mathcal{F}, \mathbb{P})$ is a family $\{\mathcal{F}\}_{t\geq 0}$ of time-indexed sub-σ-fields of $\mathcal{F}$ satisfying $\mathcal{F}_s \subset \mathcal{F}_s$ for any $0 \leq s \leq t$. A filtration $\{\mathcal{F}\}_{t\geq 0}$ satisfies the *usual conditions* if for every t in $\mathbb{R}_+$, $\mathcal{F}_t$ contains all the $\mathbb{P}$-negligible sets in $\mathcal{F}$, and $\mathcal{F}_t = \bigcap_{s>t} \mathcal{F}_s$. The collection $\left(\Omega, \mathcal{F}, \{\mathcal{F}\}_{t\geq 0}, \mathbb{P}\right)$ is referred to as a filtered probability space.

A stochastic process $X_t = (X_t)_{t\in[0,T]}$ is a family of functions such that for every $t \in [0, T]$, $\omega \mapsto X_t(\omega)$ is a measurable function (random variable) in a probability space $(\Omega, \mathcal{F}, \mathbb{P})$, i.e., the pre-image of any Borel set under X is in $\mathcal{F}$. The maps $t \mapsto X_t(\omega)$ are called *trajectories* or the *sample paths* of X_t, and it is said that X_t is continuous if its trajectories are continuous in a subset of probability one. Given a filtration $\{\mathcal{F}_t\}_{t\geq 0}$ on $(\Omega, \mathcal{F}, \mathbb{P})$, X_t is called $\{\mathcal{F}_t\}_{t\geq 0}$-adapted if $\omega \mapsto X_t(\omega)$ is $\mathcal{F}_t$-measurable for every t in $[0, T]$.

Stochastic processes can take either real or complex values. Complex random variables are functions whose real and imaginary parts are real random variables. Thus, the real

and imaginary parts of a complex stochastic process are themselves real random processes. Consequently, a complex stochastic process can be treated as a real one, albeit with increased dimensionality.

Next, we provide a brief introduction to stochastic differential equations. We follow the classical formulation by studying real-valued stochastic processes. Nonetheless, SDEs can be used to investigate more general processes, including complex-valued stochastic processes. For instance, the last can be achieved by analyzing the associated real system.

An Itô stochastic differential equation is defined by

$$\begin{cases} dX_t = b(t, X_t)dt + \displaystyle\sum_{k=1}^{m} \sigma_k(t, X_t)dW_t^k \qquad \forall\ t \in [0, T], \\ X_0 = x_0, \end{cases} \tag{1.1}$$

where $b : [0, T] \times \mathbb{R}^d \longrightarrow \mathbb{R}^d$ is called drift coefficient, $\sigma = (\sigma_1 | \cdots | \sigma_m) : [0, T] \times \mathbb{R}^d \longrightarrow \mathbb{R}^{d\times m}$ is called diffusion term, $W = (W^1, W^2, \ldots, W^m)$ is an m-dimensional Brownian motion defined on a filtered complete probability space $\left(\Omega, \mathcal{F}, \{\mathcal{F}\}_{t\geq 0}, \mathbb{P}\right)$, and $x_0 \in \mathbb{R}^d$ is the initial value. Due to the non-differentiability of Brownian motion paths, (1.1) represents an integral equation expressed as

$$X_t = x_0 + \int_0^t b(s, X_s)\, ds + \sum_{k=1}^{m} \int_0^t \sigma_k(s, X_s)\, dW_s^k \qquad \forall\, t \in [0, T]. \tag{1.2}$$

Here, the second term on the right-hand side corresponds to a stochastic integral, often called the Itô integral, a generalization of the Riemann–Stieltjes integral in stochastic analysis. Among its most notable properties, we emphasize that it is always a centered random variable, i.e.,

$$\mathbb{E}\left(\int_0^t F_s\, dW_s\right) = 0$$

and satisfies the Itô isometry

$$\mathbb{E}\left(\left(\int_0^t F_s\, dW_s\right)^2\right) = \mathbb{E}\left(\int_0^t F_s^2\, ds\right), \tag{1.3}$$

asuming, for instace, $F \in \mathbf{L}^2(\Omega \times [0,T])$, i.e.,

$$\|F\|_{\mathbf{L}^2(\Omega\times[0,T])} := \mathbb{E}\left(\int_0^T F_s^2\, ds\right) < \infty.$$

Note that the left-hand side of (1.3) corresponds to the variance of the Itô integral. The stochastic integral is also applicable to broader integrators, specifically semimartingales (see, e.g., [83]).

We have not yet discussed the conditions that the stochastic process X in equation (1.2) must satisfy. Depending on these conditions, the coefficients of the SDE must meet specific hypotheses. Assuming that these hypotheses are fulfilled, the Itô's lemma states that any smooth bounded transformation of X also possesses a SDE with respect to the same Brownian motion. Specifically, for any $f \in C_b^{1,2}([0,T]\times\mathbb{R}^d)$, we get

$$\begin{aligned} f(t,X_t) =& f(0,X_0) + \int_0^t \frac{\partial f}{\partial s}(s,X_s)\, ds + \sum_{i=1}^d \int_0^t b^i(s,X_s)\frac{\partial f}{\partial x_i}(s,X_s)\, ds \\ &+ \sum_{i=1}^d \sum_{k=1}^m \int_0^t \sigma_k^i(s,X_s)\frac{\partial f}{\partial x}(s,X_s)\, dW_s^k \\ &+ \frac{1}{2}\sum_{i,j=1}^m \sum_{k=1}^m \int_0^t \sigma_k^i(s,X_s)\sigma_k^j(s,X_s)\frac{\partial^2 f}{\partial x_i x_j}(s,X_s)\, ds, \end{aligned}$$

for $t \in [0,T]$. This result is fundamental in the investigation of Itô processes. In particular, this identity serves as the stochastic calculus counterpart of the chain rule.

There is no singular definition for a solution of a stochastic differential equation. SDEs can be studied from a pathwise perspective, focusing on finding a stochastic process that satisfies (1.2) for a given Brownian motion. Alternatively, they can be examined from a distributional perspective by finding a suitable Brownian motion and stochastic process that match the distribution of (1.2). The coefficients of the SDE must satisfy specific hypotheses depending on the type of solution under investigation.

A strong or pathwise solution of (1.2) is a stochastic process X with continuous trajectories, adapted to the filtration generated by x_0 and W_s for $0 \le s \le t$, that satisfies:

$$\mathbb{P}\left(\forall\, t \in [0,T] : X_t = x_0 + \int_0^t b(s,X_s)ds + \sum_{k=1}^m \int_0^t \sigma^k(s,X_s)dW_s\right) = 1. \tag{1.4}$$

The SDE (1.2) has unique pathwise solution X if for any other strong solution X^*,

$$\mathbb{P}\big(X_t(w) = X_t^*(w), \forall\, t \in [0,T]\big) = 1.$$

A weak or distributional solution of (1.2) is a tuple

$$\big((X,W),(\Omega,\mathcal{F},\mathbb{P}),\{\mathcal{F}_t\}_{t\geq 0}\big) \tag{1.5}$$

such that $\big(\Omega,\mathcal{F},\{\mathcal{F}_t\}_{t\geq 0},\mathbb{P}\big)$ is a filtered probability space satisfying the usual conditions, W is an m-dimensional $\{\mathcal{F}_t\}_{t\geq 0}$-Brownian motion on $(\Omega,\mathcal{F},\mathbb{P})$, and X is a continuous $\{\mathcal{F}_t\}_{t\geq 0}$-adapted process such that (1.4) holds. The solution (1.5) of the SDE (1.2) is unique in law if for any other weak solution $\big((X^*,W^*),(\Omega^*,\mathcal{F}^*,\mathbb{P}^*),\{\mathcal{F}_t^*\}_{t\geq 0}\big)$, the laws of X and X^* are equal, i.e.,

$$\mathbb{P}\left(X_{t_1}\in B_1,\ldots,X_{t_n}\in B_n\right) = \mathbb{P}^*\left(X_{t_1}^*\in B_1,\ldots,X_{t_n}^*\in B_n\right)$$

holds for all $n\in\mathbb{N}$, $t_1,\ldots,t_n>0$, and Borel sets $B_1,\ldots,B_n$. Note that any strong solution of the Itô SDE (1.2) is a weak solution, and when the pathwise uniqueness holds, the uniqueness in law also holds.

The *standard hypothesis* for the existence and uniqueness of strong solution for the Itô SDE (1.2) are:

- The coefficients b and σ are globally Lipschitz continuous, i.e., there is $K>0$ such that

$$||b(t,x)-b(t,y)|| + \sum_{k=1}^{m}\left|\left|\sigma^k(t,x)-\sigma^k(t,y)\right|\right| \leq K\|x-y\|, \tag{1.6}$$

  for any $t\in[0,T]$ and $x,y\in\mathbb{R}^d$.

- The coefficients b and σ has at most linear growth, i.e., there is $K>0$ such that

$$||b(t,x)||^2 + \sum_{k=1}^{m}\left|\left|\sigma^k(t,x)\right|\right|^2 \leq K\left(1+\|x\|^2\right);$$

  for any $t\in[0,T]$ and $x\in\mathbb{R}^d$.

- For each $x\in\mathbb{R}^d$, the functions $b(\cdot,x),\sigma^1(\cdot,x),\ldots,\sigma^m(\cdot,x):[0,T]\longrightarrow\mathbb{R}^d$ are right continuous with left limits.

These hypotheses can be relaxed to locally Lipschitz continuous coefficients and one-side Lipschitz continuous coefficients.

For many phenomena, studying the long-term behavior of the SDE (1.2) is essential. Specifically, the stability of the system and its ergodicity. In essence, stability of a SDE means insensitivity of its solutions to small changes in the initial value or the parameters of the system. There are different stability criteria, with significant attention given to almost sure stability and moment stability. In essence, almost sure stability (moment stability) implies that the solution of the stochastic differential equation will decay towards the trivial solution for any given initial value as time tends to infinity, almost surely (in terms of moments).

Ergodicity for an SDE can be described as the property where the long-time behavior of the system can be studied by observing its sample paths. In essence, it implies that the statistical properties of the system can be inferred from a single trajectory over a sufficiently long period. For an accurate description, let us adopt the standard hypothesis and consider X_t the unique, strong solution of (1.1). Subsequently, The family of linear operators $\{\mathbf{P}_t\}_{t\geq 0}$ defined for any Borel measurable function $\varphi : \mathbb{R}^d \to \mathbb{R}$ and $t \geq 0$ by

$$\mathbf{P}_t\varphi(x) = \mathbb{E}\big(\varphi\left(X_t\right) \mid X_0 = x_0\big)$$

is a Markov semigroup (strong Markov whenever b and σ are autonomous). A probability measure μ in $(\Omega, \mathcal{F}, \mathbb{P})$ is said to be invariant for X_t if it is invariant under the action of the Markov semigroup, i.e.,

$$\int_{\mathbb{R}^n} \mathbf{P}_t\varphi(x)\, d\mu(x) = \int_{\mathbb{R}^n} \varphi(x)\, d\mu(x),$$

for all bounded functions φ. Furthermore, X_t is said to be ergodic on $\mathbb{R}^n$ if for any initial condition $X_0 = x$,

$$\lim_{t\to\infty} \frac{1}{T} \int_0^T \varphi\left(X_t\right) = \int_{\mathbb{R}^n} \varphi(x)\, d\mu(x), \tag{1.7}$$

for all $\varphi \in \mathbf{L}^2(\mathbb{R}^n, \mu)$. Here we note that a SDE is called ergodic if its solution is ergodic. In addition, the right-hand side of (1.7) is called the *limit value* of φ, a useful quantity in several random systems. For sufficient regularity conditions leading to (1.7), refer to [52].

1.2 Numerical Approximation for Stochastic Differential Equations

A numerical approximation of an SDE is an iterative rule that generates a sequence of approximate values $X^{\Delta} = \left\{X_n^{\Delta}\right\}_{n=0}^{N}$ for the solution of (1.1). These values are computed over a partition $\{t_n\}_{n=0}^{N}$ of $[0,T]$ characterized by the step-size $\Delta = \max_{k=0,\ldots,N-1}(t_{k+1} - t_k)$. Numerical methods can approximate the trajectories or the probability distribution of the solution of SDE (1.1). Consequently, there are different notions of convergence. Namely, in this work, we examine the strong, pathwise, and weak convergence, each with its rate, which typically differs.

On the one hand, strong and pathwise convergences focus on the approximation of the sample paths of the solution. The first considers the expected value of the error in the approximation of the trajectories, while the second focuses on the error for a single sample path. Specifically, a numerical approximation X^{Δ} converges strongly with order $p > 0$ at time T if there exist $K_T > 0$, which does not depend on Δ, and $\Delta_0 > 0$ such that

$$\mathbb{E}\left(\sup_{n=0,\ldots,N}\left|X_{t_n} - X_n^{\Delta}\right|\right) \leq K_T \Delta^p, \tag{1.8}$$

for every $\Delta \in [0, \Delta_0]$. Alternatively, X^{Δ} converges pathwise with order $\gamma > 0$ at time T if there exist $K_T > 0$, which does not depend on Δ, and $\Delta_0 > 0$ such that

$$\sup_{n=0,\ldots,N}\left|X_{t_n}(\omega) - X_n^{\Delta}(\omega)\right| \leq K_T \Delta^{\gamma}, \tag{1.9}$$

for every $\Delta \in [0, \Delta_0]$.

On the other hand, weak convergence focuses on approximating the law of the solution by computing the error in the approximation of the expected value of any smooth mapping of the solution. Specifically, a numerical approximation X^{Δ} converges weakly with order $q > 0$ at time T if for each function $\varphi \in \mathcal{C}_P^{2(q+1)}(\mathbb{R}^d, \mathbb{R})$ there exist $K_{\varphi,T} > 0$, which does not depend on Δ, and $\Delta_0 > 0$ such that

$$\left|\mathbb{E}\left(\varphi\left(X_T\right)\right) - \mathbb{E}\left(\varphi\left(X_N^{\Delta}\right)\right)\right| \leq K_{\varphi,T} \Delta^q, \tag{1.10}$$

for each $\Delta \in [0, \Delta_0]$. Here we said that $\varphi : \mathbb{R}^d \longrightarrow \mathbb{R}$ belongs to $\mathcal{C}_P^L(\mathbb{R}^d, \mathbb{R})$ iff $(t, x) \rightarrow$

$\varphi(x) \in \mathcal{C}_P^L([0,T]\times\mathbb{R}^d,\mathbb{R})$, where $\mathcal{C}_P^L([0,T]\times\mathbb{R}^d,\mathbb{R})$ denote the set of all the functions $f : [0,T]\times\mathbb{R}^d \longrightarrow \mathbb{R}$ such that

$$|\partial_{x_1,\dots,x_l} f(t,x)| \leq K\left(1+\|x\|^q\right),$$

for $0 \leq l \leq L$, $K > 0$, and $q \in \mathbb{N}$.

Besides the convergence rate of numerical methods, other stability properties are considered in the standard literature on stochastic numerics [14, 56, 70]. A stable numerical method produces consistent and accurate results even when the step-size Δ increases. This can be understood from (1.8), (1.9) or (1.10), where the constants K depend on the simulation time T. That means that the results produced by the numerical approximations may deteriorate for large values of T, requiring sufficiently small time-steps Δ to mitigate this effect. Many numerical stability criteria have been considered to study the ability of numerical methods to reproduce the long-term behavior presented by the SDE. In particular, almost sure stability and moment stability for SDEs are among the most desirable properties to be replicated by numerical approximations.

Several numerical integrators for SDEs have been studied under the hypothesis of global Lipschitz continuity (1.6). The most classical method is the Euler-Maruyama scheme [65]. Namely, the Euler-Maruyama method for the SDE (1.1) is given by

$$X_{n+1}^{\Delta} = X_n^{\Delta} + b\left(t_n, X_n^{\Delta}\right)\Delta_n + \sqrt{\Delta_n}\sum_{k=1}^{m}\sigma_k\left(t_n, X_n^{\Delta}\right)\Delta W_n^k,$$

where $\Delta_n = t_{n+1} - t_n$ and $\Delta W_n^k = W_{t_{n+1}}^k - W_{t_n}^k$. The Euler-Maruyama method is known for its weak order of convergence of 1 and a strong order of convergence of $1/2$. One limitation of this method is its dependence on the discretization parameter Δ, which needs to be sufficiently small to ensure a.s. exponential stability [15, 38]. This constraint is a recurring consideration in explicit numerical methods.

In addition to the Euler-Maruyama method, several other noteworthy numerical methods are commonly used for simulating stochastic differential equations. These methods, such as the Milstein method [68], the Itô-Taylor methods [53], and the Runge-Kutta methods [13, 89], offer higher orders of convergence compared to the Euler-Maruyama method. However, these explicit numerical methods may still require small step-sizes Δ to ensure stability.

Exponential schemes offer an alternative approach to standard methods and have shown

promising performance in numerous numerical experiments [8, 46, 74]. In particular, when dealing with SDEs involving additive noise, exponential schemes demonstrate good performance, while standard explicit methods exhibit numerical instabilities. Exponential schemes are explicit numerical approximations. Subsequently, they rely on the global Lipschitz continuity of the SDE to achieve convergence.

Explicit numerical methods can become highly unstable or even diverge if the global Lipschitz condition is not satisfied. [40, 66, 70]. Alternatively, numerical methods such as semi-implicit methods [55, 86], balanced methods [2, 64, 69], tamed methods [41, 49, 96], and truncated methods [33, 34, 63] may overcome these issues. These alternative methods are designed to operate under less restrictive conditions, allowing for superlinear growth, one-sided Lipschitz continuity, or global monotonicity. Nevertheless, these numerical methods involve a greater numerical complexity, and their assumptions remain restrictive. As a consequence, their applicability is limited to specific models.

Chapter 2

Rate of convergence of an exponential scheme for the non-linear stochastic Schrödinger equation with finite-dimensional state space

2.1 Introduction

This work develops the numerical solution of the stochastic Schrödinger equation describing the evolution of open quantum systems, also called the quantum state diffusion model and the non-linear Belavkin equation. We consider a small quantum system with state space $\mathfrak{h}_1 \otimes \mathfrak{h}_2 \otimes \cdots \otimes \mathfrak{h}_n$ that interacts with a heat bath. We focus on the case where $\mathfrak{h}_1, \mathfrak{h}_2, \cdots, \mathfrak{h}_n$ are finite-dimensional Hilbert spaces, and so, to simplify notation, we represent $\mathfrak{h}_1 \otimes \mathfrak{h}_2 \otimes \cdots \otimes \mathfrak{h}_n$ by $\mathbb{C}^d$ equipped with the scalar product $\langle \cdot, \cdot \rangle$ inherited from $\mathfrak{h}_1 \otimes \mathfrak{h}_2 \otimes \cdots \otimes \mathfrak{h}_n$. The internal dynamics of the small quantum system are determined by the time-dependent Hamiltonian $H(t) \in \mathbb{C}^{d \times d}$, which is a self-adjoint operator in $\mathbb{C}^d$ for any time $t \in [0, T]$. The interactions between the small quantum system and the environment are modeled by the time-dependent linear operators $L_1(t), \ldots, L_m(t) \in \mathbb{C}^{d \times d}$. So, we address the numerical solution of the following Itô stochastic differential equation (SDE) on $\mathbb{C}^d$:

$$X_t = X_0 + \int_0^t \left(G(s) X_s + g(s, X_s) \right) ds + \sum_{k=1}^{m} \int_0^t \sigma_k(s, X_s) \, dW_s^k \qquad \forall t \in [0, T], \tag{2.1}$$

where $\|X_0\| = 1$, $W^1, \ldots, W^m$ are independent real Brownian motions,

$$G(s) = -i\,H(s) - \frac{1}{2}\sum_{k=1}^{m} L_k(s)^* L_k(s),$$

$$g(s,z) = \sum_{k=1}^{m}\left(\mathrm{Re}\langle z, L_k(s)\,z\rangle L_k(s)\,z - \frac{1}{2}\mathrm{Re}^2\left(\langle z, L_k(s)\,z\rangle\right) z\right),$$

and

$$\sigma_k(s,z) = L_k(s)\,z - \mathrm{Re}\langle z, L_k(s)\,z\rangle z$$

(see, e.g., [7, 11, 97] for derivations of (2.1)). The complex SDE (2.1) has a unique strong solution (see, e.g., [7, 73]), which satisfies $\|X_t\| = 1$ for all $t \in [0,T]$.

The evolution of quantum measurement processes is described by the operator $|X_t\rangle\langle X_t|$, which is written using Dirac notation. Namely, $|X_t\rangle\langle X_t|$ represents the density operator conditioned on the measurement outcomes (see, e.g., [7, 11, 97] for some derivations). In the homodyne or heterodyne measurement of the observable $L_k(t)$, for instance, the integral from 0 to t of the photocurrent is proportional to

$$W_t^k + 2\int_0^t \mathrm{Re}\left(tr\left(L_k(s)\,|X_s\rangle\langle X_s|\right)\right)ds = W_t^k + 2\int_0^t \mathrm{Re}\langle X_s, L_k(s)\,X_s\rangle ds.$$

On the other hand, the Gorini-Kossakowski-Lindblad-Sudarshan quantum master equation

$$\frac{d}{dt}\rho_t = G(t)\,\rho_t + \rho_t G(t)^* + \sum_{k=1}^{m} L_k(t)\,\rho_t L_k(t)^* \tag{2.2}$$

describes the evolution of the density operator ρ_t, which is the unit-trace positive operator acting on $\mathfrak{h}_1 \otimes \mathfrak{h}_2 \otimes \cdots \otimes \mathfrak{h}_n$ that represents the quantum state of the physical system. We have that $\rho_t = \mathbb{E}\left(|X_t\rangle\langle X_t|\right)$ (see, e.g., [7, 76] for details, and [23] for a recent development). That's why it is said that the quantum density operator ρ_t is unraveled in the quantum trajectories $|X_t\rangle\langle X_t|$. If d is not small enough (in the range of tens), then the calculation of the mean value of the quantum observable A (i.e., $tr(A\rho_t)$) by computing $\mathbb{E}\left(\langle X_t, AX_t\rangle\right)$ via Monte Carlo methods has great advantages over the numerical solution of (2.2) (see, e.g., [10, 11, 36, 82, 87, 97]), which involves d^2 unknown complex functions. Hence, (2.1) is widely used for the numerical solution of (2.2), together with the quantum-jump version of (2.1) (see, e.g., [11, 97])).

This paper deals with the computation of the mean value of $\varphi(X_t)$, when φ is smooth. We focus on the following Euler-Exponential scheme developed by [73, 77] that solves accurately (2.1) with low computational cost (see, e.g., [10, 11, 58, 77] for alternative schemes).

Scheme 1. *Suppose that* $0 = \tau_0 < \tau_1 < \cdots < \tau_N = T$ *are real numbers, and take* $\Delta_n = \tau_{n+1} - \tau_n$. *Let* $\xi_1^1, \ldots, \xi_1^m, \ldots, \xi_N^1, \ldots, \xi_N^m$ *be independent and identically distributed (i.i.d.) real random variables with variance* 1, *and moments of any order. Assume that the distribution of* ξ_n^k *is symmetric with respect to* 0. *Let* $\hat{Y}_0$ *be a random variable independent of the* ξ_n^k*'s satisfying* $\|\hat{Y}_0\| = 1$. *Then, we recursively define*

$$Y_{n+1} = \mathrm{e}^{G(\tau_n)\Delta_n}\left(\hat{Y}_n + g\left(\tau_n, \hat{Y}_n\right)\Delta_n + \sqrt{\Delta_n}\sum_{k=1}^{m}\sigma_k\left(\tau_n, \hat{Y}_n\right)\xi_{n+1}^k\right)$$

and

$$\hat{Y}_{n+1} = Y_{n+1}/\left\|Y_{n+1}\right\|,$$

where $n = 0, \ldots, N-1$.

First, we obtain that the rate of convergence of $\mathbb{E}\left(\varphi\left(\hat{Y}_N\right)\right)$ to $\mathbb{E}(\varphi(X_T))$ with respect to the maximum step-size of $(\tau_n)_{n=0,\ldots,N}$ is equal to 1 for any function φ whose partial Wirtinger derivatives up to order 4 have polynomial growth. An example of such φ is $\varphi(x) = \langle x, Ax\rangle^2$, which appears in the computation of both the variance of $\langle X_t, AX_t\rangle$ and the average of the quantum variance of the observable A at time t, i.e., $\mathbb{E}(\langle X_t, A^2X_t\rangle) - \mathbb{E}(\langle X_t, AX_t\rangle^2)$. Previously, [73] proved that $\mathbb{E}\left(\left\langle \hat{Y}_N, A\,\hat{Y}_N\right\rangle\right)$ converges linearly to $\mathbb{E}(\langle X_T, A\,X_T\rangle)$ whenever the distribution of ξ_{n+1}^k has compact support. This excludes to take $\xi_{n+1}^k = W_{\tau_{n+1}}^k - W_{\tau_n}^k$, a choice used, for instance, in the Multilevel Monte Carlo methods (see, e.g., [28, 29]). Here, we drop the assumption that the support of ξ_{n+1}^k is compact. At the same time, we establish that $\left|\mathbb{E}(\varphi(X_T)) - \mathbb{E}\left(\varphi\left(\hat{Y}_N\right)\right)\right|$ is less than or equal to a constant multiplied by $\max_{n=0,\ldots,N-1}(\tau_{n+1} - \tau_n)$ for a general class of functions φ. This allows us to select adequate step-sizes $\tau_{n+1} - \tau_n$ for achieving a desired global error.

Second, we study for the first time, to the best of our knowledge, the application of the Talay-Tubaro extrapolation procedure to the numerical solution of (2.1). In [92] the Romberg-Richardson extrapolation method for ordinary differential equations is extended to solve globally Lipschitz real SDEs by weak second-order schemes based on the Euler and Milstein schemes (see, e.g., [31, 56, 70]). In this paper, we obtain the leading term of the error $\mathbb{E}(\varphi(X_T)) - \mathbb{E}\left(\varphi\left(\hat{Y}_N\right)\right)$, where $\hat{Y}_N$ follows Scheme 1. Then, we prove that the rate

of convergence of $2\,\mathbb{E}\left(\varphi\left(\hat{Y}_{2N}\left(\bar{\tau}\right)\right)\right) - \mathbb{E}\left(\varphi\left(\hat{Y}_{N}\left(\tau\right)\right)\right)$ to $\mathbb{E}\left(\varphi\left(X_T\right)\right)$ is equal to 2, where $\hat{Y}_n\left(\tau\right)$ is as in Scheme 1 and $\hat{Y}_n\left(\bar{\tau}\right)$ is given by Scheme 1 with $\left(\tau_n\right)_{n=0\ldots,N}$ replaced by the discretization $\left(\bar{\tau}_n\right)_{n=0\ldots,2N}$ obtained by halving the step-sizes of τ_n. This yields a weak second-order approximation of $\mathbb{E}\varphi\left(X_T\right)$ that inherits the good dynamical properties of Scheme 1 and has a low computational cost.

We face two obstacles in the error analysis. Since the coefficients of (2.1) are not globally Lipschitz, the techniques currently used to estimate the rate of weak convergence of the numerical schemes for locally Lipschitz SDEs (see, e.g., [9, 35, 40, 78, 91]) do not apply to (2.1), at least no directly. In Section 2.5.3.2 we overcome the first obstacle by introducing a localization procedure that allows us to treat (2.1) by using a globally Lipschitz SDE whose drift and diffusion coefficients coincide with those of (2.1) in the unit ball. To this end, we exploit the fact that $\left\|\hat{Y}_{n+1}\right\| = 1$ and $\left\|X_t\right\| = 1$. Moreover, Scheme 1 involves the map $Y_{n+1} \mapsto Y_{n+1}/\left\|Y_{n+1}\right\|$ that has a singularity at 0. In order to treat the singularity appearing in the projection onto the unit sphere, we derive a short-time asymptotic expansion of $Y_{n+1}/\left\|Y_{n+1}\right\|$ with respect to the step-size.

Third, we study the strong convergence of Scheme 1, which ensures the convergence of the trajectories of Scheme 1 with $\xi_{n+1}^k = (W_{\tau_{n+1}}^k - W_{\tau_n}^k)/\sqrt{\Delta_n}$. Namely, we prove that the rate of strong convergence of Scheme 1 is equal to $1/2$. This, together with the linear order of weak convergence of Scheme 1, provides a theoretical basis for the numerical solution of (2.1) by the Multilevel Monte Carlo method (see, e.g., [28]) with Scheme 1 as integrator. Other studies on the strong convergence of the numerical schemes for locally Lipschitz SDEs are, e.g., [39, 95].

We organize the paper as follows. Section 2.2 sets up notation and basic definitions. Section 2.3 addresses the rates of strong and weak convergence of Scheme 1. Section 2.4 provides a numerical experiment with a quantum oscillator in the interaction representation. All proofs are deferred to Section 2.5.

2.2 Notation

The scalar product $\langle\cdot,\cdot\rangle$ is anti-linear in the first variable. The partial Wirtinger derivatives are, by definition,

$$\partial_{z_k} f(z) = \frac{1}{2}\left(\frac{\partial}{\partial x_k} - \mathrm{i}\,\frac{\partial}{\partial y_k}\right) f(x + \mathrm{i}\,y) \tag{2.3a}$$

$$\partial_{\overline{z_k}} f(z) = \frac{1}{2}\left(\frac{\partial}{\partial x_k} + \mathrm{i}\,\frac{\partial}{\partial y_k}\right) f(x + \mathrm{i}\,y) \tag{2.3b}$$

where $k = 1, \ldots, d$, $z = x + \mathrm{i}\,y$ with $x = (x_1, \ldots, x_d), y = (y_1, \ldots, y_d) \in \mathbb{R}^d$, and the complex-valued function $(x, y) \mapsto f(x + \mathrm{i}\,y)$ has partial derivatives of first order (see, e.g., [48, 84]). For each $n \in \mathbb{N}$ we consider the multi-index set

$$\mathcal{P}_n = \left\{(\alpha_1, \ldots, \alpha_{2d}) : \alpha_k \in \mathbb{N} \cup \{0\}, \sum_{k=1}^{2d} |\alpha_k| = n\right\}.$$

Then, for any $z = (z_1, \ldots, z_d) \in \mathbb{C}^d$ and $\alpha \in \mathcal{P}_n$ we define

$$z^\alpha = z_1^{\alpha_1} \cdots z_d^{\alpha_d}\, \overline{z_1}^{\alpha_{d+1}} \cdots \overline{z_d}^{\alpha_{2d}}$$

and

$$\partial^\alpha = \frac{\partial^{\alpha_1}}{\partial_{z_1}^{\alpha_1}} \cdots \frac{\partial^{\alpha_d}}{\partial_{z_d}^{\alpha_d}}\, \frac{\partial^{\alpha_{d+1}}}{\partial_{\overline{z_1}}^{\alpha_{d+1}}} \cdots \frac{\partial^{\alpha_{2d}}}{\partial_{\overline{z_d}}^{\alpha_{2d}}}.$$

As usual $\mathcal{P}_0 = \{0\}$ and ∂^0 stands for the identity operator.

Consider $n, L \in \mathbb{Z}_+$. We denote by $\mathcal{WC}^{n,L}\left([t_0, T] \times \mathbb{C}^d, \mathbb{C}\right)$ (resp. $\mathcal{WC}^L\left(\mathbb{C}^d, \mathbb{C}\right)$) the set of all $f : [t_0, T] \times \mathbb{C}^d \to \mathbb{C}$ (resp. $f : \mathbb{C}^d \to \mathbb{C}$) such that $\partial_t^\ell f$ and $\partial^\alpha f$ are continuous functions for any $\ell \leq n$ and $|\alpha| \leq L$. By definition, a function $f \in \mathcal{WC}^{n,L}\left([t_0, T] \times \mathbb{C}^d, \mathbb{C}\right)$ (resp. $f \in \mathcal{WC}^L\left(\mathbb{C}^d, \mathbb{C}\right)$) belongs to $\mathcal{WC}_P^L\left([t_0, T] \times \mathbb{C}^d, \mathbb{C}\right)$ (resp. $\mathcal{WC}_P^L\left(\mathbb{C}^d, \mathbb{C}\right)$) iff

$$|\partial^\alpha f(t, z)| \leq K_\alpha(T)\left(1 + \|z\|^{q_\alpha}\right) \qquad \forall t \in [t_0, T] \text{ and } z \in \mathbb{C}^d \tag{2.4}$$

whenever $|\alpha| \leq L$. Here and subsequently, $\|z\| = \sqrt{\langle z, z\rangle}$, and we use the same symbols $K(\cdot)$, K, and q for different nonnegative increasing functions, real numbers, and natural numbers, respectively. A family of functions $f_\theta \in \mathcal{WC}^L\left(\mathbb{C}^d, \mathbb{C}\right)$, with $\theta \in \Theta$, belongs uniformly to $\mathcal{WC}_P^L\left(\mathbb{C}^d, \mathbb{C}\right)$ iff (2.4) holds uniformly for all f_θ, i.e.

$$|\partial^\alpha f_\theta(z)| \leq K_\alpha\left(1 + \|z\|^{q_\alpha}\right) \qquad \forall z \in \mathbb{C}^d$$

for all $|\alpha| \leq L$ and $\theta \in \Theta$.

2.3 Rates of strong and weak convergence

From Lemma 2.3.1, given below, we obtain that we can project Y_{n+1} onto the unit sphere, and so Scheme 1 is well-defined.

Lemma 2.3.1. *Assume the setup of Scheme 1. Then, $Y_{n+1} \neq 0$ for all $n = 0, \ldots, N-1$.*

Proof. Deferred to Section 2.5.2. □

Next, we establish that the rate of weak convergence of Scheme 1 is equal to 1 provided that φ and the partial Wirtinger derivatives of φ up to order 4 have polynomial growth. From [35] we have that the Euler scheme could converge weakly with a rate slower than 1 when applied to SDEs with non-globally Lipschitz smooth coefficients. And worse still, the Euler scheme diverges, in the weak sense with a fixed time horizon, in some cases where the SDE coefficients grow superlinearly (see, e.g., [40]). The property $\left\|\hat{Y}_{n+1}\right\| = 1$ allows us to use a regularized Kolmogorov equation, together with$\|X_t\| = 1$, to overcome the difficulties caused by the fact that the coefficients of (2.1) are not globally Lipschitz. On the other hand, we obtain $\left\|\hat{Y}_{n+1}\right\| = 1$ by projecting Y_{n+1} onto the unit ball, and so the map $Y_{n+1} \mapsto \hat{Y}_{n+1}$ has a singularity at 0, which adds complexity to the convergence analysis.

Theorem 2.3.1. *Let $H, L_k : [0,T] \to \mathbb{C}^{d\times d}$ be continuously differentiable. Suppose that X is the solution to (2.1) with $\|X_0\| = 1$. Consider $(\hat{Y}_n)_{n=1\ldots,N}$ given by Scheme 1 with $\hat{Y}_0 = X_0$. If $\varphi \in \mathcal{WC}_P^4\left(\mathbb{C}^d, \mathbb{C}\right)$, then there exists an increasing function $K(\cdot)$ depending on φ such that for any time discretization $(\tau_n)_{n=0,\ldots,N}$ we have*

$$\left|\mathbb{E}\left(\varphi\left(X_T\right)\right) - \mathbb{E}\left(\varphi\left(\hat{Y}_N\right)\right)\right| \leq K(T) \max_{n=0,\ldots,N-1}\left(\tau_{n+1} - \tau_n\right).$$

Here, $K(\cdot)$ does not depend on the time discretization (τ_n) and the natural number N.

Proof. The desired result follows from Proposition 2.5.2 given in Section 2.5.3. □

In Theorem 2.3.1 we use the partial Wirtinger derivatives –rather than the classical complex derivative– to describe the regularity of φ. This enables us to consider a wide range of functions φ. For example, $\varphi(x) = \langle x, Ax\rangle$, where $A \in \mathbb{C}^{d\times d}$ is a non-null matrix, has continuous partial Wirtinger derivatives of any order, while $x \mapsto \langle x, Ax\rangle$ is not a holomorphic

function. Moreover, using the Wirtinger derivatives we re-write the Kolmogorov equation corresponding to an SDE on $\mathbb{C}^d$ as two Kolmogorov equations on $\mathbb{R}^{2d}$, and so its regularity properties follow from known results on the Kolmogorov equation with real variables.

Next, we modify the proof of Theorem 2.3.1 to obtain the leading term of the error $\mathbb{E}(\varphi(X_T)) - \mathbb{E}(\varphi(\hat{Y}_N))$. To this end, we adapt the error analysis carried out in [92].

Theorem 2.3.2. *Let X be the solution of (2.1) with $\|X_0\| = 1$. Assume that the functions $H, L_k : [0,T] \to \mathbb{C}^{d\times d}$ have continuous second derivatives. Consider $(\hat{Y}_n)_{n=0\ldots,N}$ given by Scheme 1 with $\hat{Y}_0 = X_0$. If $\varphi \in \mathcal{WC}_P^9\left(\mathbb{C}^d, \mathbb{C}\right)$, then there exists a function $\Psi \in \mathcal{WC}_P^{0,4}\left([0,T]\times\mathbb{C}^d, \mathbb{C}\right)$ and an increasing function $K(\cdot)$ depending on φ such that for any time discretization $(\tau_n)_{n=0,\ldots,N}$ we have*

$$\left|\mathbb{E}\left(\varphi\left(X_T\right)\right) - \mathbb{E}\left(\varphi\left(\hat{Y}_N\right)\right) - \sum_{n=0}^{N-1}\Delta_n \int_{\tau_n}^{\tau_{n+1}} \mathbb{E}\Psi\left(s, X_s\right) ds\right| \leq K\left(T\right)\left(\max_{n=0,\ldots,N-1}\Delta_n\right)^2$$

where $\Delta_n = \tau_{n+1} - \tau_n$. Here, $K(\cdot)$ and Ψ do not depend on $(\tau_n)_{n=0,\ldots,N}$ and N.

Proof. Deferred to Section 2.5.4. □

From Theorem 2.3.2 we deduce that the extrapolation procedure introduced by [92] applies to Scheme 1. i.e., in the notation of Corollary 2.3.1, we have that $2\,\mathbb{E}\left(\varphi\left(\hat{Y}_{2N}\left(\bar{\tau}\right)\right)\right) - \mathbb{E}\left(\varphi\left(\hat{Y}_N\left(\tau\right)\right)\right)$ is a second-order approximation of $\mathbb{E}\left(\varphi\left(X_T\right)\right)$, which requires one and one-half times the amount of evaluations of Scheme 1.

Corollary 2.3.1. *Assume that X is the solution of (2.1) with $\|X_0\| = 1$. Suppose that $H, L_k : [0,T] \to \mathbb{C}^{d\times d}$ have continuous second derivatives. Consider the discretization $\tau = (\tau_n)_{n=0\ldots,N}$, where $0 = \tau_0 < \tau_1 < \cdots < \tau_N = T$, and define*

$$\bar{\tau}_n = \begin{cases} \tau_k & \text{if } n = 2k \\ \left(\tau_k + \tau_{k+1}\right)/2 & \text{if } n = 2k+1 \end{cases},$$

i.e. the partition $\bar{\tau} = (\bar{\tau}_n)_{n=0\ldots,2N}$ of $[0,T]$ is obtained by halving the step-sizes of τ. Let $\hat{Y}_n(\tau)$ and $\hat{Y}_n(\bar{\tau})$ be given by Scheme 1 with discretization τ and $\bar{\tau}$, respectively. If $\hat{Y}_0(\tau) = \hat{Y}_0(\bar{\tau}) = X_0$, then for any time discretization $(\tau_n)_{n=0,\ldots,N}$ we have

$$\left|\mathbb{E}\left(\varphi\left(X_T\right)\right) - \left(2\,\mathbb{E}\left(\varphi\left(\hat{Y}_{2N}\left(\bar{\tau}\right)\right)\right) - \mathbb{E}\left(\varphi\left(\hat{Y}_N\left(\tau\right)\right)\right)\right)\right| \leq K\left(T\right)\max_{n=0,\ldots,N-1}\left(\tau_{n+1} - \tau_n\right)^2.$$

Here, $K(\cdot)$ does not depend on the time discretization $(\tau_n)_{n=0,\dots,N}$ and the natural number N.

Using the short-time asymptotic expansion of $\hat{Y}_{n+1}$ obtained in the proof of Theorem 2.3.1 we now establish that Scheme 1 converges strongly with order 1/2.

Theorem 2.3.3. *Let X be solution of (2.1) and $\hat{Y}$ given by Scheme 1 with $\xi_{n+1}^k = (W_{\tau_{n+1}}^k - W_{\tau_n}^k)/\sqrt{\Delta_n}$. Assume that $\|X_0\| = 1$, and $\hat{Y}_0 = X_0$. Then, for any $p \in \mathbb{N}$ we have*

$$\max_{n=0,\dots,N} \mathbb{E}\left(\left\|X_{\tau_n} - \hat{Y}_n\right\|^{2p}\right) \leq K_p(T) \max_{n=0,\dots,N-1} (\tau_{n+1} - \tau_n)^p,$$

where $K_p(T) \geq 0$ does not depend on the discretization $0 = \tau_0 < \tau_1 < \cdots < \tau_N = T$.

Proof. Deferred to Section 2.5.5. □

Remark 2.3.1. *The implementation of Scheme 1 requires the computation of the matrix exponential $\exp(G(\tau_n)\Delta_n)$ times a vector (see, e.g., [72] for a review). This calculation can be done by using Krylov subspace methods whenever $G(\tau_n)$ is a sparse matrix, which is common in many physical systems. If d is less than a few thousand, we compute $\exp(G(\tau_n))$ by means of Padé approximations combined with a scaling and squaring strategy, and so we calculate only one matrix exponential when we take a sample from each integration step of Scheme 1.*

2.4 Example

2.4.1 Physical system and previous results

We deal with the open quantum system with state space $\mathfrak{h} = l^2(\mathbb{Z}_+)$ described by the Hamiltonian

$$\mathcal{H} = \mathrm{i}\left(a^\dagger - a\right) + a^\dagger a,$$

and the Gorini-Kossakowski-Sudarshan-Lindblad operators

$$\mathcal{L}_1 = 0.2a,\ \mathcal{L}_2 = 0.01a^2,\ \mathcal{L}_3 = 0.1a^\dagger a, \text{ and } \mathcal{L}_4 = 0.1a^\dagger,$$

where $a^\dagger$ and a are the creation and annihilation operators. We recall that the domain of $a^\dagger$ and a is $\left\{x \in l^2(\mathbb{Z}_+) : \sum_{k\geq 0} k\,|\langle e_k, x\rangle|^2 < +\infty\right\}$, where $(e_k)_{k\in\mathbb{Z}_+}$ is the canonical orthonormal

basis for $l^2(\mathbb{Z}_+)$. The creation operator $a^\dagger$ is defined by $a^\dagger e_k = \sqrt{k+1}\, e_{k+1}$ for all $k \in \mathbb{Z}_+$, and the annihilation operator a is given by $a\, e_k = \sqrt{k}\, e_{k-1}$ for any $k > 0$, and $a\, e_0 = 0$. The Number operator is equal to $a^\dagger a$. Thus, the evolution of the quantum system is described by the mean values of functions of $|X_t^\infty\rangle\langle X_t^\infty|$, where we use the Dirac notation and X_t^∞ is the solution of (2.1) with $H = \mathcal{H}$ and $L_k = \mathcal{L}_k$ for any $k = 1, \ldots, 4$. The existence and weak uniqueness of the regular solution to (2.1) with an infinite-dimensional state-space is proved in, e.g., [25, 80].

For instance, the model under consideration describes a single mode of a quantized electromagnetic field in interaction with a heat bath. In the Hamiltonian $\mathcal{H}$, the term $a^\dagger a$ is the Hamiltonian of the quantum harmonic oscillator, where the energy origin has been redefined to eliminate the vacuum fluctuation energy, and i $\left(a^\dagger - a\right)$ represents a linear pumping produced by an electric field (see, e.g., [36]). Moreover, $\mathcal{L}_1$ and $\mathcal{L}_2$ add the damping caused by photon emissions, $\mathcal{L}_3$ induces pure dephasing, and $\mathcal{L}_4$ models photon gain (see, e..g., [11, 21, 94]).

We approximate X_t^∞ by the solution X_t of (2.1) with

$$X_0 = P_d\, X_0^\infty / \left\| P_d\, X_0^\infty \right\|, \qquad H = P_d\, \mathcal{H}, \qquad \text{and } L_k = P_d\, \mathcal{L}_k$$

for all $k = 1, \ldots, 4$, where $P_d : l^2(\mathbb{Z}_+) \to \mathbb{C}^{d+1}$ is the projection on the linear manifold spanned by $\{e_k : k = 0, \ldots, d\}$. The numerical experiment of Section 6 of [73] examines the computation of $\mathbb{E}\left\langle X_t, a^\dagger a X_t \right\rangle$ by using Scheme 1, the explicit Euler scheme, and a version of the implicit Euler method, the two later ones are projected onto the unit sphere in each time integration step. In [73], the performance of Scheme 1 outshone that of the other two numerical methods.

As in [73] we compute $\mathbb{E}\left\langle X_t, a^\dagger a X_t \right\rangle$ with $X_0^\infty = e_6$. We take $d = 50$. This selection allows us to get $\mathbb{E}\left\langle X_t, a^\dagger a X_t \right\rangle$ by calculating the explicit solution $\mathcal{T}_t \in \mathbb{C}^{(d+1)\times(d+1)}$ of the adjoint quantum master equation

$$\frac{d}{dt}\mathcal{T}_t = G^*\mathcal{T}_t + \mathcal{T}_t G + \sum_{k=1}^{n} L_k^* \mathcal{T}_t L_k, \qquad \mathcal{T}_0 = P_d\, a^\dagger a \tag{2.5}$$

since $\mathbb{E}\left\langle X_t, a^\dagger a\, X_t \right\rangle = \langle X_0, \mathcal{T}_t X_0 \rangle$. In Figure 2.1 the solid line shows the interpolate values of $\langle e_6, \mathcal{T}_t\, e_6 \rangle$, which are the reference values for $\mathbb{E}\left\langle X_t, a^\dagger a\, X_t \right\rangle$. It is worth pointing out that the numerical solution of (2.5) has serious drawbacks if d is large (see, e.g., [11, 36, 82]), and

according to Proposition 6.1 of [75] we have that for any $p \in \mathbb{N}$,

$$\left|\mathbb{E}\left\langle X_t, P_d\, a^\dagger a\, X_t\right\rangle - \mathbb{E}\left\langle X_t^\infty, P_d\, a^\dagger a\, X_t^\infty\right\rangle\right| \leq K_p\left(\frac{1}{d^{p-2}} + \frac{1}{d^{2p-5}}\right) \qquad \forall d \geq 6.$$

2.4.2 The Talay-Tubaro extrapolation method

We illustrate the good behavior of the Talay-Tubaro extrapolation of Scheme 1 given by Corollary 2.3.1. To this end, we compute $\mathbb{E}\left\langle X_{T_j}, a^\dagger a X_{T_j}\right\rangle$ for $T_j = 0.94\, j$ with $j = 1, \ldots, 10$;from Figure 2.1 we see that $\mathbb{E}\left\langle X_t, P_d\, a^\dagger a\, X_t\right\rangle$ reaches a peak value at approximately $T_{10} = 9.4$. We run Scheme 1 with two constant step-sizes $\tau_{n+1} - \tau_n = 2\Delta$, and $\bar{\tau}_{n+1} - \bar{\tau}_n = \Delta$, where $\Delta = 9.4/N$. Thus, according to Corollary 2.3.1 we have

$$\mathbb{E}\left\langle X_{T_j}, a^\dagger a\, X_{T_j}\right\rangle \approx 2\,\mathbb{E}\left(\varphi\left(\hat{Y}_{2N_j}\left(\bar{\tau}\right)\right)\right) - \mathbb{E}\left(\varphi\left(\hat{Y}_{N_j}\left(\tau\right)\right)\right),$$

where $2\,N_j\,\Delta = T_j$ and $\varphi\left(x\right) = \langle x, a^\dagger a\, x\rangle$. Using sample-sizes of 10^8 we compute the sample means of $\varphi\left(\hat{Y}_{2N_j}\left(\bar{\tau}\right)\right)$ and $\varphi\left(\hat{Y}_{N_j}\left(\tau\right)\right)$. Figure 2.1 illustrates the performance of the extrapolation method based on Scheme 1 for the step-sizes $\Delta = 9.4/60, 9.4/80, 9.4/160$. The circles represent the estimated values of $\mathbb{E}\left(\varphi\left(\hat{Y}_{2N_j}\left(\bar{\tau}\right)\right)\right)$, and the crosses stand for the estimated values of $2\,\mathbb{E}\left(\varphi\left(\hat{Y}_{2N_j}\left(\bar{\tau}\right)\right)\right) - \mathbb{E}\left(\varphi\left(\hat{Y}_{N_j}\left(\tau\right)\right)\right)$. We get more accurate estimations of $\mathbb{E}\left\langle X_{T_j}, a^\dagger a\, X_{T_j}\right\rangle$ when we use smaller step-sizes Δ. In Figure 2.1 we see that both Scheme 1 and the Talay-Tubaro extrapolation method reproduce well the oscillatory behavior of the quantum mean value of the number operator, even if we use large step-sizes. Moreover, Figure 2.1 highlights the very good accuracy of the extrapolation method described by Corollary 2.3.1.

Figure 2.2 and Table 2.1 provide the errors

$$\epsilon_1\left(\Delta\right) = \max_{j=0,1,\ldots,10}\left|\mathbb{E}\left(\varphi\left(X_{T_j}\right)\right) - \frac{1}{M}\sum_{k=1}^{M}\varphi\left(\hat{Y}_{2N_j}^k\left(\bar{\tau}\right)\right)\right|, \tag{2.6}$$

and

$$\epsilon_2\left(\Delta\right) = \max_{j=0,1,\ldots,10}\left|\mathbb{E}\left(\varphi\left(X_{T_j}\right)\right) - \frac{1}{M}\sum_{k=1}^{M}\left(2\,\varphi\left(\hat{Y}_{2N_j}^k\left(\bar{\tau}\right)\right) - \varphi\left(\hat{Y}_{N_j}^k\left(\tau\right)\right)\right)\right|, \tag{2.7}$$

corresponding to the Monte Carlo simulation of Scheme 1 and the Talay-Tubaro extrap-

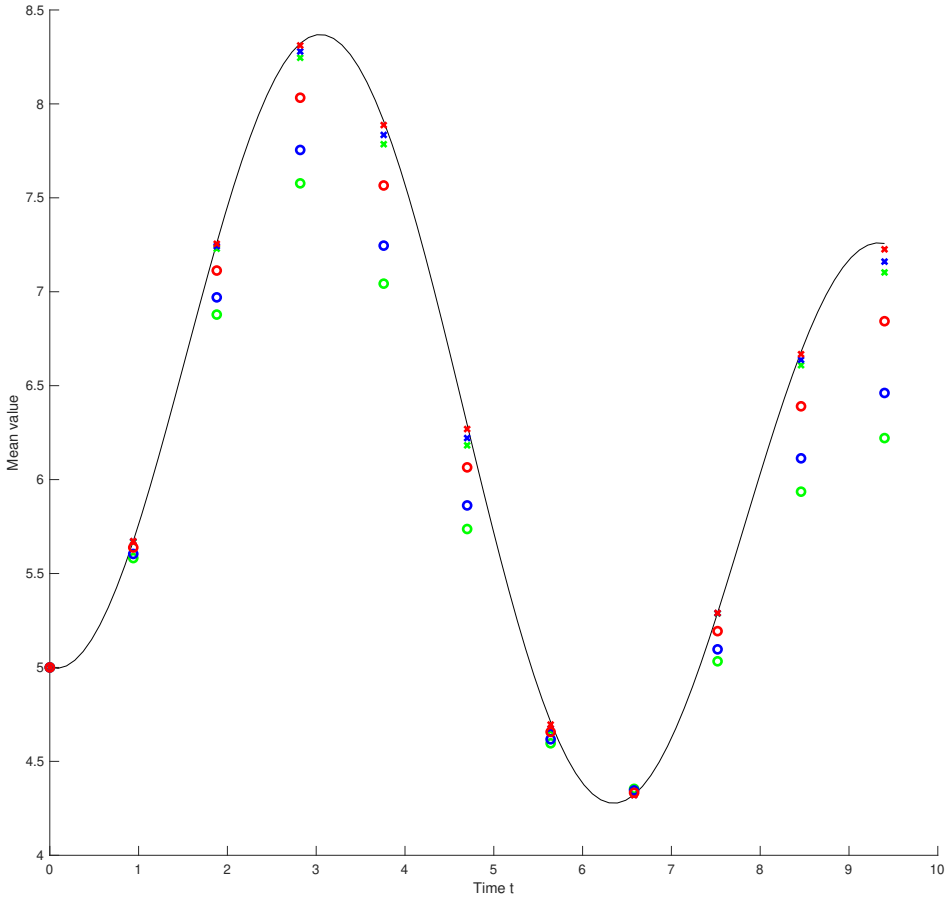

Figure 2.1: *Computation of* $\mathbb{E}\langle X_t, a^\dagger a\, X_t\rangle$*, with* $X_0^\infty = e_6$ *and* $d = 50$*, by Scheme 1 (circles) and the Talay-Tubaro extrapolation of Scheme 1 (crosses). Here,* $\Delta = 0.1567, 0.1175, 0.0588$*, and smaller step-sizes* Δ *yield better approximations. The solid line represents the reference values.*

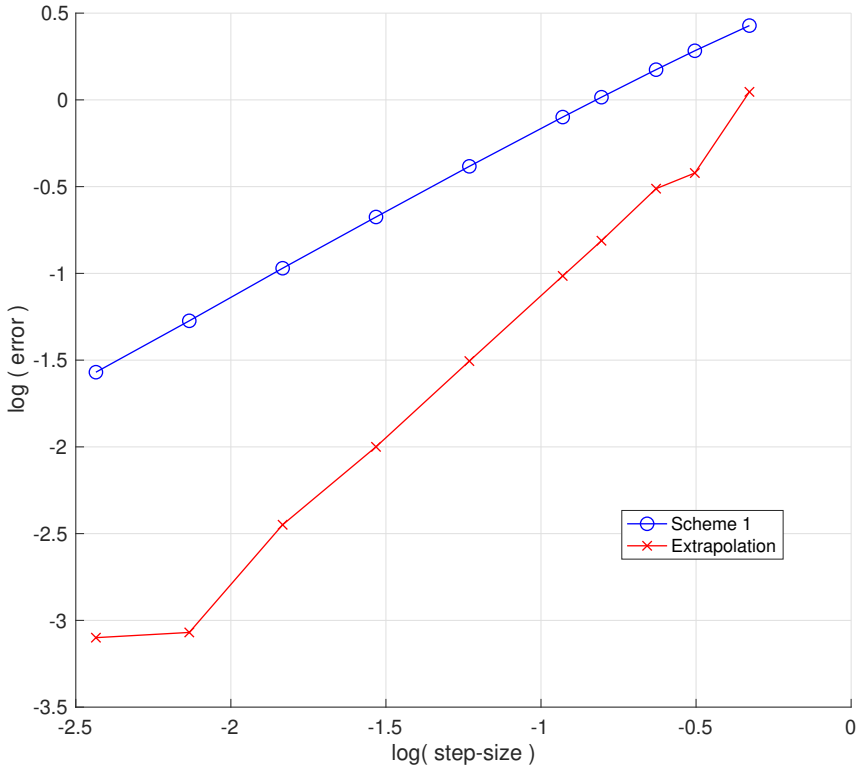

Figure 2.2: *The base* 10 *logarithm of the errors* $\epsilon_1(\Delta)$*, indicated by circles, and* $\epsilon_2(\Delta)$*, indicated by cross, as a function of the base* 10 *logarithm of the step-size* Δ*.*

olation method, respectively. Here, the sample size is equal to 10^8 (i.e., $M = 10^8$), and $\hat{Y}^1_{2N_j}(\bar{\tau}), \ldots, \hat{Y}^M_{2N_j}(\bar{\tau})$ (respectively, $\hat{Y}^1_{N_j}(\tau), \ldots, \hat{Y}^M_{N_j}(\tau)$) are independent random variables distributed according to the law of $\hat{Y}_{2N_j}(\bar{\tau})$ (respectively, $\hat{Y}_{N_j}(\tau)$). A confidence interval for $\mathbb{E}\left(\varphi\left(\hat{Y}_{2N_j}(\bar{\tau})\right)\right)$ with the confidence level of 90 % is given by

$$\left|\mathbb{E}\left(\varphi\left(\hat{Y}_{2N_j}(\bar{\tau})\right)\right) - \frac{1}{M}\sum_{k=1}^{M}\varphi\left(\hat{Y}^k_{2N_j}(\bar{\tau})\right)\right| \leq \mathrm{E}^j_1(\Delta),$$

where

$$\mathrm{E}^j_1(\Delta) = \frac{1.65}{\sqrt{M}}\left(\frac{1}{M}\sum_{k=1}^{M}\varphi\left(\hat{Y}^k_{2N_j}(\bar{\tau})\right)^2 - \left(\frac{1}{M}\sum_{k=1}^{M}\varphi\left(\hat{Y}^k_{2N_j}(\bar{\tau})\right)\right)^2\right)^{1/2}$$

(see, e.g., Section 2.2.2 of [30]). Similarly, the endpoints of a confidence interval for the Talay-

Δ	0.47	0.3133	0.2350	0.1567	0.1175	0.0588	0.0294	0.0147	0.0073	0.0037
N	20	30	40	60	80	160	320	640	1280	2560
$\epsilon_1(\Delta)$	2.6799	1.9188	1.4931	1.0361	0.7959	0.4139	0.2113	0.1071	0.0533	0.0269
$10^4\,\mathrm{E}_1(\Delta)$	6.5405	7.2363	7.5933	7.9575	8.1427	8.4283	8.5746	8.65	8.6865	8.7062
$\epsilon_2(\Delta)$	1.1120	0.3788	0.3078	0.1542	0.0967	0.0312	0.0100	0.0036	0.00085	0.00079
$10^4\,\mathrm{E}_2(\Delta)$	9.7197	9.5701	9.4686	9.1625	9.0110	8.8164	8.7623	8.7451	8.7356	8.7309

Table 2.1: *Errors* (2.6) *and* (2.7) *appearing in the computation of* $\mathbb{E}\left\langle X_{T_j}, a^\dagger a X_{T_j}\right\rangle$ *with* $X_0^\infty = e_6$ *and* $d = 50$*, by using Scheme 1 and the Talay-Tubaro extrapolation of Scheme 1. Here,* $T_j = 0.94\,j$ *with* $j = 0, 1, \ldots, 10$*.*

Tubaro approximation $2\,\mathbb{E}\left(\varphi\left(\hat{Y}_{2N_j}(\bar{\tau})\right)\right) - \mathbb{E}\left(\varphi\left(\hat{Y}_{N_j}(\tau)\right)\right)$ at the approximate confidence level 90 % are $\frac{1}{M}\sum_{k=1}^{M}\left(2\,\varphi\left(\hat{Y}^k_{2N_j}(\bar{\tau})\right) - \varphi\left(\hat{Y}^k_{N_j}(\tau)\right)\right) \pm \mathrm{E}_2^j(\Delta)$, where $\mathrm{E}_2^j(\Delta)$ is equal to

$$\frac{1.65}{\sqrt{M}}\left(\frac{1}{M}\sum_{k=1}^{M}\left(2\,\varphi\left(\hat{Y}^k_{2N_j}(\bar{\tau})\right) - \varphi\left(\hat{Y}^k_{N_j}(\tau)\right)\right)^2 - \left(\frac{1}{M}\sum_{k=1}^{M}\left(2\,\varphi\left(\hat{Y}^k_{2N_j}(\bar{\tau})\right) - \varphi\left(\hat{Y}^k_{N_j}(\tau)\right)\right)\right)^2\right)^{1/2}.$$

Table 2.1 also presents the values of

$$\mathrm{E}_\ell(\Delta) = \max_{j=0,1,\ldots,10} \mathrm{E}_\ell^j(\Delta) \tag{2.8}$$

with $\ell = 1, 2$.

According to Figure 2.2 and Table 2.1, we have that the extrapolation method, given by Corollary 2.3.1, improves the accuracy of Scheme 1. Applying a non-linear regression analysis, we find that the estimated convergence rates of the errors ϵ_1 and ϵ_2 are 0.88054 and 2.073, respectively, in good agreement with Theorem 2.3.1 and Corollary 2.3.1. This motivates to apply the Talay-Tubaro extrapolation procedure in the numerical simulation of open quantum systems.

2.4.3 Multilevel Monte Carlo method

We calculate $\mathbb{E}\left\langle X_{T_j}, a^\dagger a\, X_{T_j}\right\rangle$ by sampling Scheme 1 with the Multilevel Monte Carlo method (MLMC), where $j = 1, \ldots, 10$. Let $\left(\hat{Y}_{n,\ell}\right)_{n=0,\ldots,N_\ell}$ denote Scheme 1 with constant step-size $\tau_{n+1} - \tau_n = T_{10}/N_\ell$, where $N_\ell = 2^\ell N_0$. We take $N_0 = 20$, and so the step-size of the level 0

Tol	0.1	0.05	0.01	0.005
$\bar{\epsilon}_3$	0.0976	0.0619	0.0132	0.0053
L	7	8	11	11
Total number of steps	$1.1335 \cdot 10^7$	$2.2894 \cdot 10^7$	$4.6357 \cdot 10^8$	$1.6346 \cdot 10^9$
$\bar{\epsilon}_1\left(T/N_{L-2}\right)$	0.1165	0.0474	0.0309	0.0181
$\bar{\epsilon}_1\left(T/N_{L-1}\right)$	0.0766	0.0996	0.0234	0.0361
$\bar{\epsilon}_1\left(T/N_L\right)$	0.1092	0.0766	0.0456	0.0361

Table 2.2: *Errors appearing in the computation of* $\mathbb{E}\left\langle X_{T_j}, a^\dagger a\, X_{T_j}\right\rangle$ *with* $X_0^\infty = e_6$ *and* $d = 50$ *by using the Multilevel Monte Carlo method with starting step-size* 0.47.

is equal to $9.4/20 = 0.47$. Since $\tau_{2^{\ell+1}j} = 2^{\ell+1} j \frac{9.4}{10\, 2^{\ell+1}} = 0.94\, j$,

$$\begin{aligned}\mathbb{E}\varphi\left(X_{T_j}\right) \approx \mathbb{E}\varphi\left(\hat{Y}_{2^{L+1}j,L}\right) &= \mathbb{E}\varphi\left(\hat{Y}_{2\,j,0}\right) + \sum_{\ell=1}^{L}\left(\mathbb{E}\varphi\left(\hat{Y}_{2^{\ell+1}j,\ell}\right) - \mathbb{E}\varphi\left(\hat{Y}_{2^{\ell}j,\ell-1}\right)\right) \\ &\approx \frac{1}{M_0}\sum_{u=1}^{M_0}\varphi\left(\hat{Y}^{u,0}_{2\,j,0}\right) + \sum_{\ell=1}^{L}\frac{1}{M_\ell}\sum_{u=1}^{M_\ell}\left(\varphi\left(\hat{Y}^{u,\ell}_{2^{\ell+1}j,\ell}\right) - \varphi\left(\hat{Y}^{u,\ell}_{2^{\ell}j,\ell-1}\right)\right),\end{aligned}$$

where $j = 1, \ldots, 10$, and $\hat{Y}^{u,0}_{2\,j,0}$, $\left(\hat{Y}^{u,\ell}_{2^{\ell+1}j,\ell}, \hat{Y}^{u,\ell}_{2^{\ell}j,\ell-1}\right)$ are independent random variables distributed according to the laws of $\hat{Y}_{2\,j,0}$, $\left(\hat{Y}_{2^{\ell+1}j,\ell}, \hat{Y}_{2^{\ell}j,\ell-1}\right)$, respectively. We automatically adjust the parameters L, $M_0, \ldots, M_L$ by using the MLMC described in Section 3 of [28], with the Euler-Maruyama scheme replaced by Scheme 1. We define the cost function at level ℓ with $\ell \geq 1$ (resp. $\ell = 0$) to be the number of steps taken by $\hat{Y}_{\cdot,\ell}$ and $\hat{Y}_{\cdot,\ell-1}$ (resp. $\hat{Y}_{\cdot,0}$). Table 2.2 provides the error $\bar{\epsilon}_3$ defined by

$$\max_{0\leq j\leq 10}\left|\mathbb{E}\left(\varphi\left(X_{T_j}\right)\right) - \frac{1}{M_0}\sum_{u=1}^{M_0}\varphi\left(\hat{Y}^{u,0}_{2\,j,0}\right) - \sum_{\ell=1}^{L}\frac{1}{M_\ell}\sum_{u=1}^{M_\ell}\left(\varphi\left(\hat{Y}^{u,\ell}_{2^{\ell+1}j,\ell}\right) - \varphi\left(\hat{Y}^{u,\ell}_{2^{\ell}j,\ell-1}\right)\right)\right|,$$

together with the total number of steps taken by Scheme 1, which is equal to $M_L N_L + \sum_{k=0}^{L-1}\left(M_k + M_{k+1}\right)N_k$. Moreover, Table 2.2 presents the error $\bar{\epsilon}_1\left(T/N_\ell\right)$ obtained by using the same total number of steps taken by Scheme 1 in the MLMC, i.e., by sampling $\left(M_L N_L + \sum_{k=0}^{L-1}\left(M_k + M_{k+1}\right)N_k\right)/N_\ell$-times Scheme 1 with step-size T_{10}/N_ℓ. According to Table 2.2 we have that the MLMC achieves the global error specified by the user. To this end, the MLMC finds the appropriate number of levels L and sample-sizes M_ℓ.

Δ	0.47	0.3133	0.2350	0.1567	0.1175	0.0588	0.0294	0.0147	0.0073
N	20	30	40	60	80	160	320	640	1280
$\epsilon_2(\Delta)$	1.11	0.3641	0.3062	0.1491	0.1055	0.042	0.0136	0.0119	0.0057
$\epsilon_4(\Delta)$	4.7456	8.8647	13.3929	21.9222	30.0058	44.0654	44.0172	0.1577	0.0362

Table 2.3: *Errors appearing in the computation of* $\mathbb{E}\left\langle X_{T_j}, a^\dagger a X_{T_j}\right\rangle$ *with* $X_0^\infty = e_6$, $d = 50$, *and* $T_j = 0.94\, j$ *with* $j = 0, 1, \ldots, 10$. *We use the Talay-Tubaro extrapolation of Scheme 1* ($\epsilon_2(\Delta)$), *and the QuTiP library* ($\epsilon_4(\Delta)$).

2.4.4 The QuTip toolbox

In this section we compute $\mathbb{E}\left\langle X_{T_j}, a^\dagger a X_{T_j}\right\rangle$ using the current version of the open-source software *Quantum Toolbox in Python* (see, e.g., [47]). We use version 4.7.1 of the *QuTiP* library, which can be found at `https://qutip.org`. We solve (2.1) using the *QuTiP* routine *ssesolve* with the solver option 'platen', as we present in Code 2.3. Thus, we run an implementation of the stochastic Runge-Kutta method stated in the equation (7.47) of [11], which was designed by Platen (see, e.g., [56] for a version of this scheme that achieves the second weak order of convergence for globally Lipschitz real SDEs).

In Table 2.3 we compare the Talay-Tubaro extrapolation of Scheme 1 with the *QuTiP* function *ssesolve*. We restrict the sample-size to $4 \cdot 10^5$ and the step-size to 9.4/1280, because the intensive memory usage of Code 2.3 results in the Pyton reboot in more computationally demanding cases (we use a computer with an Intel Xeon E5-2699 v4 (44) processor and 64 GB of RAM). In Table 2.3, $\epsilon_4(\Delta)$ is defined by (2.6) with $\frac{1}{M}\sum_{k=1}^{M}\varphi\left(\hat{Y}_{2N_j}^k(\bar{\tau})\right)$ replaced by the expectation values provided by Code 2.3. As in Table 2.1, the error $\epsilon_2(\Delta)$ is given by (2.7). The highest estimated deviation of the values of $\epsilon_2(\Delta)$ presented in Table 2.3 is $\max_\Delta \mathrm{E}_2(\Delta) = 0.0153$, where $\mathrm{E}_2(\Delta)$ is given by (2.8).

According to Table 2.3 we have that the method given by Corollary 2.3.1 outperforms the *QuTiP* function *ssesolve* in terms of accuracy. In this example, Table 2.3 suggests that the stochastic Runge-Kutta method designed by Platen shows numerical instabilities when $\Delta \geq 0.0294$.

```python
from qutip import *
import numpy as np

if __name__ == '__main__':
    # Set the Hamiltonian H
    d = 50
    a  = destroy(d+1)
    H = 1j*(a.dag() - a) + a.dag()* a

    # Set the initial state
    x0 = np.zeros([d+1,1])
    x0[5] = 1
    State0 = Qobj(x0) # Initial state.

    # Set the uniform time discretization of [0,T]
    T = 9.4
    N = 1280
    times = np.linspace(0.0, T, N+1)

    # Set the stochastic colapse operators L_k
    sc_ops = [0.2*a, 0.01*a*a, 0.1*a.dag()*a, 0.1*a.dag()]

    e_ops = [a.dag()*a] # Number operator
    ntraj = int(0.4*1e5) # Number of trajectories
    num_cpus = 22 # Number of cpus used by ssesolve function.

    Data = ssesolve( H, State0, times, sc_ops= sc_ops,
             e_ops=e_ops, method="homodyne", solver='platen',
             ntraj=ntraj, map_func=parallel_map,
             map_kwargs={'num_cpus' : num_cpus})
```

Figure 2.3: *The Python module that computes* $\mathbb{E}\left\langle X_{T_j}, a^\dagger a X_{T_j}\right\rangle$ *using the routine ssesolve of QuTiP*

2.5 Proofs

2.5.1 Preliminaries

For completeness, we present the extension of two classical theorems to the framework of the Wirtinger calculus. For instance, the following Taylor's formula is used in complex-valued signal processing.

Theorem 2.5.1. *Suppose that $f \in \mathcal{WC}^k\left(\mathbb{C}^d, \mathbb{C}\right)$ with $k \in \mathbb{C}$. Let $z_0, z \in \mathbb{C}^d$. Then*

$$f\left(z_0 + z\right) = \sum_{|\alpha| \leq k-1} \partial^\alpha f\left(z_0\right) \frac{z^\alpha}{\alpha!} + k \sum_{|\alpha|=k} \frac{z^\alpha}{\alpha!} \int_0^1 \left(1-t\right)^{k-1} \partial^\alpha f\left(z_0 + t\, z\right) dt. \tag{2.9}$$

Proof. Using the chain rule for Wirtinger's derivatives (see, e.g., [48, 84]) we get

$$\frac{d}{dt} f\left(z_0 + t\, z\right) = \sum_{|\alpha|=1} \partial^\alpha f\left(z_0 + t\, z\right) z^\alpha,$$

and so $f\left(z_0 + z\right) = f\left(z_0\right) + \sum_{|\alpha|=1} z^\alpha \int_0^1 \partial_z^\alpha f\left(z_0 + t\, z\right) dt$. As in the derivation of the classical Taylor's formula, using induction and applying integration by parts formula we obtain the theorem. □

Applying (2.3) gives

$$\partial_{z_j\, z_k} = \frac{1}{4}\left(\frac{\partial^2}{\partial x_j\, x_k} - \frac{\partial^2}{\partial y_j\, y_k}\right) - \frac{\mathrm{i}}{4}\left(\frac{\partial^2}{\partial x_j\, y_k} + \frac{\partial^2}{\partial y_j\, x_k}\right), \tag{2.10a}$$

$$\partial_{\overline{z_j}\,\overline{z_k}} = \frac{1}{4}\left(\frac{\partial^2}{\partial x_j\, x_k} - \frac{\partial^2}{\partial y_j\, y_k}\right) + \frac{\mathrm{i}}{4}\left(\frac{\partial^2}{\partial x_j\, y_k} + \frac{\partial^2}{\partial y_j\, x_k}\right), \tag{2.10b}$$

$$\partial_{z_j\,\overline{z_k}} = \frac{1}{4}\left(\frac{\partial^2}{\partial x_j\, x_k} + \frac{\partial^2}{\partial y_j\, y_k}\right) + \frac{\mathrm{i}}{4}\left(\frac{\partial^2}{\partial x_j\, y_k} - \frac{\partial^2}{\partial y_j\, x_k}\right). \tag{2.10c}$$

The following Itô formula for complex-valued semimartingales has been used in the study of conformal martingales.

Theorem 2.5.2. *Let $Z_t = \left(Z_t^1, \ldots, Z_t^d\right)$ with $Z_t^k = X_t^k + \mathrm{i}\, Y_t^k$, where X_t^k, Y_t^k are continuous real semimartingales. Assume that $f \in \mathcal{WC}^{1,2}\left([t_0, T] \times \mathbb{C}^d, \mathbb{C}\right)$. Then, for all $t \in [t_0, T]$ we*

have

$$\begin{aligned} f(t,Z_t) =& f(t_0,Z_{t_0}) + \int_{t_0}^t \partial_t f(s,Z_s)\,ds + \sum_{k=1}^d \int_{t_0+}^t \partial_{z_k} f(s,Z_s)\,dZ_s^k \\ &+ \sum_{k=1}^d \int_{t_0+}^t \partial_{\overline{z_k}} f(s,Z_s)\,d\overline{Z^k}_s + \frac{1}{2}\sum_{j,k=1}^d \int_{t_0+}^t \partial_{z_j\,z_k} f(s,Z_s)\,d\left[Z^j,Z^k\right]_s \\ &+ \frac{1}{2}\sum_{j,k=1}^d \int_{t_0+}^t \partial_{\overline{z_j}\,\overline{z_k}} f(s,Z_s)\,d\left[\overline{Z^j},\overline{Z^k}\right]_s \\ &+ \sum_{j,k=1}^d \int_{t_0+}^t \partial_{z_j\,\overline{z_k}} f(s,Z_s)\,d\left[Z^j,\overline{Z^k}\right]_s. \end{aligned}$$

Proof. Applying the Itô formula to $(t,X_t,Y_t)\mapsto f(t,X_t+\mathrm{i}\,Y_t)$ we get

$$\begin{aligned} f(t,Z_t) =& f(t_0Z_0) + \int_{t_0}^t \partial_t f(s,Z_s)\,ds + \sum_{k=1}^d \int_{t_0+}^t \frac{\partial}{\partial x_k} f(s,Z_s)\,dX_s^k \\ &+ \sum_{k=1}^d \int_{t_0+}^t \frac{\partial}{\partial y_k} f(s,Z_s)\,dY_s^k + \frac{1}{2}\sum_{j,k=1}^d \int_{t_0+}^t \frac{\partial^2}{\partial x_j\,x_k} f(s,Z_s)\,d\left[X^j,X^k\right]_s \\ &+ \frac{1}{2}\sum_{j,k=1}^d \int_{t_0+}^t \frac{\partial^2}{\partial y_j\,y_k} f(s,Z_s)\,d\left[Y^j,Y^k\right]_s \\ &+ \sum_{j,k=1}^d \int_{t_0+}^t \frac{\partial^2}{\partial x_j\,y_k} f(s,Z_s)\,d\left[X^j,Y^k\right]_s, \end{aligned}$$

where $X_t=\mathrm{Re}\,(Z_t)$ and $Y_t=\mathrm{Im}\,(Z_t)$ (see, e.g, [83, 85]). Replacing X_t^ℓ and Y_t^ℓ by $\left(Z_t^\ell+\overline{Z_t^\ell}\right)/2$ and $\mathrm{i}\left(\overline{Z_t^\ell}-Z_t^\ell\right)/2$, respectively, we obtain the desire formula after basic algebraic manipulations involving (2.3) and (2.10). □

2.5.2 Proof of Lemma 2.3.1

Proof. Let

$$\widetilde{Y}_{n+1} = \hat{Y}_n + g\left(\tau_n,\hat{Y}_n\right)\Delta_n + \sqrt{\Delta_n}\sum_{k=1}^m \sigma_k\left(\tau_n,\hat{Y}_n\right)\xi_{n+1}^k. \tag{2.11}$$

Since $\mathrm{Re}\langle z, \sigma_k(s,z)\rangle = 0$ whenever $\|z\| = 1$, using $\|\hat{Y}_n\| = 1$ yields

$$\mathrm{Re}\langle \hat{Y}_n, \widetilde{Y}_{n+1}\rangle = 1 + \Delta_n \mathrm{Re}\langle \hat{Y}_n, g\left(\tau_n, \hat{Y}_n\right)\rangle = 1 + \frac{\Delta_n}{2}\sum_{k=1}^{m} \mathrm{Re}^2\langle \hat{Y}_n, L_k(\tau_n)\,\hat{Y}_n\rangle.$$

Therefore, $\mathrm{Re}\langle \hat{Y}_n, \widetilde{Y}_{n+1}\rangle \geq 1$, and so $\widetilde{Y}_{n+1} \neq 0$. This gives $e^{G(\tau_n)\Delta_n}\widetilde{Y}_{n+1} \neq 0$. □

2.5.3 Proof of Theorem 2.3.1

2.5.3.1 Asymptotic behavior of Scheme 1

In Scheme 1 the preliminary approximation Y_{n+1} is projected onto the unit sphere. The following lemma allows us to treat theoretically the singularity at 0 of the function $z \mapsto z/\|z\|$.

Lemma 2.5.1. *For any non-zero $z \in \mathbb{C}^d$ we have*

$$\left|\frac{z}{\|z\|} - z - \frac{z}{2}\left(1 - \|z\|^2\right) - \frac{3}{8}z\left(1 - \|z\|^2\right)^2\right| \leq \left|1 - \|z\|^2\right|^3.$$

Proof. Let $r > 0$. Since

$$\frac{1}{r} - 1 - \frac{1}{2}\left(1 - r^2\right) = \frac{\left(1 - r^2\right)^2}{2\,r}\left(\frac{1}{1+r} + \frac{1}{(1+r)^2}\right)$$

(see, e.g., proof of Lemma 5.4 of [78]),

$$\frac{1}{r} - 1 - \frac{1}{2}\left(1 - r^2\right) - \frac{3}{8}\left(1 - r^2\right)^2 = \frac{\left(1 - r^2\right)^2}{2}\left(\frac{1}{r\,(1+r)} + \frac{1}{r\,(1+r)^2} - \frac{3}{4}\right).$$

This gives

$$\frac{1}{r} - 1 - \frac{1}{2}\left(1 - r^2\right) - \frac{3}{8}\left(1 - r^2\right)^2 = \frac{\left(1 - r^2\right)^3}{8\,r}\left(\frac{6 + 3\,r}{(1+r)^2} + \frac{2}{(1+r)^3}\right).$$

Applying elementary calculus, we get $(6 + 3\,r)/(1+r)^2 + 2/(1+r)^3 \leq 8$. Hence, taking $r = \|z\|$ yields

$$\left|\frac{1}{\|z\|} - 1 - \frac{1}{2}\left(1 - \|z\|^2\right) - \frac{3}{8}\left(1 - \|z\|^2\right)^2\right| \|z\| \leq \frac{\left|1 - \|z\|^2\right|^3}{\|z\|}\,\|z\|,$$

and the lemma follows. □

Next, we study the short-time asymptotic behavior of $\|Y_{n+1}\|$.

Notation 1. *By $\mathfrak{G}_0$ we mean the σ-algebra generated by $\hat{Y}_0$. For a given discretization $(\tau_n)_{n=0,\dots,N}$ of $[0,T]$, $\mathfrak{G}_n$ stands for the σ-algebra generated by $\hat{Y}_0$, $W^k_{\tau_j}$, ξ^k_j, where $k=1,\dots,m$ and $j=1,\dots,n$. Let $\mathbb{E}(\cdot \mid \mathfrak{G}_n)$ denote the conditional expectation given $\mathfrak{G}_n$. We write $(\mathcal{O}_n)_{n=1,\dots,N}$ for different collections of N random variables such that $\mathcal{O}_n$ is $\mathfrak{G}_n$-measurable, and*

$$\mathbb{E}\left(\|\mathcal{O}_{n+1}\|^p \mid \mathfrak{G}_n\right) \leq K_p(T) \qquad \forall n=0,\dots,N-1,$$

for any $p\in\mathbb{N}$, where $K_p(\cdot)>0$ is a nonnegative increasing function that does not depends on the partition $(\tau_k)_{k=0,\dots,N}$ and $N\in\mathbb{N}$. In addition to T, $K_p(T)>0$ could depend on m, d, some moments of the ξ^k_1's, and the supremum on $[0,T]$ of $\|G(t)\|$ and $\|L_k(s)\|$.

Lemma 2.5.2. *Assume that $H, L_k : [0,T]\to\mathbb{C}^{d\times d}$ are continuous. Consider $(\hat{Y}_n)_{n=1\dots,N}$ defined by Scheme 1, and set $G_n = G(\tau_n)$, $g_n = g(\tau_n,\hat{Y}_n)$, and $\sigma_{k,n} = \sigma_k(\tau_n,\hat{Y}_n)$. Then,*

$$\begin{aligned}
\|Y_{n+1}\|^2 - 1 = {}& \Delta_n\left(\sum_{k=1}^m \|\sigma_{k,n}\|^2\left(\left(\xi^k_{n+1}\right)^2-1\right)+\sum_{j\neq k}\langle\sigma_{j,n},\sigma_{k,n}\rangle\xi^j_{n+1}\xi^k_{n+1}\right)\\
&+2\Delta_n^{3/2}\sum_{k=1}^m\left(\mathrm{Re}\langle\hat{Y}_n,(G_n+G_n^*)\,\sigma_{k,n}\rangle+\mathrm{Re}\langle g_n,\sigma_{k,n}\rangle\right)\xi^k_{n+1}\\
&+\Delta_n^2\left(\left\|G_n\hat{Y}_n\right\|^2+2\,\mathrm{Re}\langle\hat{Y}_n,(G_n+G_n^*)\,g_n\rangle+\mathrm{Re}\langle G_n^2\hat{Y}_n,\hat{Y}_n\rangle+\|g_n\|^2\right)\\
&+\Delta_n^2\left(\sum_{k=1}^m 2\mathrm{Re}\langle G_n\sigma_{k,n},\sigma_{k,n}\rangle\left(\xi^k_{n+1}\right)^2+\sum_{j\neq k}\langle\sigma_{j,n},(G_n+G_n^*)\,\sigma_{k,n}\rangle\xi^j_{n+1}\xi^k_{n+1}\right)\\
&+2\Delta_n^{5/2}\sum_{k=1}^m\left(\mathrm{Re}\langle G_n\hat{Y}_n,G_n\sigma_{k,n}\rangle+\ \mathrm{Re}\langle g_n,(G_n+G_n^*)\,\sigma_{k,n}\rangle\right)\xi^k_{n+1}\\
&+\Delta_n^{5/2}\sum_{k=1}^m\mathrm{Re}\langle\left(G_n^2+(G_n^*)^2\right)\hat{Y}_n,\sigma_{k,n}\rangle\xi^k_{n+1}+\mathcal{O}_{n+1}\Delta_n^3,
\end{aligned}$$

where the sum over $j\neq k$ means the sum over all $j,k=1,\dots,m$ with $j\neq k$.

Proof. Since

$$Y_{n+1}=\left(I+G_n\Delta_n+\frac{1}{2}G_n^2\Delta_n^2+O\left(\Delta_n^3\right)\right)\left(\hat{Y}_n+g_n\Delta_n+\sqrt{\Delta_n}\sum_{k=1}^m\sigma_{k,n}\xi^k_{n+1}\right),$$

$$
\begin{aligned}
&\|Y_{n+1}\|^2 \\
&= \left\|(I+G_n\Delta_n)\,\hat{Y}_n\right\|^2 + 2\Delta_n\,\mathrm{Re}\langle(I+G_n\Delta_n)\,\hat{Y}_n,(I+G_n\Delta_n)\,g_n\rangle + \Delta_n^2\,\mathrm{Re}\langle\hat{Y}_n,G_n^2\hat{Y}_n\rangle \\
&\quad + \sum_{k=1}^{m} 2\sqrt{\Delta_n}\,\mathrm{Re}\langle(I+G_n\Delta_n)\,\hat{Y}_n,(I+G_n\Delta_n)\,\sigma_{k,n}\rangle\xi_{n+1}^k + \Delta_n^{5/2}\sum_{k=1}^{m}\mathrm{Re}\langle\hat{Y}_n,G_n^2\sigma_{k,n}\rangle\xi_{n+1}^k \\
&\quad + \Delta_n^2\,\|(I+G_n\Delta_n)\,g_n\|^2 + \sum_{k=1}^{m} 2\Delta_n^{3/2}\,\mathrm{Re}\langle(I+G_n\Delta_n)\,g_n,(I+G_n\Delta_n)\,\sigma_{k,n}\rangle\xi_{n+1}^k \\
&\quad + \Delta_n\left\|\sum_{k=1}^{m}(I+G_n\Delta_n)\,\sigma_{k,n}\,\xi_{n+1}^k\right\|^2 + \Delta_n^{5/2}\sum_{k=1}^{m}\mathrm{Re}\langle G_n^2\hat{Y}_n,\sigma_{k,n}\rangle\xi_{n+1}^k + \mathcal{O}_{n+1}\Delta_n^3.
\end{aligned}
$$

More precisely, here the random variable $\mathcal{O}_{n+1}$ is equal to

$$
\begin{aligned}
&\mathrm{Re}\langle\hat{Y}_n,G_n^2g_n\rangle + \sum_{k=1}^{m}\mathrm{Re}\langle\sigma_{k,n},G_n^2\sigma_{k,n}\rangle(\xi_{n+1}^k)^2 + 2\mathrm{Re}\langle g_n+G_n\hat{Y}_n,\frac{1}{2}G_n^2\hat{Y}_n+G_ng_n\rangle \\
&+ 2\sum_{k=1}^{m}\|G_n\sigma_{k,n}\|^2(\xi_{n+1}^k)^2 + \Delta_n^{1/2}\sum_{k=1}^{m}\mathrm{Re}\langle\sigma_{k,n},G_n^2g_n\rangle\xi_{n+1}^k \\
&+ \Delta_n^{1/2}\left(\sum_{k=1}^{m}\mathrm{Re}\langle g_n+G_n\hat{Y}_n,G_n^2\sigma_{k,n}\rangle\xi_{n+1}^k + \sum_{k=1}^{m}2\mathrm{Re}\langle G_n\sigma_{k,n},\frac{1}{2}G_n^2\hat{Y}_n+G_ng_n\rangle\xi_{n+1}^k\right) \\
&+ \Delta_n\left(\mathrm{Re}\langle g_n+G_n\hat{Y}_n,G_n^2g_n\rangle + \sum_{k=1}^{m}\mathrm{Re}\langle G_n\sigma_{k,n},G_n^2\sigma_{k,n}\rangle(\xi_{n+1}^k)^2 + 2\left\|\frac{1}{2}G_n^2\hat{Y}_n+G_ng_n\right\|^2\right) \\
&+ \Delta_n^{3/2}\left(\sum_{k=1}^{m}\mathrm{Re}\langle G_n\sigma_{k,n},G_n^2g_n\rangle\xi_{n+1}^k + \sum_{k=1}^{m}\mathrm{Re}\langle\frac{1}{2}G_n^2\hat{Y}_n+G_ng_n,G_n^2\sigma_{k,n}\rangle\xi_{n+1}^k\right) \\
&+ \Delta_n^2\left(\mathrm{Re}\langle\frac{1}{2}G_n^2\hat{Y}_n+G_ng_n,G_n^2g_n\rangle + \frac{1}{2}\sum_{k=1}^{m}||G_n\sigma_{k,n}||^2\,(\xi_{n+1}^k)^2\right) \\
&+ \Delta_n^{5/2}\sum_{k=1}^{m}\mathrm{Re}\langle G_n\sigma_{k,n},G_n^2g_n\rangle\xi_{n+1}^k \\
&+ \Delta_n^3\left(\frac{1}{2}\left||G_n^2g_n\right|\right|^2 + \left\|G_n^3\left(\sum_{k=0}^{\infty}\frac{\Delta_n^kG_n^k}{(k+3)!}\right)\left(\hat{Y}_n+g_n\Delta_n+\sqrt{\Delta_n}\sum_{k=1}^{m}\sigma_{k,n}\xi_{n+1}^k\right)\right\|^2\right).
\end{aligned}
$$

Using $\mathrm{Re}\langle \hat{Y}_n, \sigma_{k,n}\rangle = 0$ and $2\,\mathrm{Re}\langle \hat{Y}_n, G_n\hat{Y}_n + g_n\rangle + \sum_{k=1}^m \|\sigma_{k,n}\|^2 = 0$ we obtain

$$\begin{aligned}
\|Y_{n+1}\|^2 = {} & \left\|\hat{Y}_n\right\|^2 + \Delta_n^2 \left\|G_n\hat{Y}_n\right\|^2 + 2\Delta_n^2\,\mathrm{Re}\langle \hat{Y}_n, (G_n + G_n^*)\, g_n\rangle \\
& + 2\sum_{k=1}^m \left(\Delta_n^{3/2}\mathrm{Re}\langle \hat{Y}_n, (G_n + G_n^*)\,\sigma_{k,n}\rangle + \Delta_n^{5/2}\mathrm{Re}\langle G_n\hat{Y}_n, G_n\sigma_{k,n}\rangle\right)\xi_{n+1}^k \\
& + \Delta_n^2\left(\mathrm{Re}\langle G_n^2\hat{Y}_n, \hat{Y}_n\rangle + \|g_n\|^2\right) + \Delta_n^{5/2}\sum_{k=1}^m \mathrm{Re}\langle \left(G_n^2 + (G_n^*)^2\right)\hat{Y}_n, \sigma_{k,n}\rangle\xi_{n+1}^k \\
& + 2\sum_{k=1}^m \left(\Delta_n^{3/2}\,\mathrm{Re}\langle g_n, \sigma_{k,n}\rangle + \Delta_n^{5/2}\,\mathrm{Re}\langle g_n, (G_n + G_n^*)\,\sigma_{k,n}\rangle\right)\xi_{n+1}^k \\
& + \Delta_n\sum_{k=1}^m \|\sigma_{k,n}\|^2\left(\left(\xi_{n+1}^k\right)^2 - 1\right) + 2\Delta_n^2\sum_{k=1}^m \mathrm{Re}\langle G_n\sigma_{k,n}, \sigma_{k,n}\rangle\left(\xi_{n+1}^k\right)^2 \\
& + \sum_{j\neq k}\left(\Delta_n\langle \sigma_{j,n}, \sigma_{k,n}\rangle + \Delta_n^2\langle \sigma_{j,n}, (G_n + G_n^*)\,\sigma_{k,n}\rangle\right)\xi_{n+1}^j\xi_{n+1}^k + \mathcal{O}_{n+1}\Delta_n^3.
\end{aligned}$$

As $\|\hat{Y}_n\| = 1$, collecting terms we get the lemma. □

Using Lemmata 2.5.1 and 2.5.2, together with careful algebraic manipulations, we establish the short-time asymptotic behavior of $\hat{Y}_{n+1}$.

Lemma 2.5.3. *Let $\left(\hat{Y}_n\right)_{n=1\ldots,N}$ be given by Scheme 1. Suppose that $H, L_k : [0,T] \to \mathbb{C}^{d\times d}$ are continuous, and choose $G_n = G(\tau_n)$, $g_n = g(\tau_n, \hat{Y}_n)$, and $\sigma_{k,n} = \sigma_k(\tau_n, \hat{Y}_n)$. Then,*

$$\hat{Y}_{n+1} = \hat{Y}_n + \left(G_n\hat{Y}_n + g_n\right)\Delta_n + \sqrt{\Delta_n}\sum_{k=1}^m \sigma_{k,n}\xi_{n+1}^k + \sum_{j=1}^4 \Delta_n^{(j+1)/2}\Gamma_{j,n+1} + \mathcal{O}_{n+1}\Delta_n^3, \quad (2.12)$$

where $(\Gamma_{4,n})_{n=1,\ldots;N}$ is of the type $(\mathcal{O}_n)_{n=1,\ldots,N}$ with $\mathbb{E}\left(\Gamma_{4,n+1} \mid \mathfrak{G}_n\right) = 0$,

$$\Gamma_{1,n+1} = \frac{1}{2}e^{G_n\Delta_n}\hat{Y}_n\left(\sum_{k=1}^m \|\sigma_{k,n}\|^2\left(1 - \left(\xi_{n+1}^k\right)^2\right) - \sum_{j\neq k}\langle \sigma_{j,n}, \sigma_{k,n}\rangle\xi_{n+1}^j\xi_{n+1}^k\right),$$

$$\begin{aligned}\Gamma_{2,n+1} = &\sum_{k=1}^{m} G_n\sigma_{k,n}\,\xi_{n+1}^k - \frac{1}{2}e^{G_n\Delta_n}\sum_{\ell,k=1}^{m}\sigma_{\ell,n}\,\|\sigma_{k,n}\|^2\left(\left(\xi_{n+1}^k\right)^2-1\right)\xi_{n+1}^\ell\\ &- e^{G_n\Delta_n}\hat{Y}_n\sum_{k=1}^{m}\left(\mathrm{Re}\langle\hat{Y}_n,(G_n+G_n^*)\,\sigma_{k,n}\rangle+\mathrm{Re}\langle g_n,\sigma_{k,n}\rangle\right)\xi_{n+1}^k\\ &- \frac{1}{2}e^{G_n\Delta_n}\sum_{\ell=1}^{m}\sum_{j\neq k}\sigma_{\ell,n}\langle\sigma_{j,n},\sigma_{k,n}\rangle\xi_{n+1}^j\xi_{n+1}^k\xi_{n+1}^\ell,\end{aligned}$$

and

$$\begin{aligned}\Gamma_{3,n+1} = &\,G_n\,g_n+\frac{1}{2}G_n^2\hat{Y}_n - e^{G_n\Delta_n}\hat{Y}_n\sum_{k=1}^{m}\mathrm{Re}\langle G_n\sigma_{k,n},\sigma_{k,n}\rangle\left(\xi_{n+1}^k\right)^2\\ &+\frac{3}{8}\hat{Y}_n\left(\sum_{k=1}^{m}\|\sigma_{k,n}\|^2\left(\left(\xi_{n+1}^k\right)^2-1\right)+\sum_{j\neq k}\langle\sigma_{j,n},\sigma_{k,n}\rangle\xi_{n+1}^j\xi_{n+1}^k\right)^2\\ &-\frac{1}{2}e^{G_n\Delta_n}\hat{Y}_n\left(\left\|G_n\hat{Y}_n\right\|^2+2\,\mathrm{Re}\langle\hat{Y}_n,(G_n+G_n^*)\,g_n\rangle+\mathrm{Re}\langle G_n^2\hat{Y}_n,\hat{Y}_n\rangle\right)\\ &-\frac{1}{2}e^{G_n\Delta_n}\hat{Y}_n\left(\sum_{j\neq k}\left(\langle\sigma_{j,n},(G_n+G_n^*)\,\sigma_{k,n}\rangle\right)\xi_{n+1}^j\xi_{n+1}^k+\|g_n\|^2\right)\\ &-\frac{1}{2}e^{G_n\Delta_n}g_n\left(\sum_{k=1}^{m}\|\sigma_{k,n}\|^2\left(\left(\xi_{n+1}^k\right)^2-1\right)+\sum_{j\neq k}\langle\sigma_{j,n},\sigma_{k,n}\rangle\xi_{n+1}^j\xi_{n+1}^k\right)\\ &-e^{G_n\Delta_n}\sum_{k,\ell=1}^{m}\left(\mathrm{Re}\langle\hat{Y}_n,(G_n+G_n^*)\,\sigma_{k,n}\rangle+\mathrm{Re}\langle g_n,\sigma_{k,n}\rangle\right)\sigma_{\ell,n}\xi_{n+1}^k\xi_{n+1}^\ell.\end{aligned}$$

Proof. Using

$$Y_{n+1} = \left(I+G_n\Delta_n+\frac{1}{2}G_n^2\Delta_n^2+O\left(\Delta_n^3\right)\right)\left(\hat{Y}_n+g_n\Delta_n+\sqrt{\Delta_n}\sum_{k=1}^{m}\sigma_{k,n}\xi_{n+1}^k\right),$$

gives

$$\begin{aligned}Y_{n+1} = &\,\hat{Y}_n+\Delta_n\left(G_n\hat{Y}_n+g_n\right)+\sqrt{\Delta_n}\sum_{k=1}^{m}\sigma_{k,n}\xi_{n+1}^k+\Delta_n^{3/2}\sum_{k=1}^{m}G_n\sigma_{k,n}\xi_{n+1}^k\\ &+\Delta_n^2\left(G_ng_n+\frac{1}{2}G_n^2\hat{Y}_n\right)+\frac{1}{2}\Delta_n^{5/2}\sum_{k=1}^{m}G_n^2\sigma_{k,n}\xi_{n+1}^k+\mathcal{O}_{n+1}\Delta_n^3.\end{aligned}$$

Applying Lemma 2.5.2 we obtain

$$\begin{aligned}
&\left(\|Y_{n+1}\|^2-1\right)^2\\
&=\mathcal{O}_{n+1}\Delta_n^3+\Delta_n^2\left(\sum_{k=1}^m\|\sigma_{k,n}\|^2\left(\left(\xi_{n+1}^k\right)^2-1\right)+\sum_{j\neq k}\langle\sigma_{j,n},\sigma_{k,n}\rangle\xi_{n+1}^j\xi_{n+1}^k\right)^2\\
&\quad+4\Delta_n^{5/2}\sum_{k,\ell=1}^m\|\sigma_{k,n}\|^2\left(\mathrm{Re}\langle\hat{Y}_n,\left(G_n+G_n^*\right)\sigma_{\ell,n}\rangle+\mathrm{Re}\langle g_n,\sigma_{\ell,n}\rangle\right)\left(\left(\xi_{n+1}^k\right)^2-1\right)\xi_{n+1}^\ell\\
&\quad+4\Delta_n^{5/2}\sum_{j\neq k}\sum_{\ell=1}^m\langle\sigma_{j,n},\sigma_{k,n}\rangle\left(\mathrm{Re}\langle\hat{Y}_n,\left(G_n+G_n^*\right)\sigma_{\ell,n}\rangle+\mathrm{Re}\langle g_n,\sigma_{\ell,n}\rangle\right)\xi_{n+1}^j\xi_{n+1}^k\xi_{n+1}^\ell.
\end{aligned}$$

Since

$$Y_{n+1}=\left(I+O\left(\Delta_n\right)\right)\left(\hat{Y}_n+g_n\Delta_n+\sqrt{\Delta_n}\sum_{k=1}^m\sigma_{k,n}\xi_{n+1}^k\right),$$

$$\begin{aligned}
&Y_{n+1}\left(1-\|Y_{n+1}\|^2\right)^2\\
&=\mathcal{O}_{n+1}\Delta_n^3+\hat{Y}_n\Delta_n^2\left(\sum_{k=1}^m\|\sigma_{k,n}\|^2\left(\left(\xi_{n+1}^k\right)^2-1\right)+\sum_{j\neq k}\langle\sigma_{j,n},\sigma_{k,n}\rangle\xi_{n+1}^j\xi_{n+1}^k\right)^2\\
&\quad+4\hat{Y}_n\Delta_n^{5/2}\sum_{k,\ell=1}^m\|\sigma_{k,n}\|^2\left(\mathrm{Re}\langle\hat{Y}_n,\left(G_n+G_n^*\right)\sigma_{\ell,n}\rangle+\mathrm{Re}\langle g_n,\sigma_{\ell,n}\rangle\right)\left(\left(\xi_{n+1}^k\right)^2-1\right)\xi_{n+1}^\ell\\
&\quad+4\hat{Y}_n\Delta_n^{5/2}\sum_{j\neq k}\sum_{\ell=1}^m\langle\sigma_{j,n},\sigma_{k,n}\rangle\left(\mathrm{Re}\langle\hat{Y}_n,\left(G_n+G_n^*\right)\sigma_{\ell,n}\rangle+\mathrm{Re}\langle g_n,\sigma_{\ell,n}\rangle\right)\xi_{n+1}^j\xi_{n+1}^k\xi_{n+1}^\ell.
\end{aligned}$$

Using Lemma 2.5.2, together with

$$Y_{n+1}=e^{G_n\Delta_n}\left(\hat{Y}_n+g_n\Delta_n+\sqrt{\Delta_n}\sum_{k=1}^m\sigma_{k,n}\xi_{n+1}^k\right),$$

we get

$$
\begin{aligned}
&\left(\|Y_{n+1}\|^2-1\right)Y_{n+1}\\
&=\Delta_n e^{G_n\Delta_n}\hat{Y}_n\left(\sum_{k=1}^m\|\sigma_{k,n}\|^2\left(\left(\xi_{n+1}^k\right)^2-1\right)+\sum_{j\neq k}\langle\sigma_{j,n},\sigma_{k,n}\rangle\xi_{n+1}^j\xi_{n+1}^k\right)\\
&\quad+2\Delta_n^{3/2}e^{G_n\Delta_n}\hat{Y}_n\sum_{k=1}^m\left(\mathrm{Re}\langle\hat{Y}_n,\left(G_n+G_n^*\right)\sigma_{k,n}\rangle+\mathrm{Re}\langle g_n,\sigma_{k,n}\rangle\right)\xi_{n+1}^k\\
&\quad+\Delta_n^{3/2}e^{G_n\Delta_n}\sum_{k,\ell=1}^m\sigma_{\ell,n}\|\sigma_{k,n}\|^2\left(\left(\xi_{n+1}^k\right)^2-1\right)\xi_{n+1}^\ell\\
&\quad+\Delta_n^{3/2}e^{G_n\Delta_n}\sum_{\ell=1}^m\sum_{j\neq k}\sigma_{\ell,n}\langle\sigma_{j,n},\sigma_{k,n}\rangle\xi_{n+1}^j\xi_{n+1}^k\xi_{n+1}^\ell\\
&\quad+\Delta_n^2e^{G_n\Delta_n}\hat{Y}_n\left(\left\|G_n\hat{Y}_n\right\|^2+2\,\mathrm{Re}\langle\hat{Y}_n,\left(G_n+G_n^*\right)g_n\rangle+\mathrm{Re}\langle G_n^2\hat{Y}_n,\hat{Y}_n\rangle+\|g_n\|^2\right)\\
&\quad+\Delta_n^2e^{G_n\Delta_n}\hat{Y}_n\left(2\sum_{k=1}^m\mathrm{Re}\langle G_n\sigma_{k,n},\sigma_{k,n}\rangle\left(\xi_{n+1}^k\right)^2+\sum_{j\neq k}\left(\langle\sigma_{j,n},\left(G_n+G_n^*\right)\sigma_{k,n}\rangle\right)\xi_{n+1}^j\xi_{n+1}^k\right)\\
&\quad+\Delta_n^2e^{G_n\Delta_n}g_n\left(\sum_{k=1}^m\|\sigma_{k,n}\|^2\left(\left(\xi_{n+1}^k\right)^2-1\right)+\sum_{j\neq k}\langle\sigma_{j,n},\sigma_{k,n}\rangle\xi_{n+1}^j\xi_{n+1}^k\right)\\
&\quad+2\Delta_n^2e^{G_n\Delta_n}\sum_{k,\ell=1}^m\left(\mathrm{Re}\langle\hat{Y}_n,\left(G_n+G_n^*\right)\sigma_{k,n}\rangle+\mathrm{Re}\langle g_n,\sigma_{k,n}\rangle\right)\sigma_{\ell,n}\xi_{n+1}^k\xi_{n+1}^\ell\\
&\quad+2\Delta_n^{5/2}e^{G_n\Delta_n}\hat{Y}_n\sum_{k=1}^m\left(\mathrm{Re}\langle G_n\hat{Y}_n,G\sigma_{k,n}\rangle+\ \mathrm{Re}\langle g_n,\left(G_n+G_n^*\right)\sigma_{k,n}\rangle\right)\xi_{n+1}^k\\
&\quad+2\Delta_n^{5/2}e^{G_n\Delta_n}g_n\sum_{k=1}^m\left(\mathrm{Re}\langle\hat{Y}_n,\left(G_n+G_n^*\right)\sigma_{k,n}\rangle+\mathrm{Re}\langle g_n,\sigma_{k,n}\rangle\right)\xi_{n+1}^k\\
&\quad+\Delta_n^{5/2}e^{G_n\Delta_n}\sum_{\ell=1}^m\left(\left\|G_n\hat{Y}_n\right\|^2+2\,\mathrm{Re}\langle\hat{Y}_n,\left(G_n+G_n^*\right)g_n\rangle+\|g_n\|^2\right)\sigma_{\ell,n}\xi_{n+1}^\ell\\
&\quad+\Delta_n^{5/2}e^{G_n\Delta_n}\sum_{\ell=1}^m\left(\sum_{k=1}^m2\mathrm{Re}\langle G_n\sigma_{k,n},\sigma_{k,n}\rangle\left(\xi_{n+1}^k\right)^2+\mathrm{Re}\langle G_n^2\hat{Y}_n,\hat{Y}_n\rangle\right)\sigma_{\ell,n}\xi_{n+1}^\ell\\
&\quad+\Delta_n^{5/2}e^{G_n\Delta_n}\sum_{\ell=1}^m\sum_{j\neq k}\sigma_{\ell,n}\left(\langle\sigma_{j,n},\left(G_n+G_n^*\right)\sigma_{k,n}\rangle\right)\xi_{n+1}^j\xi_{n+1}^k\xi_{n+1}^\ell\\
&\quad+\Delta_n^{5/2}e^{G_n\Delta_n}\hat{Y}_n\sum_{k=1}^m\mathrm{Re}\langle\left(G_n^2+\left(G_n^*\right)^2\right)\hat{Y}_n,\sigma_{k,n}\rangle\xi_{n+1}^k+\mathcal{O}_{n+1}\Delta_n^3.
\end{aligned}
$$

From Lemma 2.5.2 it follows that $\|Y_{n+1}\|^2 - 1 = \mathcal{O}_{n+1}\Delta_n$, and hence $\left(\|Y_{n+1}\|^2 - 1\right)^3 = \mathcal{O}_{n+1}\Delta_n^3$. According to Lemma 2.3.1 we have that $Y_{n+1} \neq 0$, and so applying Lemma 2.5.1 yields

$$\hat{Y}_{n+1} = Y_{n+1} + \frac{Y_{n+1}}{2}\left(1 - \|Y_{n+1}\|^2\right) + \frac{3}{8}Y_{n+1}\left(1 - \|Y_{n+1}\|^2\right)^2 + \mathcal{O}_{n+1}\Delta_n^3. \tag{2.13}$$

In (2.13) we collect the terms with coefficients $\Delta_n^{(j+1)/2}$ in the asymptotic development of Y_{n+1}, $Y_{n+1}\left(1 - \|Y_{n+1}\|^2\right)/2$ and $3\,Y_{n+1}\left(1 - \|Y_{n+1}\|^2\right)^2/8$, where $j = 1, \ldots, 4$. This yields (2.12) with

$$\begin{aligned}
\Gamma_{4,n+1} = {} & \frac{1}{2}\sum_{k=1}^{m} G_n^2\sigma_{k,n}\xi_{n+1}^k - e^{G_n\Delta_n}\hat{Y}_n\sum_{k=1}^{m}\left(\mathrm{Re}\langle G_n\hat{Y}_n, G\sigma_{k,n}\rangle + \mathrm{Re}\langle g_n, (G_n + G_n^*)\,\sigma_{k,n}\rangle\right)\xi_{n+1}^k \\
& - e^{G_n\Delta_n} g_n\sum_{k=1}^{m}\left(\mathrm{Re}\langle\hat{Y}_n, (G_n + G_n^*)\,\sigma_{k,n}\rangle + \mathrm{Re}\langle g_n, \sigma_{k,n}\rangle\right)\xi_{n+1}^k \\
& - \frac{1}{2}e^{G_n\Delta_n}\sum_{\ell=1}^{m}\left(\left\|G_n\hat{Y}_n\right\|^2 + 2\,\mathrm{Re}\langle\hat{Y}_n, (G_n + G_n^*)\,g_n\rangle + \|g_n\|^2\right)\sigma_{\ell,n}\xi_{n+1}^\ell \\
& - \frac{1}{2}e^{G_n\Delta_n}\sum_{\ell=1}^{m}\left(\sum_{k=1}^{m} 2\mathrm{Re}\langle G_n\sigma_{k,n}, \sigma_{k,n}\rangle\left(\xi_{n+1}^k\right)^2 + \mathrm{Re}\langle G_n^2\hat{Y}_n, \hat{Y}_n\rangle\right)\sigma_{\ell,n}\xi_{n+1}^\ell \\
& - \frac{1}{2}e^{G_n\Delta_n}\sum_{\ell=1}^{m}\sum_{j\neq k}\sigma_{\ell,n}\left(\langle\sigma_{j,n}, (G_n + G_n^*)\,\sigma_{k,n}\rangle\right)\xi_{n+1}^j\xi_{n+1}^k\xi_{n+1}^\ell \\
& - \frac{1}{2}e^{G_n\Delta_n}\hat{Y}_n\sum_{k=1}^{m}\mathrm{Re}\langle\left(G_n^2 + (G_n^*)^2\right)\hat{Y}_n, \sigma_{k,n}\rangle\xi_{n+1}^k \\
& + \frac{3}{2}\hat{Y}_n\sum_{k,\ell=1}^{m}\|\sigma_{k,n}\|^2\left(\mathrm{Re}\langle\hat{Y}_n, (G_n + G_n^*)\,\sigma_{\ell,n}\rangle + \mathrm{Re}\langle g_n, \sigma_{\ell,n}\rangle\right)\left(\left(\xi_{n+1}^k\right)^2 - 1\right)\xi_{n+1}^\ell \\
& + \frac{3}{2}\hat{Y}_n\sum_{j\neq k}\sum_{\ell=1}^{m}\langle\sigma_{j,n}, \sigma_{k,n}\rangle\left(\mathrm{Re}\langle\hat{Y}_n, (G_n + G_n^*)\,\sigma_{\ell,n}\rangle + \mathrm{Re}\langle g_n, \sigma_{\ell,n}\rangle\right)\xi_{n+1}^j\xi_{n+1}^k\xi_{n+1}^\ell.
\end{aligned}$$

Since the distribution of the ξ_n^k's is symmetric about 0, $\mathbb{E}\left(\Gamma_{4,n+1} \mid \mathfrak{G}_n\right) = 0$. □

2.5.3.2 Localization procedure

We will associate (2.1) with a globally Lipschitz SDE whose coefficients coincide with the drift and diffusion coefficients of (2.1) in the (closed) unit ball. According to the smooth

Urysohn lemma we have that there exists a function $\widetilde{\rho} \in C^{\infty}(\mathbb{R}, [0,1])$ such that $\widetilde{\rho}(r) = 1$ for all $r \in [0,1]$, and $\widetilde{\rho}(r) = 0$ whenever $|r| \geq \sqrt{2}$. Then, we set

$$\rho(z) = \widetilde{\rho}\left(\|z\|^2\right) \qquad \forall z \in \mathbb{C}^d.$$

As a smooth cutoff function $\widetilde{\rho}$ we can take, for instance, $\widetilde{\rho} = \chi_{[-b,b]} * \varrho_{\epsilon}$, where $\chi_{[-b,b]}$ is the characteristic function of the ball centered at 0 with radius $1 < b < \sqrt{2}$, and $\varrho_{\epsilon}(r) = \eta(r/\epsilon)/\epsilon$ with $0 < \epsilon < \min\{b-1, \sqrt{2}-b\}$ and

$$\eta(r) = \begin{cases} C \exp\left(\frac{1}{|r|^2-1}\right) & \text{if} \quad |r| \leq 1 \\ 0 & \text{if} \quad |r| > 1 \end{cases}.$$

Here, C is the normalizing constant of the the standard mollifier η.

Since $z \mapsto \|z\|^2$ belongs to $\mathcal{WC}^{\infty}(\mathbb{C}^d, \mathbb{C})$, $\rho \in \mathcal{WC}^{\infty}(\mathbb{C}^d, \mathbb{C})$. In this section, we consider the globally Lipschitz SDE

$$Z_t^{s,\zeta} = \zeta + \int_s^t a\left(r, Z_r^{s,\zeta}\right) dr + \sum_{k=1}^{m} \int_s^t b_k\left(r, Z_r^{s,\zeta}\right) dW_r^k \qquad \forall t \in [s,T], \tag{2.14}$$

with ζ being $\mathfrak{F}_s$-measurable,

$$a(t,z) = (G(t)\, z + g(t,z))\, \rho(z), \qquad \text{and } b_k(t,z) = \sigma_k(t,z)\, \rho(z), \tag{2.15}$$

where g, G, σ_k are as in (2.1) and Theorem 2.3.1. The solution of (2.14), with $\|X_0\| = 1$, satisfies $\|X_t\| = 1$ for all $t \in [0,T]$.Therefore, using the uniqueness of the solution to (2.14) we deduce that $Z_t^{s,X_s} = X_t$ for all $t \in [s,T]$, because $\rho(z) = 1$ for any $\|z\| \leq 1$.

Applying classical results on the real-valued Kolmogorov equations (see, e.g., [57, 73, 90, 92]) we study the complex-valued Kolmogorov equation associated to (2.14).

Proposition 2.5.1. *Suppose that $H, L_k : [0,T] \to \mathbb{C}^{d\times d}$ are continuous functions. Let the functions φ_θ, with $\theta \in \Theta$, belong uniformly to $\mathcal{WC}_P^{2+L}(\mathbb{C}^d, \mathbb{C})$, where $L \in \mathbb{Z}_+$. Take*

$$u_\theta(s,z) = \mathbb{E}\left(\varphi_\theta\left(Z_T^{s,z}\right)\right) \qquad \forall s \in [0,T],$$

where $Z_T^{s,z}$ *is given by* (2.14)*. Then,* $u_\theta \in \mathcal{WC}_P^{1,2+L}\left([0,T]\times\mathbb{C}^d,\mathbb{C}\right)$*,*

$$\left|\partial^\alpha u_\theta(t,z)\right| \le K_\alpha(T)\left(1+\|z\|^{q_\alpha}\right) \qquad \forall z\in\mathbb{C}^d \text{ and } \forall t\in[0,T] \tag{2.16}$$

for any $\theta\in\Theta$ *and* $|\alpha|\le 2+L$*, and*

$$\begin{cases} \partial_s u_\theta(s,z) = -\mathcal{L}\,u_\theta(s,z) & if\, s\in[0,T] \text{ and } z\in\mathbb{C}^d \\ u_\theta(T,z) = \varphi_\theta(z) & if\, z\in\mathbb{C}^d \end{cases},$$

where

$$\mathcal{L} = \sum_{\alpha\in\mathcal{P}_1} a^\alpha \partial^\alpha + \frac{1}{2}\sum_{\ell=1}^m \sum_{\alpha\in\mathcal{P}_2} b_\ell^\alpha \partial^\alpha.$$

Moreover, for all $\alpha\in\mathcal{P}_k$ *with* $k\le L$ *we have that* $\partial_t\partial_z^\alpha u_\theta$ *is a continuous function, and*

$$\partial_t\partial_z^\alpha u_\theta = -\partial_z^\alpha \mathcal{L}(u_\theta).$$

Proof. Throughout the proof, for every $z\in\mathbb{C}^d$ we define $\vec{z}$ to be $(\mathrm{Re}(z),\mathrm{Im}(z))^\top\in\mathbb{R}^{2d}$. Then, the SDE (2.14) is equivalent to

$$\overrightarrow{Z_t^{s,\zeta}} = \vec{\zeta} + \int_s^t \vec{a}\left(r,\overrightarrow{Z_r^{s,\zeta}}\right)dr + \sum_{\ell=1}^m \int_s^t \vec{b}_\ell\left(r,\overrightarrow{Z_r^{s,\zeta}}\right)dW_r^\ell \qquad \forall t\in[s,T],$$

where $\vec{a}(r,\vec{z}) = \overrightarrow{a(r,z)}$ and $\vec{b}_\ell(r,\vec{z}) = \overrightarrow{b_\ell(r,z)}$. Since

$$u_\theta(s,z) = \mathbb{E}\left(\mathrm{Re}\left(\varphi_\theta\right)\left(Z_T^{s,z}\right)\right) + i\,\mathbb{E}\left(\mathrm{Im}\left(\varphi_\theta\right)\left(Z_T^{s,z}\right)\right),$$

we consider

$$u_\theta(s,z) = u_\theta^R(s,\vec{z}) + \mathrm{i}\,u_\theta^I(s,\vec{z}), \tag{2.17}$$

where $u_\theta^R(s,\vec{z}) = \mathbb{E}(\mathrm{Re}(\varphi_\theta)(\overrightarrow{Z_T^{s,z}}))$, and $u_\theta^I(s,\vec{z}) = \mathbb{E}(\mathrm{Im}(\varphi_\theta)(\overrightarrow{Z_T^{s,z}}))$. Here, by abuse of notation, $f(\vec{z}) = f(z)$.

Let $f\in\mathcal{WC}^2\left(\mathbb{C}^d,\mathbb{C}\right)$. Replacing $\partial^\alpha f(z)$ by the right-hand side of (2.3) yields

$$\sum_{\alpha\in\mathcal{P}_1} a^\alpha(t,z)\,\partial^\alpha f(z) = \sum_{k=1}^d \mathrm{Re}\left(a^k(t,z)\right)\frac{\partial}{\partial x_k} f(x+\mathrm{i}\,y) + \sum_{k=1}^d \mathrm{Im}\left(a^k(t,z)\right)\frac{\partial}{\partial y_k} f(x+\mathrm{i}\,y)$$

for all $z = x + i\,y$. Similarly, using (2.10) we obtain

$$\begin{aligned}\sum_{\alpha\in\mathcal{P}_2} b_\ell^\alpha(t,z)\,\partial^\alpha f(z) = &\sum_{j,k=1}^{d} \mathrm{Re}\left(b_\ell^j(t,z)\right)\mathrm{Re}\left(b_\ell^k(t,z)\right)\frac{\partial^2}{\partial x_j\,x_k}f(x+\mathrm{i}\,y)\\ &+\sum_{j,k=1}^{d} \mathrm{Im}\left(b_\ell^j(t,z)\right)\mathrm{Im}\left(b_\ell^k(t,z)\right)\frac{\partial^2}{\partial y_j\,y_k}f(x+\mathrm{i}\,y)\\ &+2\sum_{j,k=1}^{d} \mathrm{Re}\left(b_\ell^j(t,z)\right)\mathrm{Im}\left(b_\ell^k(t,z)\right)\frac{\partial^2}{\partial x_j\,y_k}f(x+\mathrm{i}\,y)\,.\end{aligned}$$

Hence,

$$\mathcal{L}f(z) = \widetilde{\mathcal{L}}f(\vec{z})\,, \tag{2.18}$$

where

$$\widetilde{\mathcal{L}}f(\vec{z}) = \vec{a}(r,\vec{z})\cdot\nabla_{\vec{z}}f(\vec{z}) + \frac{1}{2}\sum_{\ell=1}^{m}\vec{b}_\ell(t,\vec{z})^\top Hf(\vec{z})\,\vec{b}_\ell(t,\vec{z})$$

with $Hf(\vec{z})$ being the Hessian matrix of $f(\vec{z})$.

Since $\vec{a}$, $\vec{b}_\ell$ and all the partial derivatives of $\vec{a}$, $\vec{b}_\ell$ (with respect to the state variables) are continuous functions with compact support, classical results on Kolmogorov's equation (see, e.g., [57, 73, 90, 92]) ensure that: (i) u_θ^R, u_θ^I belong to $\mathcal{C}_P^{1,2+L}\left([0,T]\times\mathbb{R}^{2d},\mathbb{R}\right)$, and for any $\theta\in\Theta$ and $|\alpha|\leq 2+L$ we have

$$\max\left\{\left|\partial_{\vec{z}}^\alpha u_\theta^R(t,\vec{z})\right|,\left|\partial_{\vec{z}}^\alpha u_\theta^I(t,\vec{z})\right|\right\}\leq K_\alpha(T)\left(1+\|\vec{z}\|^{q_\alpha}\right)$$

for all $\vec{z}\in\mathbb{R}^{2d}$ and $t\in[0,T]$; (ii) for all $\vec{z}\in\mathbb{R}^{2d}$ and $t\in[0,T]$, $\partial_t u_\theta^R(t,\vec{z}) = -\widetilde{\mathcal{L}}\,u_\theta^R(t,\vec{z})$ and $\partial_t u_\theta^I(t,\vec{z}) = -\widetilde{\mathcal{L}}\,u_\theta^I(t,\vec{z})$; and (iii) for any standard multi-index α satisfying $|\alpha|\leq L$ we have that $\partial_t\partial_{\vec{z}}^\alpha u_\theta^R$, $\partial_t\partial_{\vec{z}}^\alpha u_\theta^I$ are continuous functions, and $\partial_t\partial_{\vec{z}}^\alpha u_\theta^R = -\partial_{\vec{z}}^\alpha\widetilde{\mathcal{L}}u_\theta^R$, $\partial_t\partial_{\vec{z}}^\alpha u_\theta^I = -\partial_{\vec{z}}^\alpha\widetilde{\mathcal{L}}u_\theta^I$. Combining (ii), (2.17), and (2.18) yields

$$\partial_t u_\theta(t,z) = \partial_t u_\theta(t,\vec{z}) = -\widetilde{\mathcal{L}}u_\theta(t,\vec{z}) = -\mathcal{L}u_\theta(t,z)\,.$$

From (i) and (2.17) we obtain (2.16), and (iii) completes the proof.

□

2.5.3.3 Proof of generalized version of Theorem 2.3.1

First, we compare the main conditional moments of the increments of Scheme 1 with those of the Euler scheme. For this purpose, we apply Lemma 2.5.3.

Lemma 2.5.4. *Let $H, L_k : [0,T] \to \mathbb{C}^{d\times d}$ be continuously differentiable functions. Let $(\hat{Y}_n)_{n=1\ldots,N}$ be as in Scheme 1. Consider*

$$E^n_{\tau_{n+1}} = \hat{Y}_n + \left(G(\tau_n)\hat{Y}_n + g\left(\tau_n, \hat{Y}_n\right)\right)(\tau_{n+1}-\tau_n) + \sum_{k=1}^{m} \sigma_k\left(\tau_n, \hat{Y}_n\right)\left(W^k_{\tau_{n+1}} - W^k_{\tau_n}\right).$$

Then, for any $|\alpha| \le 5$ there exist $c_\alpha \in \mathcal{WC}^{1,\infty}_P\left([0,T]\times\mathbb{C}^d, \mathbb{C}\right)$ such that

$$\mathbb{E}\left(\left(\hat{Y}_{n+1} - \hat{Y}_n\right)^\alpha \mid \mathfrak{G}_n\right) - \mathbb{E}\left(\left(E^n_{\tau_{n+1}} - \hat{Y}_n\right)^\alpha \mid \mathfrak{G}_n\right) = c_\alpha\left(\tau_n, \hat{Y}_n\right)\Delta_n^2 + \mathbb{E}\left(\mathcal{O}_{n+1} \mid \mathfrak{G}_n\right)\Delta_n^3.$$

Proof. Since $\mathbb{E}(\left(\xi^k_{n+1}\right)^2) = 1$ and the distribution of ξ^k_{n+1} is symmetric around 0,

$$\mathbb{E}\left(\Gamma_{1,n+1} \mid \mathfrak{G}_n\right) = \mathbb{E}\left(\Gamma_{2,n+1} \mid \mathfrak{G}_n\right) = 0.$$

Using Lemma 2.5.3 we get

$$\mathbb{E}\left(\hat{Y}_{n+1} - \hat{Y}_n \mid \mathfrak{G}_n\right) = \left(G_n\hat{Y}_n + g_n\right)\Delta_n + \mathbb{E}\left(\Gamma_{3,n+1} \mid \mathfrak{G}_n\right)\Delta_n^2 + \mathbb{E}\left(\mathcal{O}_{n+1} \mid \mathfrak{G}_n\right)\Delta_n^3,$$

because $\mathbb{E}\left(\Gamma_{4,n+1} \mid \mathfrak{G}_n\right) = 0$. Hence,

$$\mathbb{E}\left(\hat{Y}_{n+1} - \hat{Y}_n \mid \mathfrak{G}_n\right) - \mathbb{E}\left(E^n_{\tau_{n+1}} - \hat{Y}_n \mid \mathfrak{G}_n\right) = \mathbb{E}\left(\Gamma_{3,n+1} \mid \mathfrak{G}_n\right)\Delta_n^2 + \mathbb{E}\left(\mathcal{O}_{n+1} \mid \mathfrak{G}_n\right)\Delta_n^3.$$

Let $|\alpha| = 2$. Then, $\alpha = \alpha_1 + \alpha_2$, with $|\alpha_1| = |\alpha_2| = 1$. Lemma 2.5.3 leads to

$$\begin{aligned}\mathbb{E}\left(\left(\hat{Y}_{n+1} - \hat{Y}_n\right)^\alpha \mid \mathfrak{G}_n\right) = \left(G_n\hat{Y}_n + g_n\right)^\alpha \Delta_n^2 + \Delta_n \sum_{k=1}^{m} (\sigma_{k,n})^\alpha \\ + \Delta_n^2 \sum_{k=1}^{m}\left(\sigma^{\alpha_1}_{k,n}\,\mathbb{E}\left(\Gamma^{\alpha_2}_{2,n+1}\xi^k_{n+1} \mid \mathfrak{G}_n\right) + \sigma^{\alpha_2}_{k,n}\,\mathbb{E}\left(\Gamma^{\alpha_1}_{2,n+1}\xi^k_{n+1} \mid \mathfrak{G}_n\right)\right) \\ + \mathbb{E}\left(\Gamma^\alpha_{1,n+1} \mid \mathfrak{G}_n\right)\Delta_n^2 + \mathbb{E}\left(\mathcal{O}_{n+1} \mid \mathfrak{G}_n\right)\Delta_n^3.\end{aligned}$$

Therefore,

$$\begin{aligned}\mathbb{E}\left(\left(\hat{Y}_{n+1}-\hat{Y}_n\right)^{\alpha} \mid \mathfrak{G}_n\right) - \mathbb{E}\left(\left(E^n_{\tau_{n+1}}-\hat{Y}_n\right)^{\alpha} \mid \mathfrak{G}_n\right) \\ = \Delta_n^2 \sum_{k=1}^{m} \left(\sigma_{k,n}^{\alpha_1}\, \mathbb{E}\left(\Gamma_{2,n+1}^{\alpha_2}\xi_{n+1}^k \mid \mathfrak{G}_n\right) + \sigma_{k,n}^{\alpha_2}\, \mathbb{E}\left(\Gamma_{2,n+1}^{\alpha_1}\xi_{n+1}^k \mid \mathfrak{G}_n\right)\right) \\ + \mathbb{E}\left(\Gamma_{1,n+1}^{\alpha} \mid \mathfrak{G}_n\right)\Delta_n^2 + \mathbb{E}\left(\mathcal{O}_{n+1} \mid \mathfrak{G}_n\right)\Delta_n^3.\end{aligned}$$

Assume that $|\alpha| = 3$. Thus, $\alpha = \alpha_1 + \alpha_2 + \alpha_3$, with $|\alpha_1| = |\alpha_2| = |\alpha_3| = 1$. Applying Lemma 2.5.3 gives

$$\begin{aligned}\mathbb{E}\left(\left(\hat{Y}_{n+1}-\hat{Y}_n\right)^{\alpha} \mid \mathfrak{G}_n\right) = \Delta_n^2 \sum_{k=1}^{m} \sum_{\{\beta_1,\beta_2,\beta_3\}=\{\alpha_1,\alpha_2,\alpha_3\}} \left(G_n\hat{Y}_n + g_n\right)^{\beta_1} (\sigma_{k,n})^{\beta_2} (\sigma_{k,n})^{\beta_3} \\ + \Delta_n^2 \sum_{k,j=1}^{m} \sum_{\{\beta_1,\beta_2,\beta_3\}=\{\alpha_1,\alpha_2,\alpha_3\}} \mathbb{E}\left(\sigma_{k,n}^{\beta_1}\sigma_{j,n}^{\beta_2}\Gamma_{1,n+1}^{\beta_3}\xi_{n+1}^k\xi_{n+1}^j \mid \mathfrak{G}_n\right) \\ + \mathbb{E}\left(\mathcal{O}_{n+1} \mid \mathfrak{G}_n\right)\Delta_n^3.\end{aligned}$$

This yields

$$\begin{aligned}\mathbb{E}\left(\left(\hat{Y}_{n+1}-\hat{Y}_n\right)^{\alpha} \mid \mathfrak{G}_n\right) - \mathbb{E}\left(\left(E^n_{\tau_{n+1}}-\hat{Y}_n\right)^{\alpha} \mid \mathfrak{G}_n\right) \\ = \Delta_n^2 \sum_{k,j=1}^{m} \sum_{\{\beta_1,\beta_2,\beta_3\}=\{\alpha_1,\alpha_2,\alpha_3\}} \mathbb{E}\left(\sigma_{k,n}^{\beta_1}\sigma_{j,n}^{\beta_2}\Gamma_{1,n+1}^{\beta_3}\xi_{n+1}^k\xi_{n+1}^j \mid \mathfrak{G}_n\right) + \mathbb{E}\left(\mathcal{O}_{n+1} \mid \mathfrak{G}_n\right)\Delta_n^3.\end{aligned}$$

If $|\alpha| = 4$, then

$$\begin{aligned}\mathbb{E}\left(\left(\hat{Y}_{n+1}-\hat{Y}_n\right)^{\alpha} \mid \mathfrak{G}_n\right) &= \mathbb{E}\left(\left(\sum_{k=1}^{m}\sigma_{k,n}\xi_{n+1}^k\right)^{\alpha} \mid \mathfrak{G}_n\right)\Delta_n^2 + \mathbb{E}\left(\mathcal{O}_{n+1} \mid \mathfrak{G}_n\right)\Delta_n^3 \\ &= \mathbb{E}\left(\left(E^n_{\tau_{n+1}}-\hat{Y}_n\right)^{\alpha} \mid \mathfrak{G}_n\right) + \mathbb{E}\left(\mathcal{O}_{n+1} \mid \mathfrak{G}_n\right)\Delta_n^3.\end{aligned}$$

In case $|\alpha| = 5$, from Lemma 2.5.3 we obtain

$$\mathbb{E}\left(\left(\hat{Y}_{n+1}-\hat{Y}_n\right)^{\alpha} \mid \mathfrak{G}_n\right) = \mathbb{E}\left(\mathcal{O}_{n+1} \mid \mathfrak{G}_n\right)\Delta_n^3,$$

and so

$$\mathbb{E}\left(\left(\hat{Y}_{n+1}-\hat{Y}_n\right)^{\alpha} \mid \mathfrak{G}_n\right)-\mathbb{E}\left(\left(E^n_{\tau_{n+1}}-\hat{Y}_n\right)^{\alpha} \mid \mathfrak{G}_n\right)=\mathbb{E}\left(\mathcal{O}_{n+1} \mid \mathfrak{G}_n\right)\Delta_n^3.$$

□

The following proposition is an extension of Theorem 2.3.1, which considers only one function φ_θ.

Proposition 2.5.2. *Let the assumptions of Theorem 2.3.1 hold. If the functions φ_θ, with $\theta \in \Theta$, belong uniformly to $\mathcal{WC}^4_P\left(\mathbb{C}^d,\mathbb{C}\right)$, then*

$$\sup_{\theta\in\Theta}\left|\mathbb{E}\left(\varphi_\theta\left(X_T\right)\right)-\mathbb{E}\left(\varphi_\theta\left(\hat{Y}_N\right)\right)\right| \le K\left(T\right)\max_{n=1,\ldots,N}\left(\tau_{n+1}-\tau_n\right).$$

for any partition $(\tau_n)_{n=0,\ldots,N}$.

Proof. We use the methodology introduced by Milstein and Talay that obtains the global rate of weak convergence of the numerical schemes for SDEs by means of the Kolmogorov equations. To this end, we define

$$u_\theta\left(s,z\right)=\mathbb{E}\,\varphi_\theta\left(Z_T^{s,z}\right) \qquad\qquad \forall s\in[0,T],$$

where $z\in\mathbb{C}^d$ and $Z_T^{s,z}$ is the solution of (2.14). From the definition of (2.14) it follows that $Z_t^{0,X_0}=X_t$ for all $t\in[0,T]$ in case $\|X_0\|=1$. Therefore,

$$\mathbb{E}\,u_\theta\left(0,X_0\right)=\mathbb{E}\left(u_\theta\left(0,X_0\right)\mid X_0\right)=\mathbb{E}\,\varphi_\theta\left(X_T\right).$$

Since $\hat{Y}_0=X_0$,

$$\begin{aligned}\mathbb{E}\,\varphi_\theta\left(\hat{Y}_N\right)-\mathbb{E}\,\varphi_\theta\left(X_T\right)&=\mathbb{E}\,u_\theta\left(T,\hat{Y}_N\right)-\mathbb{E}\,u_\theta\left(0,X_0\right)\\&=\mathbb{E}\,u_\theta\left(0,\hat{Y}_0\right)-\mathbb{E}\,u_\theta\left(0,X_0\right)\\&\quad+\sum_{n=0}^{N-1}\left(\mathbb{E}\,u_\theta\left(\tau_{n+1},\hat{Y}_{n+1}\right)-\mathbb{E}\,u_\theta\left(\tau_n,\hat{Y}_n\right)\right)\\&=\sum_{n=0}^{N-1}\left(\mathbb{E}\,\Phi_1^n+\mathbb{E}\,\Phi_2^n\right),\end{aligned}$$

where $\Phi_1^n = u_\theta\left(\tau_{n+1}, E^n_{\tau_{n+1}}\right) - u_\theta\left(\tau_n, \hat{Y}_n\right)$,

$$\Phi_2^n = u_\theta\left(\tau_{n+1}, \hat{Y}_{n+1}\right) - u_\theta\left(\tau_{n+1}, \hat{Y}_n\right) + u_\theta\left(\tau_{n+1}, \hat{Y}_n\right) - u_\theta\left(\tau_{n+1}, E^n_{\tau_{n+1}}\right),$$

and

$$E_t^n = \hat{Y}_n + \left(G\left(\tau_n\right)\hat{Y}_n + g\left(\tau_n, \hat{Y}_n\right)\right)\left(t - \tau_n\right) + \sum_{k=1}^{m} \sigma_k\left(\tau_n, \hat{Y}_n\right)\left(W_t^k - W_{\tau_n}^k\right)$$

for all $t \in [\tau_n, \tau_{n+1}]$. This gives

$$\left|\mathbb{E}\,\varphi_\theta\left(\hat{Y}_N\right) - \mathbb{E}\,\varphi_\theta\left(X_T\right)\right| \leq \sum_{n=0}^{N-1}\left(\left|\mathbb{E}\,\Phi_1^n\right| + \left|\mathbb{E}\,\Phi_2^n\right|\right). \tag{2.19}$$

By Proposition 2.5.1, $u_\theta \in \mathcal{WC}_P^4\left([0,T]\times\mathbb{C}^d, \mathbb{C}\right)$. Combining Theorem 2.5.2 with Proposition 2.5.1 we obtain

$$\begin{aligned}\mathbb{E}\left(\Phi_1^n \mid \mathfrak{G}_n\right) &= \int_{\tau_n}^{\tau_{n+1}} \mathbb{E}\left(\frac{\partial}{dt}u\left(t, E_t^n\right) + \mathcal{L}_{\tau_n,\hat{Y}_n}\left(u\right)\left(t, E_t^n\right) \mid \mathfrak{G}_n\right) dt \\ &= \int_{\tau_n}^{\tau_{n+1}} \mathbb{E}\left(-\mathcal{L}\left(u\right)\left(t, E_t^n\right) + \mathcal{L}_{\tau_n,\hat{Y}_n}\left(u\right)\left(t, E_t^n\right) \mid \mathfrak{G}_n\right) dt,\end{aligned}$$

where

$$\mathcal{L}_{\tau_n,\hat{Y}_n} = \sum_{\alpha\in\mathcal{P}_1} a^\alpha\left(\tau_n, \hat{Y}_n\right)\partial^\alpha + \frac{1}{2}\sum_{\ell=1}^{m}\sum_{\alpha\in\mathcal{P}_2} b_\ell^\alpha\left(\tau_n, \hat{Y}_n\right)\partial^\alpha.$$

Combining (2.15) with $\|\hat{Y}_n\| = 1$ we deduce that $b_\ell\left(\tau_n, \hat{Y}_n\right) = \sigma_\ell\left(\tau_n, \hat{Y}_n\right)$ and $a\left(\tau_n, \hat{Y}_n\right) = G\left(\tau_n\right)\hat{Y}_n + g\left(\tau_n, \hat{Y}_n\right)$. Hence,

$$\mathcal{L}_{\tau_n,\hat{Y}_n} = \sum_{\alpha\in\mathcal{P}_1}\left(G\left(\tau_n\right)\hat{Y}_n + g\left(\tau_n, \hat{Y}_n\right)\right)^\alpha\partial^\alpha + \frac{1}{2}\sum_{\ell=1}^{m}\sum_{\alpha\in\mathcal{P}_2}\sigma_\ell^\alpha\left(\tau_n, \hat{Y}_n\right)\partial^\alpha.$$

Since $\mathcal{L}_{\tau_n,\hat{Y}_n}(u)(\tau_n, \hat{Y}_n) = \mathcal{L}(u)(\tau_n, \hat{Y}_n)$, applying first Theorem 2.5.2 and then Proposition

2.5.1 we get

$$\mathbb{E}\left(\Phi_1^n \mid \mathfrak{G}_n\right) = \int_{\tau_n}^{\tau_{n+1}} \int_{\tau_n}^{t} \mathbb{E}\left(-\mathcal{L}_1\left(u\right)\left(s, E_s^n\right) + \mathcal{L}^2\left(u\right)\left(s, E_s^n\right) \mid \mathfrak{G}_n\right) ds\, dt$$
$$+ \int_{\tau_n}^{\tau_{n+1}} \int_{\tau_n}^{t} \mathbb{E}\left(\mathcal{L}^2_{\tau_n, \hat{Y}_n}\left(u\right)\left(s, E_s^n\right) - 2\,\mathcal{L}_{\tau_n, \hat{Y}_n}\left(\mathcal{L}\left(u\right)\right)\left(s, E_s^n\right) \mid \mathfrak{G}_n\right) ds\, dt,$$

where

$$\mathcal{L}_1 = \sum_{\alpha \in \mathcal{P}_1} \left(\frac{\partial}{\partial t} a^\alpha\right) \partial^\alpha + \frac{1}{2} \sum_{\ell=1}^{m} \sum_{\alpha \in \mathcal{P}_2} \left(\frac{\partial}{\partial t} b_\ell^\alpha\right) \partial^\alpha.$$

From (2.16) it follows that

$$\left|\mathbb{E}\left(\Phi_1^n \mid \mathfrak{G}_n\right)\right| \leq K\left(T\right)\left(\tau_{n+1} - \tau_n\right)^2 \qquad \forall n = 0, \ldots, N-1 \tag{2.20}$$

for all $\theta \in \Theta$.

We now turn to $\mathbb{E}\Phi_2^n$. Since $u_\theta \in \mathcal{WC}_P^4\left([0,T] \times \mathbb{C}^d, \mathbb{C}\right)$, applying Theorem 2.5.1 gives

$$u_\theta\left(\tau_{n+1}, \hat{Y}_{n+1}\right) - u_\theta\left(\tau_{n+1}, \hat{Y}_n\right) = \sum_{k=1}^{3} \sum_{\alpha \in \mathcal{P}_k} \frac{1}{\alpha!} \partial_z^\alpha u_\theta\left(\tau_{n+1}, \hat{Y}_n\right)\left(\hat{Y}_{n+1} - \hat{Y}_n\right)^\alpha + R_{n+1,\theta}^4\left(\hat{Y}_{n+1}\right)$$

and

$$u_\theta\left(\tau_{n+1}, E_{\tau_{n+1}}^n\right) - u_\theta\left(\tau_{n+1}, \hat{Y}_n\right) = \sum_{k=1}^{3} \sum_{\alpha \in \mathcal{P}_k} \frac{1}{\alpha!} \partial_z^\alpha u_\theta\left(\tau_{n+1}, \hat{Y}_n\right)\left(E_{\tau_{n+1}}^n - \hat{Y}_n\right)^\alpha + R_{n+1,\theta}^4\left(E_{\tau_{n+1}}^n\right),$$

where

$$R_{n+1,\theta}^k\left(z\right) = k \sum_{|\alpha|=k} \frac{\left(z - \hat{Y}_n\right)^\alpha}{\alpha!} \int_0^1 \left(1-t\right)^{k-1} \partial_z^\alpha u_\theta\left(\tau_{n+1}, \hat{Y}_n + t\left(z - \hat{Y}_n\right)\right) dt.$$

According to (2.16) we have that

$$\left|\partial_z^\alpha u_\theta\left(\tau_{n+1}, \hat{Y}_n + t\left(z - \hat{Y}_n\right)\right)\right| \leq K\left(T\right)\left(1 + \|z\|^q\right) \qquad \forall \theta \in \Theta, n \leq N-1 \tag{2.21}$$

for any $t \in [0,1]$, and $|\alpha| = 4$. Therefore,

$$\left|\mathbb{E}\left(R^4_{n+1,\theta}\left(\hat{Y}_{n+1}\right) \mid \mathfrak{G}_n\right)\right| \leq K(T) \sum_{|\alpha|=4} \frac{1}{\alpha!} \left|\mathbb{E}\left(\left(\hat{Y}_{n+1} - \hat{Y}_n\right)^\alpha \mid \mathfrak{G}_n\right)\right|.$$

By Lemma 2.5.3, $\hat{Y}_{n+1} - \hat{Y}_n = \sqrt{\tau_{n+1} - \tau_n}\mathcal{O}_{n+1}$, which implies

$$\left|\mathbb{E}\left(\left(\hat{Y}_{n+1} - \hat{Y}_n\right)^\alpha \mid \mathfrak{G}_n\right)\right| \leq K(T)(\tau_{n+1} - \tau_n)^2.$$

Combining (2.21) with the Cachy-Schwarz inequality for conditional expectations we obtain

$$\begin{aligned}
\left|\mathbb{E}\left(R^4_{n+1,\theta}\left(E^n_{\tau_{n+1}}\right) \mid \mathfrak{G}_n\right)\right| &\leq K(T) \sum_{|\alpha|=4} \frac{1}{\alpha!} \mathbb{E}\left(\left|\left(E^n_{\tau_{n+1}} - \hat{Y}_n\right)^\alpha\right| \left(1 + \left\|E^n_{\tau_{n+1}}\right\|^q\right) \mid \mathfrak{G}_n\right) \\
&\leq K(T)\left(\mathbb{E}\left(\left\|E^n_{\tau_{n+1}} - \hat{Y}_n\right\|^8 \mid \mathfrak{G}_n\right)\right)^{1/2}\left(1 + \mathbb{E}\left(\left\|E^n_{\tau_{n+1}}\right\|^{2q} \mid \mathfrak{G}_n\right)\right)^{1/2} \\
&\leq K(T)(\tau_{n+1} - \tau_n)^2,
\end{aligned}$$

because $E^n_{\tau_{n+1}} - \hat{Y}_n = \sqrt{\tau_{n+1} - \tau_n}\mathcal{O}_{n+1}$. Then,

$$\begin{aligned}
|\mathbb{E}(\Phi^n_2 \mid \mathfrak{G}_n)| \leq &\sum_{k=1}^{3} \sum_{\alpha \in \mathcal{P}_k} \frac{1}{\alpha!} \left|\partial^\alpha_z u_\theta\left(\tau_{n+1}, \hat{Y}_n\right)\right| \left|\mathbb{E}\left(\left(\hat{Y}_{n+1} - \hat{Y}_n\right)^\alpha - \left(E^n_{\tau_{n+1}} - \hat{Y}_n\right)^\alpha \mid \mathfrak{G}_n\right)\right| \\
&+ K(T)(\tau_{n+1} - \tau_n)^2,
\end{aligned}$$

and so (2.21) implies

$$\begin{aligned}
|\mathbb{E}(\Phi^n_2 \mid \mathfrak{G}_n)| \leq K(T) &\sum_{k=1}^{3} \sum_{\alpha \in \mathcal{P}_k} \left|\mathbb{E}\left(\left(\hat{Y}_{n+1} - \hat{Y}_n\right)^\alpha \mid \mathfrak{G}_n\right) - \mathbb{E}\left(\left(E^n_{\tau_{n+1}} - \hat{Y}_n\right)^\alpha \mid \mathfrak{G}_n\right)\right| \\
&+ K(T)(\tau_{n+1} - \tau_n)^2.
\end{aligned}$$

Lemma 2.5.4 leads to

$$\left|\mathbb{E}\left(\left(\hat{Y}_{n+1} - \hat{Y}_n\right)^\alpha - \left(E^n_{\tau_{n+1}} - \hat{Y}_n\right)^\alpha \mid \mathfrak{G}_n\right)\right| \leq K(T)(\tau_{n+1} - \tau_n)^2.$$

Hence,

$$|\mathbb{E}(\Phi^n_2 \mid \mathfrak{G}_n)| \leq K(T)(\tau_{n+1} - \tau_n)^2. \tag{2.22}$$

Combining (2.19), (2.20) and (2.22) we obtain the desired result. □

Remark 2.5.1. *In the proof of Proposition 2.5.2 we obtain that the rate of convergence of* $\mathbb{E}(\varphi_\theta(\hat{Y}_N))$ *to* $\mathbb{E}(\varphi_\theta(X_T))$ *is equal to* 1 *for any regularizing function* $\widetilde{\rho}$*. On the other hand, the constant* $K(T)$ *obtained in the proof of Proposition 2.5.2 is not optimal, because depends of* $\widetilde{\rho}$*.*

2.5.4 Proof of Theorem 2.3.2

Proof. For every $z \in \mathbb{C}^d$ we set

$$u(s,z) = \mathbb{E}\,\varphi\left(Z_T^{s,z}\right) \qquad \forall s \in [0,T],$$

where $Z_T^{s,z}$ is the solution of (2.14). Proceeding as in the proof of Proposition 2.5.2 we obtain that

$$\mathbb{E}\,\varphi\left(\hat{Y}_N\right) - \mathbb{E}\,\varphi\left(X_T\right) = \sum_{n=0}^{N-1} \left(\mathbb{E}\left(\Phi_1^n\right) + \mathbb{E}\left(\Phi_2^n\right)\right),$$

where

$$\begin{aligned}\mathbb{E}\left(\Phi_1^n \mid \mathfrak{G}_n\right) = &\int_{\tau_n}^{\tau_{n+1}} \int_{\tau_n}^{t} \mathbb{E}\left(-\mathcal{L}_1(u)\left(s, E_s^n\right) + \mathcal{L}^2(u)\left(s, E_s^n\right) \mid \mathfrak{G}_n\right) ds\, dt \\ &+ \int_{\tau_n}^{\tau_{n+1}} \int_{\tau_n}^{t} \mathbb{E}\left(\mathcal{L}^2_{\tau_n,\hat{Y}_n}(u)\left(s, E_s^n\right) - 2\,\mathcal{L}_{\tau_n,\hat{Y}_n}\left(\mathcal{L}(u)\right)\left(s, E_s^n\right) \mid \mathfrak{G}_n\right) ds\, dt,\end{aligned}$$

and

$$\Phi_2^n = u\left(\tau_{n+1}, \hat{Y}_{n+1}\right) - u\left(\tau_{n+1}, \hat{Y}_n\right) + u\left(\tau_{n+1}, \hat{Y}_n\right) - u\left(\tau_{n+1}, E^n_{\tau_{n+1}}\right).$$

According to Proposition 2.5.1 we have that $u \in \mathcal{WC}_P^{1,9}\left([0,T] \times \mathbb{C}^d, \mathbb{C}\right)$. By applying first Theorem 2.5.2 and then Proposition 2.5.1 we obtain

$$\mathbb{E}\left(\Phi_1^n \mid \mathfrak{G}_n\right) = \frac{1}{2}\left(\tau_{n+1} - \tau_n\right)^2 \Psi_1\left(\tau_n, \hat{Y}_n\right) + \int_{\tau_n}^{\tau_{n+1}} \int_{\tau_n}^{t} \int_{\tau_n}^{s} \mathbb{E}\left(\Psi_{2,n}\left(r, E_r^n\right) \mid \mathfrak{G}_n\right) dr\, ds\, dt,$$

where

$$\Psi_1(s,z) = -\mathcal{L}_1(u)(s,z) + \mathcal{L}^2(u)(s,z) + \mathcal{L}^2_{s,z}(u)(s,z) - 2\,\mathcal{L}_{s,z}\left(\mathcal{L}(u)\right)(s,z),$$

and

$$\Psi_2 = 2\,\mathcal{L}_1\mathcal{L}\,(u) - \mathcal{L}_2\,(u) - 3\,\mathcal{L}_{\tau_n,\hat{Y}_n}\mathcal{L}_1\,(u) - 3\,\mathcal{L}^2_{\tau_n,\hat{Y}_n}\mathcal{L}\,(u) + \mathcal{L}^3_{\tau_n,\hat{Y}_n}\,(u) + 3\,\mathcal{L}_{\tau_n,\hat{Y}_n}\mathcal{L}^2\,(u) + \mathcal{L}\mathcal{L}_1\,(u) - \mathcal{L}^3\,(u)$$

with

$$\mathcal{L}_2 = \sum_{\alpha\in\mathcal{P}_1}\left(\frac{\partial^2}{\partial t^2}a^\alpha\right)\partial^\alpha + \frac{1}{2}\sum_{\ell=1}^{m}\sum_{\alpha\in\mathcal{P}_2}\left(\frac{\partial^2}{\partial t^2}b^\alpha_\ell\right)\partial^\alpha.$$

Combining $u \in \mathcal{WC}^{1,9}_P\left([0,T]\times\mathbb{C}^d,\mathbb{C}\right)$ with $\|\hat{Y}_n\| = 1$ gives

$$\left|\mathbb{E}\left(\Phi^n_1 \mid \mathfrak{G}_n\right) - \frac{1}{2}\left(\tau_{n+1}-\tau_n\right)^2\Psi_1\left(\tau_n,\hat{Y}_n\right)\right| \leq K\,(T)\,\Delta^3_n, \tag{2.23}$$

where $\Delta_n = \tau_{n+1} - \tau_n$.

Theorem 2.5.1 leads to

$$\Phi^n_2 = \sum_{k=1}^{5}\sum_{\alpha\in\mathcal{P}_k}\frac{1}{\alpha!}\partial^\alpha_z u\left(\tau_{n+1},\hat{Y}_n\right)\left(\left(\hat{Y}_{n+1}-\hat{Y}_n\right)^\alpha - \left(E^n_{\tau_{n+1}}-\hat{Y}_n\right)^\alpha\right) + R^6_{n+1}\left(\hat{Y}_{n+1}\right) - R^6_{n+1}\left(E^n_{\tau_{n+1}}\right),$$

where

$$R^k_{n+1}\,(z) = k\sum_{|\alpha|=k}\frac{\left(z-\hat{Y}_n\right)^\alpha}{\alpha!}\int_0^1(1-t)^{k-1}\,\partial^\alpha_z u\left(\tau_{n+1},\hat{Y}_n + t\left(z-\hat{Y}_n\right)\right)dt.$$

An analysis similar to that in the proof of Proposition 2.5.2 shows that

$$\left|\mathbb{E}\left(R^6_{n+1}\left(\hat{Y}_{n+1}\right)\mid\mathfrak{G}_n\right)\right| + \left|\mathbb{E}\left(R^6_{n+1}\left(E^n_{\tau_{n+1}}\right)\mid\mathfrak{G}_n\right)\right| \leq K\,(T)\,\Delta^3_n.$$

Applying Lemma 2.5.4 gives

$$\left|\mathbb{E}\left(\Phi^n_2\mid\mathfrak{G}_n\right) - \left(\tau_{n+1}-\tau_n\right)^2\sum_{k=1}^{5}\sum_{\alpha\in\mathcal{P}_k}\frac{1}{\alpha!}\partial^\alpha_z u\left(\tau_{n+1},\hat{Y}_n\right)c_\alpha\left(\tau_n,\hat{Y}_n\right)\right| \leq K\,(T)\,\Delta^3_n,$$

where $c_\alpha \in \mathcal{WC}_P^{1,\infty}\left([0,T]\times\mathbb{C}^d,\mathbb{C}\right)$. Since $\partial_z^\alpha u \in \mathcal{WC}_P^{1,4}\left([0,T]\times\mathbb{C}^d,\mathbb{C}\right)$ for any $|\alpha|=5$,

$$\left|\mathbb{E}\left(\Phi_2^n \mid \mathfrak{G}_n\right) - \left(\tau_{n+1}-\tau_n\right)^2 \sum_{k=1}^{5}\sum_{\alpha\in\mathcal{P}_k}\frac{1}{\alpha!}\partial_z^\alpha u\left(\tau_n,\hat{Y}_n\right)c_\alpha\left(\tau_n,\hat{Y}_n\right)\right| \leq K\left(T\right)\Delta_n^3.$$

Then, using (2.23) yields

$$\left|\mathbb{E}\left(\Phi_1^n+\Phi_2^n \mid \mathfrak{G}_n\right) - \left(\tau_{n+1}-\tau_n\right)^2 \Psi\left(\tau_n,\hat{Y}_n\right)\right| \leq K\left(T\right)\Delta_n^3,$$

where

$$\Psi\left(t,z\right) = \frac{1}{2}\Psi_1\left(t,z\right) + \sum_{k=1}^{5}\sum_{\alpha\in\mathcal{P}_k}\frac{1}{\alpha!}\partial_z^\alpha u\left(t,z\right)c_\alpha\left(t,z\right).$$

Since $\Psi \in \mathcal{WC}_P^{1,4}\left([0,T]\times\mathbb{C}^d,\mathbb{C}\right)$, the family $\{\Psi\left(t,\cdot\right) : t\in[0,T]\}$ belongs uniformly to $\mathcal{WC}_P^4\left(\mathbb{C}^d,\mathbb{C}\right)$. Applying Proposition 2.5.2 we deduce that

$$\left|\mathbb{E}\left(\Psi\left(\tau_n,\hat{Y}_n\right)\right) - \mathbb{E}\left(\Psi\left(\tau_n,X_{\tau_n}\right)\right)\right| \leq K\left(\tau_n\right)\max_{j=1,\ldots,n-1}\Delta_j \leq K\left(T\right)\max_{j=1,\ldots,N}\Delta_j$$

for all $n=1,\ldots,N$. Hence,

$$\left|\mathbb{E}\left(\Phi_1^n+\Phi_2^n \mid \mathfrak{G}_n\right) - \left(\tau_{n+1}-\tau_n\right)^2 \mathbb{E}\Psi\left(\tau_n,X_{\tau_n}\right)\right| \leq K\left(T\right)\Delta_n^3.$$

As the first derivative of $t\mapsto\mathbb{E}\Psi\left(t,X_t\right)$ is continuous we have

$$\left|\mathbb{E}\left(\Phi_1^n+\Phi_2^n \mid \mathfrak{G}_n\right) - \left(\tau_{n+1}-\tau_n\right)\int_{\tau_n}^{\tau_{n+1}}\mathbb{E}\Psi\left(t,X_t\right)dt\right| \leq K\left(T\right)\Delta_n^3.$$

□

2.5.5 Proof of Theorem 2.3.3

Proof. Using Lemma 2.5.3 yields

$$\hat{Y}_{n+1} = \hat{Y}_n + \left(G_n\hat{Y}_n + g_n\right)\Delta_n + \sqrt{\Delta_n}\sum_{k=1}^{m}\sigma_{k,n}\xi_{n+1}^k + \sum_{j=1}^{2}\Delta_n^{(j+1)/2}\Gamma_{j,n+1} + \mathcal{O}_{n+1}\Delta_n^2,$$

and so

$$\hat{Y}_{n+1} - E^n_{\tau_{n+1}} = \Delta_n \Gamma_{1,n+1} + \Delta_n^{3/2} \Gamma_{2,n+1} + \mathcal{O}_{n+1} \Delta_n^2,$$

where $E^n_{\tau_{n+1}}$ is as in Lemma 2.5.4, and $\Gamma_{j,n+1}$ is given by Lemma 2.5.3. Therefore,

$$\mathbb{E}\left(\left\| \hat{Y}_{n+1} - E^n_{\tau_{n+1}} \right\|^{2q} \mid \mathfrak{F}_{\tau_n} \right) \leq K_p(T)\, \Delta_n^{2q}, \tag{2.24}$$

and

$$\left\| \mathbb{E}\left(\hat{Y}_{n+1} - E^n_{\tau_{n+1}} \mid \mathfrak{F}_{\tau_n} \right) \right\| \leq K(T)\, \Delta_n^2, \tag{2.25}$$

where $(\mathfrak{F}_t)_{t \geq 0}$ stands for the filtration generated by $W^1, \ldots, W^m$.

Consider

$$X^n_t = \hat{Y}_n + \int_{\tau_n}^t \left(G(s)\, X^n_s + g(s, X^n_s) \right) ds + \sum_{k=1}^m \int_{\tau_n}^t \sigma_k(s, X^n_s)\, dW^k_s \qquad \forall t \in [\tau_n, T].$$

Since $\|\hat{Y}_n\| = 1$ and $\|X^n_t\| = 1$, applying classical arguments yields

$$\left\| \mathbb{E}\left(X^n_{\tau_{n+1}} - E^n_{\tau_{n+1}} \mid \mathfrak{F}_{\tau_n} \right) \right\| \leq K(T)\, \Delta_n^2$$

and

$$\mathbb{E}\left(\left\| X^n_{\tau_{n+1}} - E^n_{\tau_{n+1}} \right\|^{2q} \mid \mathfrak{F}_{\tau_n} \right) \leq K_p(T)\, \Delta_n^{2q}$$

(see, e.g., Section 1.1.5 of [70]). Then, using (2.24) and (2.25) yields

$$\mathbb{E}\left(\left\| X^n_{\tau_{n+1}} - \hat{Y}_{n+1} \right\|^{2q} \mid \mathfrak{F}_{\tau_n} \right) \leq K_p(T)\, \Delta_n^{2q}$$

and

$$\left\| \mathbb{E}\left(X^n_{\tau_{n+1}} - \hat{Y}_{n+1} \mid \mathfrak{F}_{\tau_n} \right) \right\| \leq K(T)\, \Delta_n^2.$$

The proof is completed by using an analysis similar to that in the proof of the fundamental theorem on the mean-square order of convergence (see, e.g., [95] and Section 1.1 of [70]), together with $\|\hat{Y}_n\| = 1$ and $\|X^n_t\| = 1$. □

Chapter 3

Pathwise methods for the integration of locally Lipschitz SDE with linear multiplicative noise

3.1 Introduction

Stochastic Differential Equations (SDEs) [53, 83, 104] have become a fundamental tool for the mathematical modeling of many phenomena in which noise plays an important role. This is the case, for instance, in Biology [18, 62], Engineering [27, 88], Physical sciences [12, 20] and many other areas. In particular, SDEs are widely used for stochastic modeling in epidemiology [3, 4, 71], where models based on SDEs are typically built by incorporating randomness into deterministic models to obtain a better mathematical description of the system [17, 51, 61, 93]. In general, no exact solution can be found for these stochastic equation models. Therefore, numerical integration methods are essential for properly studying the modeled phenomena.

Currently, a wide variety of stochastic numerical methods are available for the computational integration of stochastic systems, many of which have been motivated by the need to integrate particular types of SDEs in applications [8, 13, 44, 68]. However, results on important issues related to convergence, stability, and long-time behavior of widely used standard methods are typically obtained assuming some restrictive assumptions that may not be satisfied by many SDEs. The standard literature in stochastic numerics concentrates on numerical integrators for SDEs under the hypothesis of globally Lipschitz continuous coefficients, and

when this condition is violated, the method can diverge and show a high instability, see [49, 66, 70]. Therefore, these methods cannot be reliably applied to several epidemiological models that do not meet these conditions. This is the case, for example, of the stochastic SVIR epidemic model (3.15) describing a continuous vaccination strategy with environmental noise effect, see [99]. These deficiencies have recently motivated the search for new numerical methods for SDE with non global Lipschitz coefficients. As a result, sophisticated improvements of standard integrators, including tamed versions of classic numerical schemes, have been proposed for specific SDEs systems under less restrictive conditions. However, some additional conditions (e.g. superlinearity growth, one-side Lipschitz, and global monotone condition) must still be assumed to guarantee convergence. This can limit its use in specific models, see for instance [41, 63, 78, 96] . The low performance of numerical approximations becomes even more severe when the stochastic component significantly influences the dynamics, particularly in cases involving multiplicative noise. These types of equations often appear in epidemic models, see e.g., [5, 42, 102, 103] . Here, the simulation of the system can be required on long-time intervals, thus it is desirable that the numerical integrator replicates, as best as possible, the main long-term properties of the modeled system, even in the presence of large random fluctuations.

This investigation proposes new numerical methods for effectively simulating non-globally Lipschitz SDEs with linear multiplicative noise. In particular, we provide new pathwise numerical approximation for the stochastic SVIR model (3.15) proposed in [99]. The key idea in the derivation of the numerical integrators introduced in this investigation consists in finding a continuous mapping that allows transforming the SDE defining the SVIR model into a suitable Random Differential Equation (RDE) having an Ornstein-Uhlenbeck process as the only random input parameter of the equation. In this way, the solution of the underlying SDE can be numerically obtained by first computing a numerical approximation to the solution of this auxiliary RDE and then performing an explicit inverse transformation to the numerical map used to integrate the RDE. Based on this, two specific numerical schemes are proposed in this work. Specifically, a numerical method based on an exponential method for RDE, and the other based on the Heun method for RDE. The advantage of this approach is that this conjugacy between the SDE and the auxiliary RDE essentially allows to devise integrators without the need to assume global Lipschitz conditions. Remarkably, this framework applyied to the stochastic SVIR model presented in [99], allows to devise integrators capable to outperform other extant integrators in the literature and able to approximate, with high

stability, meaningful probabilistic features of the continuous system, including its stationary distribution and ergodicity.

This chapter is organized as follows: Section 3.2 presents the approach we have adopted to devise pathwise numerical approximations for SDEs with linear multiplicative noise, along with proposing two new numerical schemes. In Section 3.3, we introduce the stochastic SVIR model and describe its main properties. Furthermore, we provide a simulation study to illustrate the practical performance of the methods introduced and conduct a comparative analysis with conventional integrators for the SVIR model.

3.2 Numerical methods based on RDE for the integration of SDE with linear multiplicative noise

In this section, we first introduce an approach to construct an invertible continuous transformation that allows us to express the solution of a SDE with linear multiplicative noise in terms of the solution of a suitable RDE. We then utilize this conjugacy between the SDE and the RDE to develop new pathwise numerical integrators for the original SDE.

3.2.1 Explicit conjugacy between SDEs and RDEs

Random differential equations, in contrast to SDEs, are a type of equations that can be studied pathwise without the need for stochastic calculus in their formulation. Consequently, deriving numerical methods for RDEs primarily relies on specialized tools from deterministic calculus. This distinction allows for the design of numerical integrators for RDEs not subject to the same restrictive convergence and stability conditions as those required for SDEs. This aspect significantly motivates exploring an invertible transformation between non-globally Lipschitz SDEs and RDEs.

Our focus is on autonomous SDEs with linear multiplicative noise. Specifically, we consider the following autonomous SDE system:

$$dX_t^i = b_i(X_t)dt + \sigma_i X_t^i \, dW_t^i \qquad t \in [0,T], \tag{3.1}$$

for $i = 1, \ldots, d$, where the drift $b : \mathbb{R}^d \longrightarrow \mathbb{R}^d$ is smooth, W_t is a d-dimentional standard Brownian motion, $x_0 \in \mathbb{R}^d$ is the initial value, and $\sigma = (\sigma_1, \ldots, \sigma_d)^\top \in \mathbb{R}^d$. To link the SDE

(3.1) with a RDE, we use a continuous invertible map $X_t \to \Phi(X_t) =: Y_t$ depending on an Ornstein-Uhlenbeck process U_t by the relation

$$Y_t^i = e^{U_t^i} X_t^i, \quad t \geq 0, \tag{3.2}$$

where the Ornstein-Uhlenbeck process is given by

$$U_t^i = u_0 - \int_0^t U_s^i \, ds - \int_0^t \sigma_i \, dW_s^i, \quad t \geq 0, \tag{3.3}$$

for $i = 1, \ldots, d$. Thus, by Itô's formula, we conclude that

$$\begin{aligned} Y_t^i &= Y_0^i + \int_0^t e^{U_s^i} X_s^i \, dU_s^i + \int_0^t e^{U_s^i} \, dX_s^i + \int_0^t e^{U_s^i} \, d[X^i, U^i]_s + \tfrac{1}{2} \int_0^t e^{U_s^i} X_s^i \, d[U^i, U^i]_s \\ &= Y_0^i - \int_0^t e^{U_s^i} X_s^i U_s^i \, ds - \sigma_i \int_0^t e^{U_s^i} X_s^i \, dW_s^i + \int_0^t e^{U_s^i} b_i(X_s) \, ds \\ &\quad + \sigma_i \int_0^t e^{U_s^i} X_s^i \, dW_s^i - \sigma_i^2 \int_0^t e^{U_s^i} X_s^i \, ds + \tfrac{1}{2} \sigma_i^2 \int_0^t e^{U_s^i} X_s^i \, ds \\ &= Y_0^i + \int_0^t e^{U_s^i} b_i \left(e^{-U_t} Y_t \right) ds - \int_0^t \left(U_s^i + \tfrac{1}{2} \sigma_i^2 \right) Y_s^i \, ds. \end{aligned}$$

where the initial value is $Y_0 = e^{U_0} X_0$, e^{U_t} denotes a vector with components $e^{U_t^i}$ for $i = 1, \ldots, d$, and b is the drift coefficient of (3.1). Hence, the auxiliary stochastic process Y_t fulfill the following RDE system:

$$\frac{dY_t}{dt} = f(Y_t, U_t) := e^{U_t} b \left(e^{-U_t} Y_t \right) - \left(U_t + \tfrac{1}{2} \sigma^2 \right) Y_t, \quad t \geq 0. \tag{3.4}$$

Now, we can numerically integrate equation (3.1) by using a numerical method for solving the RDE (3.4). In fact, let us consider a uniform partition $0 = t_0 < t_1 < \ldots < t_N = T$ of the time interval $[0, T]$, with $h = t_{n+1} - t_n < 1$ for $n = 0, \ldots, N-1$, and a numerical integrator $\hat{Y}_n$ for the RDE (3.4). In view of (3.4) we can construct the numerical approximation $\hat{X}_n$ for (3.1), defined by

$$\hat{X}_n^i = e^{-U_n^i} \hat{Y}_n^i, \qquad n = 1, \ldots, N, \ i = 1, \ldots, d \tag{3.5}$$

where U_n is a sample of the Ornstein-Uhlenbeck process (3.3) in t_n and the starting value U_0^i is selected from the stationary distribution of the Ornstein-Uhlenbeck process (3.3), i.e., $U_0^i \sim \mathcal{N}(0, \sigma_i^2/2)$, for $i = 1, \ldots, d$.

It is important to note that, since RDEs are analyzed pathwise by means of deterministic calculus, the derivation of numerical methods for RDEs is essentially carried out with specialized tools from deterministic calculus, similar to how numerical methods for deterministic equations are obtained. Therefore, convergence can typically be ensured by assuming a less stringent local Lipschitz condition on the vector field of the equation (3.4) than the global Lipschitz condition generally required for the convergence of numerical integrators for SDEs. In the sequel, two numerical methods for solving (3.4) are considered and, based on them, numerical schemes for the SDE (3.1) are proposed utilizing the strategy developed above.

3.2.2 Conjugated numerical methods

Based on the presented conjugacy between SDEs and RDEs, we propose new numerical approximations for the SDE (3.1). This is achieved by numerically integrating the conjugated RDE (3.4) using suitable numerical methods designed for RDEs. Specifically, we utilize a local linearization scheme for RDEs and the Heun method for RDEs. Henceforth, we will refer to these numerical approximations as conjugated methods.

Let $\hat{Y}_n$ be a numerical approximation for the auxiliary RDE (3.4), and let $\hat{X}_n$ represent the conjugated method for the SDE (3.1), which is obtained from the relationship described by equation (3.5). We then observe that

$$|\hat{X}_n - X_{t_n}| = |e^{-U_{t_n}}\hat{Y}_n - e^{-U_{t_n}}Y_{t_n}| = e^{-U_{t_n}}|\hat{Y}_n - Y_{t_n}|, \quad n = 1, \dots, N. \tag{3.6}$$

Subsequently, the pathwise convergence of the conjugated method $\hat{X}_n$ arises from the pathwise convergence of $\hat{Y}_n$, given that e^{-Ut} is bounded for all $t \leq T$. Furthermore, the conjugated method inherits the order of pathwise convergence from the RDE integrator.

However, over an extended period T, the quantity e^{-U_t} has the potential to grow significantly large, possibly compromising the accuracy of the approximation. To avert this scenario, we initialize U_0 with values drawn from the stationary distribution of the Ornstein-Uhlenbeck process (3.3), specifically $U_0^i \sim \mathcal{N}(0, \sigma_i^2/2)$ for $i = 1, \dots, d$. By adopting this approach, each U_t^i becomes a stationary Gaussian process, ensuring that

$$\mathbb{E}\left(U_t^i\right) = 0, \quad \textit{and} \quad \mathrm{Var}\left(U_t^i\right) = \tfrac{1}{2}\sigma_i^2, \quad t \geq 0.$$

Then, no matter how large t is, the distribution of U_t^i is very concentrated, and therefore

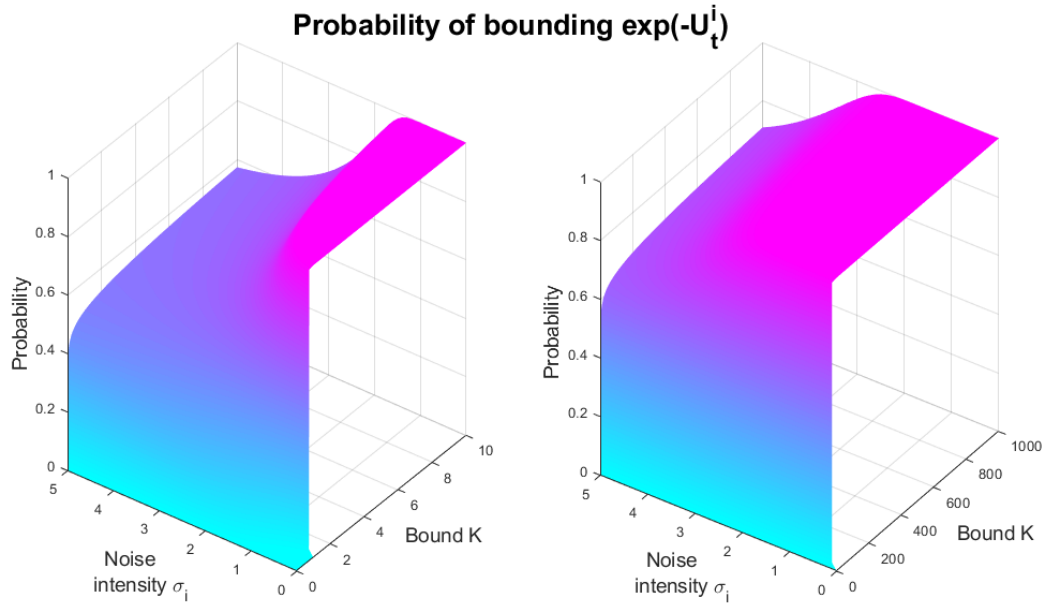

Figure 3.1: *Probabilities of bounding $e^{-U_t^i}$ by considering different bounds K and noise intensities σ_i.*

there exists a constant K such that $e^{-U_t^i} \leq K$ with high probability. In particular, 99.74% of the distribution is bounded by $e^{3\sigma_1^2/2}$. Here, the probability depends on the bound $K = K(\sigma)$. To investigate this dependence, we note that for any $K \geq 0$,

$$\begin{aligned}\mathbb{P}\left(e^{-U_t^i} \leq K\right) &= \mathbb{P}\left(U_t^i \geq -\log(K)\right) \\ &= \mathbb{P}\left(U_t^i \leq \log(K)\right) \\ &= \frac{1}{2}\left(1 + \operatorname{erf}\left(\frac{\sqrt{2}\log(K)}{\sigma_i^2}\right)\right).\end{aligned}$$

where erf refers to the error function. Using this, we calculate the probability values obtained for various bounds K and noise intensities σ_i. The results are shown in Figure 3.1, revealing that small values for the bound K emerge when the noise intensity is low. Notably, from Figure 3.2, we observe that for any intensity noise $\sigma \in [0, 5]$, there is an approximate $1/2$ probability that e^{-U_t} is bounded by values equal to or less than 1. Moreover, we also notice that for any intensity noise $\sigma \in [0, 5]$, there is an approximate 0.4 probability that e^{-U_t} is bounded by values equal to or less than 0.1.

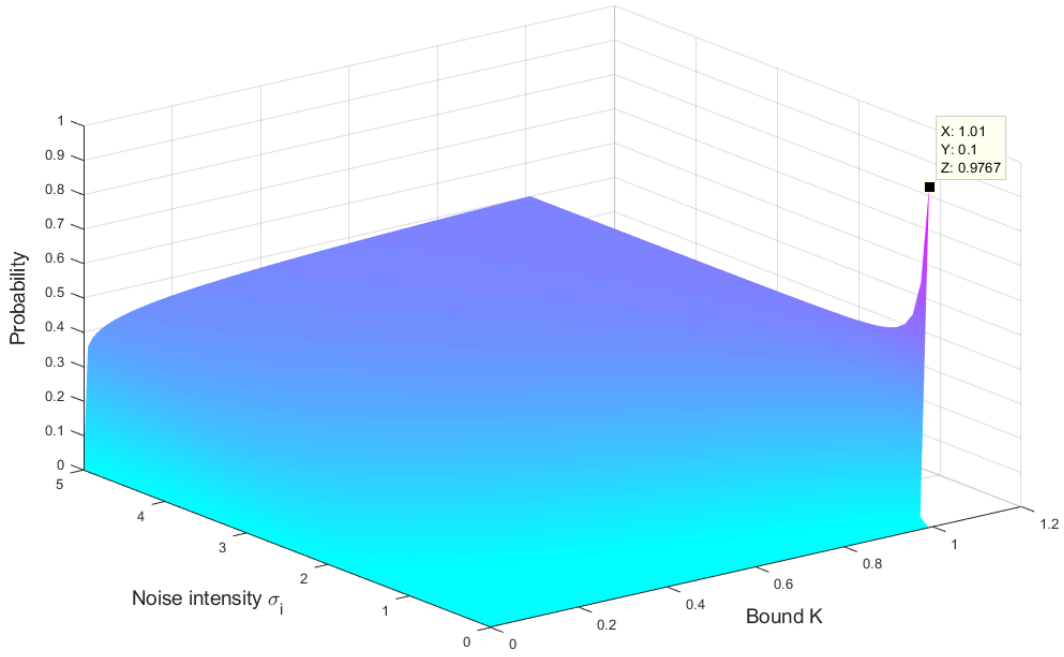

Figure 3.2: *Probabilities of bounding $e^{-U_t^i}$ by considering different bounds $K \leq 1.01$ and noise intensities $\sigma_i \in [0, 5]$.*

3.2.2.1 Conjugated Exponential Scheme

Among the numerical methods for RDE, the local linearization scheme proposed in [19] emerges as a suitable option for reproducing the stability of the system. The capability of local linearization schemes to reproduce the stability and dynamics of linear ODEs is well-known and is also hold for RDE. Additionally, numerical simulations in [19] illustrate its effectiveness even in equations with complicated noisy dynamics where conventional methods fail. Therefore, the local linearization method becomes an appealing choice for numerically solving the RDE system (3.4). Specifically, the local linearization method applied to the RDE (3.4) yields to

$$\begin{aligned}\hat{Y}_{n+1} = \hat{Y}_n &+ \int_0^h e^{J_y f(\hat{Y}_n, U_{t_n})(h-s)} f(\hat{Y}_n, U_{t_n}) ds \\ &+ \int_0^h \int_0^s e^{J_y f(\hat{Y}_n, U_{t_n})(h-s)} J_u f(\hat{Y}_n, U_{t_n}) \frac{U_{t_{n+1}} - U_{t_n}}{h} dr ds,\end{aligned} \tag{3.7}$$

where f is the vector field of the RDE, and $J_y f$ and $J_u f$ denote the Jacobian matrix of $f = f(y, u)$ with respect to y and u, respectively. According to [45], the iterative rule (3.7)

can be computed by

$$\hat{Y}_{n+1} = \hat{Y}_n + g(\hat{Y}_n, U_n; h)$$

where the vector $g(\hat{Y}_n, U_n; h)$ is defined by the block matrix

$$\begin{bmatrix} G_0(\hat{Y}_n, U_n; h) & G_1(\hat{Y}_n, U_n; h) & g(\hat{Y}_n, U_n; h) \\ \mathbf{0} & 1 & G_2(\hat{Y}_n, U_n; h) \\ \mathbf{0} & 0 & 1 \end{bmatrix} = \exp(h\mathbf{C}),$$

with

$$\mathbf{C} = \begin{bmatrix} J_y f(\hat{Y}_{t_n}, U_{t_n}) & J_u f(\hat{Y}_{t_n}, U_{t_n}) \frac{U_{n+1}-U_n}{h} & f(\hat{Y}_{t_n}, U_{t_n}) \\ \mathbf{0} & 0 & 1 \\ \mathbf{0} & 0 & 0 \end{bmatrix} \in \mathbb{R}^{(d+2)\times(d+2)}.$$

Therefore, from (3.4), we obtain the following numerical approximation for the SDE (3.1):

$$\begin{cases} \hat{X}_{n+1} = e^{-U_{n+1}} \hat{Y}_{n+1} \\ \hat{Y}_{n+1} = \hat{Y}_n + g(\hat{Y}_n, U_n; h), \end{cases} \tag{3.8}$$

Notice that the Jacobian matrices $J_y f(y,u)$ and $J_u f(y,u)$ in (3.2.2.1) can be computed directly in terms of the Jacobian $J_x b(x)$ of the drift coefficient b of the SDE (3.1):

$$\frac{\partial f_i}{\partial y_j}(y,u) = \begin{cases} \exp(u_i - u_j) \dfrac{\partial b_i}{\partial x_j}\left(e^{-u} y\right), & i \neq j, \\ \dfrac{\partial b_i}{\partial x_i}\left(e^{-u} y\right) - u_i - \dfrac{\sigma_i^2}{2}, & i = j, \end{cases} \tag{3.9}$$

and

$$\frac{\partial f_i}{\partial u_j}(y,u) = \begin{cases} -\exp(u_i - u_j) y_j \dfrac{\partial b_i}{\partial x_j}\left(e^{-u} y\right), & i \neq j, \\ e^{u_i} b_i\left(e^{-u} y\right) - y_i \dfrac{\partial b_i}{\partial x_i}\left(e^{-u} y\right) - y_i, & i = j, \end{cases} \tag{3.10}$$

where e^u denotes a vector with components e^{u_i}, for $i = 1, \ldots, d$. Furthermore, from (3.9) and (3.10), the computation of g does not require the numerical approximation $\hat{Y}_n$ of the auxiliary RDE (3.4). Instead, g can be directly computed from $\hat{X}_n$, U_{n+1}, and U_n. Thereafter, the

numerical approximation (3.8) for the SDE (3.1) can be explicitly formulated as follows:

$$\hat{X}_{n+1} = e^{-\Delta U_n}\hat{X}_n + e^{-U_{n+1}} g(\hat{X}_n, U_n; h), \tag{3.11}$$

where $\Delta U_n = U_{n+1} - U_n$. Henceforth, we shall refer to the numerical method (3.11) as the conjugated exponential scheme or the conjugated LL scheme.

3.2.2.2 Conjugated Heun Scheme

The Heun method for ODE is a multistep numerical approximation that is a Runge-Kutta method characterized by its order of convergence of two. This numerical method was adapted for RDE systems (see, e.g.,[32, 54]), performing a pathwise convergence error close to 1 for smooth vector fields. In particular, the Heun method for the RDE system (3.4) is given by

$$\hat{Y}_{n+1} = \hat{Y}_n + \frac{h}{2}\left\{ f(\hat{Y}_n, U_n) + f(\hat{Y}_n + hf(\hat{Y}_n, U_n), U_{n+1}) \right\}, \tag{3.12}$$

where f is the vector field of (3.4), and U_n is a sample of the Ornstein-Uhlenbeck process (3.3) in t_n. From this, we can compute a numerical approximation for the SDE (3.1) as $\hat{X}_{n+1} = e^{-U_{n+1}}\hat{Y}_{n+1}$. Specifically, from (3.4) we get an explicit formulation of (3.12),

$$\begin{aligned}\hat{Y}_{n+1} = \hat{Y}_n &+ \frac{h}{2}\left\{ e^{U_n} b_n + e^{U_{n+1}}\tilde{b}_n - \left(U_n + U_{n+1} + \sigma^2\right)\hat{Y}_n \right\} \\ &+ \frac{h^2}{2}\left(U_{n+1} + \frac{\sigma^2}{2}\right)\left\{ \left(U_n + \frac{\sigma^2}{2}\right)\hat{Y}_n - e^{U_n} b_n \right\},\end{aligned}$$

where e^{U_n} denotes a vector with components $e^{U_n^i}$, for $i = 1, \ldots, d$, $b_n = b\left(e^{-U_n}\hat{Y}_n\right)$,

$$\tilde{b}_n = b\left(\left\{1 - h\left(U_n + \sigma^2/2\right)\right\} e^{-U_{n+1}}\hat{Y}_n + he^{-(U_{n+1}-U_n)} b_n\right),$$

and b is the drift coefficient of (3.1). Hence, the conjugated Heun scheme for the SDE (3.1) is given by

$$\begin{aligned}\hat{X}_{n+1} = e^{-\Delta U_n}\hat{X}_n &+ \frac{h}{2}\left\{ \tilde{b}_n + e^{-\Delta U_n}\left(b_n - \left(U_n + U_{n+1} + \sigma^2\right)\hat{X}_n\right) \right\} \\ &+ \frac{h^2}{2} e^{-\Delta U_n}\left(U_{n+1} + \frac{\sigma^2}{2}\right)\left\{ \left(U_n + \frac{\sigma^2}{2}\right)\hat{X}_n - b_n \right\},\end{aligned} \tag{3.13}$$

where $\Delta U_n = U_{n+1} - U_n$. Note that in the computation of b_n and $\tilde{b}_n$, it is unnecessary to numerically approximate the auxiliary RDE (3.4). Instead, they can be directly computed from $\hat{X}_n$, U_{n+1}, and U_n. Specifically, $b_n = b(\hat{X}_n)$ and

$$\tilde{b}_n = b\left(\left\{1 - h\left(U_n + \sigma^2/2\right)\right\}\hat{X}_n + he^{-(U_{n+1}-U_n)}b_n\right).$$

3.3 Pathwise numerical simulation for the stochastic SVIR model

In this section, we address the numerical simulation of the stochastic SVIR model by employing the conjugated numerical approximations formulated in Section 3.2.1. First, we describe the stochastic SVIR model. Subsequently, we conduct a simulation study to illustrate the practical performance of the proposed methods.

3.3.1 The stochastic SVIR model

The basic compartmental model in epidemiology is the SIR model formulated by Kermack and McKendrick [50]. Thenceforth, several models have been proposed [26, 43, 60, 98]. A very remarkable adaptation of the SIR model which includes a continuous vaccination strategy was proposed in [59]. This Model is described by the following system of ODEs

$$\begin{cases} \dfrac{dS}{dt} = \mu - \beta SI - (\alpha + \mu)S, \\ \dfrac{dV}{dt} = \alpha S - \beta_1 VI - (\gamma_1 + \mu)V, \\ \dfrac{dI}{dt} = \beta SI + \beta_1 VI - (\gamma + \mu)I, \\ \dfrac{dR}{dt} = \gamma_1 V + \gamma I - \mu R. \end{cases} \tag{3.14}$$

Individuals are classified as susceptible, vaccinated, infected, or recovered, and their densities in time t are $S(t), V(t), I(t)$, and $R(t)$ respectively. Because of the recovered population R has no effect on the dynamics of S, V, and I, the system (3.14) is reduced to its three first equations. Since (3.14) monitors human populations, this model is studied on the region $\mathbb{R}^4_+ = \{(x_1, x_2, x_3, x_4) \in \mathbb{R}^4 : x_i \geq 0, \text{ for all } i = 1, 2, 3, 4\}$, its parameters, described in Table 1, are positive and it is assumed that $\beta_1 < \beta$. Moreover, the system (3.14) has a unique

Parameters	Description
μ	Recruitment rate and natural death rate
α	Vaccination rate
β	Disease transmission rate
β_1	Disease transmission rate for vaccinees before obtaining immunity
γ	Recovery rate of infected individuals
γ_1	Recovery rate of vaccinated individuals

Table 3.1: *SVIR model parameters description*

solution that remains on $\mathbb{R}^4_+$, for all $t \geq 0$.

As long as the disease does not spread, the disease-free equilibrium always exists and can be explicitly computed. However, when the disease spreads, the endemic equilibrium takes on an implicit form. The basic reproductive ratio R_0^C given by

$$R_0^C = \frac{\beta\mu}{(\mu+\alpha)(\mu+\gamma)} + \frac{\beta_1\mu\alpha}{(\mu+\gamma_1)(\mu+\alpha)(\mu+\gamma)},$$

is a threshold parameter that ensures that the SVIR Model's disease-free equilibrium is globally asymptotically stable if $R_0^C \leq 1$. Meanwhile, the endemic equilibrium is globally asymptotically stable if $R_0^C > 1$.

In [99] was investigated the dynamic behavior of the SVIR model (3.14) in random environments. Equation (3.14) is stochastically perturbed with environmental white noise and it is assumed that this perturbation is directly proportional to $S(t)$, $V(t)$, $I(t)$, and $R(t)$, yielding the stochastic SVIR model:

$$\begin{cases} dS = (\mu - \beta SI - (\alpha+\mu)S)\,dt + \sigma_1 S dW_t^1, \\ dV = (\alpha S - \beta_1 VI - (\gamma_1+\mu)V)\,dt + \sigma_2 V dW_t^2, \\ dI = (\beta SI + \beta_1 VI - (\gamma+\mu)I)\,dt + \sigma_3 I dW_t^3, \end{cases} \tag{3.15}$$

where $\sigma_i > 0$, for any $i = 1, 2, 3$, and W_t^i with $i = 1, 2, 3$ are independent Brownian motions. For this non-globally Lipschitz SDE system, several remarkable properties are established in [99]. First, system (3.15) has a unique solution $X = (S_t, V_t, I_t) \in \mathbb{R}^3_+$ for all $t \geq 0$ almost surely, provided an initial value $(S_0, V_0, I_0) \in \mathbb{R}^3_+$. This solution has the following asymptotic properties

$$\lim_{t\to\infty} \frac{X_t^i}{t} = 0, \quad a.s.; \quad \limsup_{t\to\infty} \frac{\log X_t^i}{t} \leq 0, \quad a.s.,$$

for all $i = 1, 2, 3$, and, when $\mu > \max_{k=1,2,3} \sigma_k^2/2$,

$$\lim_{t\to\infty} \frac{1}{t} \int_0^t X_s^i dW_s^i = 0, \quad a.s. \quad \forall\, i = 1, 2, 3.$$

Furthermore, two critical values can be introduced, namely,

$$R_0^s = \frac{\beta\mu}{(\mu+\alpha)(\mu+\gamma+\sigma_3^2/2)} + \frac{\beta_1\mu\alpha}{(\mu+\gamma_1)(\mu+\alpha)(\mu+\gamma+\sigma_3^2/2)},$$

and

$$\begin{aligned}\tilde{R}_0^s = &\frac{\beta\mu}{(\mu+\alpha+\sigma_1^2/2)(\mu+\gamma+\sigma_3^2/2)} \\ &+ \frac{\beta_1\mu\alpha}{(\mu+\alpha+\sigma_1^2/2)(\mu+\gamma_1+\sigma_2^2/2)(\mu+\alpha)(\mu+\gamma+\sigma_3^2/2)},\end{aligned}$$

which determines the spread of the disease. On the first hand, under the assumption $\mu > \max_{k=1,2,3} \sigma_k^2/2$, it is proved that

$$\limsup_{t\to\infty} \frac{\log I_t}{t} \leq \left(\mu+\gamma+\frac{\sigma_3^2}{2}\right)(R_0^s - 1), \qquad a.s.. \tag{3.16}$$

This implies that the disease will die out with probability one whenever $R_0^s < 1$.

On the other hand, it has been proven that

$$\limsup_{t\to\infty} \frac{1}{t} \int_0^t I_s ds \geq \frac{(\mu+\gamma+\sigma_3^2/2)\,(\tilde{R}_0^s - 1)}{(a_1+b_1)\beta + b_2\beta_1}, \qquad a.s.,$$

where $a_1 = \beta\mu/(\mu+\alpha+\sigma_1^2/2)$,

$$b_1 = \frac{\beta_1\mu\alpha}{(\mu+\alpha+\sigma_1^2/2)^2(\mu+\gamma_1+\sigma_2^2/2)}, \qquad b_2 = \frac{\beta_1\mu\alpha}{(\mu+\alpha+\sigma_1^2/2)(\mu+\gamma_1+\sigma_2^2/2)^2}.$$

i.e., the disease will prevail if $\tilde{R}_0^s > 1$.

Furthermore, when $\tilde{R}_0^s > 1$, system (3.15) has a unique stationary distribution, and its solution is ergodic. It is important to note that $R_0^s < R_0^c$, so the effect of environmental noise can suppress the outbreak of the epidemic. These results were tested by numerical simulation using the Milstein scheme which, despite being a method devised to integrate systems under

global Lipschitz conditions of the coefficients, it is commonly used for the study of stochastic epidemiological models, see for instance [17, 42, 51, 100, 101, 103].

3.3.2 Numerical-simulation results

In this section, we will illustrate the practical performance of the conjugated methods introduced in Sect. 3.2 through computer simulations. To accomplish this, we will conduct a comparative analysis with the Milstein method, as it has been considered in the literature for integrating the SVIR model [99]. Additionally, we will examine the Tamed Milstein schemes, which represent a direct enhancement of the Milstein method for integrating SDEs under non-globally Lipschitz assumptions.

3.3.2.1 Conjugated pathwise numerical approximation for the SVIR model

For the numerical simulation of the stochastic SVIR model, we utilize the conjugated pathwise numerical method proposed in Section 3.2.1. Specifically, we apply the exponential scheme (3.11) and the Heun scheme (3.13), considering the drift coefficient from (3.14), i.e.,

$$\begin{cases} b_1(x) = \mu - \beta x_1 x_3 - (\alpha + \mu)x_1, \\ b_2(x) = \alpha x1 - \beta_1 x_2 x_3 - (\gamma_1 + \mu)x_2, \\ b_3(x) = \beta x_1 x_3 + \beta_1 x_2 x_3 - (\gamma + \mu)x_3. \end{cases} \tag{3.17}$$

From (3.9) and (3.10), we note that the only necessary input for computing the iterative rule of the conjugated LL method (3.11) is the Jacobian matrix Jb. In particular, from (3.17), the Jacobian matrix Jb for the drift coefficient of the stochastic SVIR model is given by

$$Jb(x) = \begin{bmatrix} -\beta x_3 - (\alpha + \mu) & 0 & -\beta x_1 \\ \alpha & -\beta_1 x_3 - (\gamma_1 + \mu) & -\beta_1 x_2 \\ \beta x_3 & \beta_1 x_3 & \beta x_1 + \beta_1 x_2 - (\gamma + \mu) \end{bmatrix}.$$

3.3.2.2 Numerical consideration

Let us set some quantities that will be considered, for comparison purposes in the numerical experiments below. To assess the performance of the different integrators, we will measure the average results using two metrics: the trajectory error (TE), which quantifies the accuracy of

the approximation for a single trajectory, and the ergodic limit error (ELE), which measures the accuracy of the approximation for the ergodic limit. In addition, we also measure the relative results using the relative trajectory error (RTE) and the relative ergodic limit error (RELE).

Let $(t)_h = \{t_n : n = 0, 1, \ldots, N\}$ be a uniform partition of the time interval $[0, T]$ with stepsize h, defined as a sequence of times $0 = t_0 < t_1 < \ldots < t_N = T$ such that $h = t_{n+1} - t_n < 1$ for $n = 0, \ldots, N-1$. For a numerical approximation $\hat{X} = [S, V, I]$ to the solution of (3.15), the TE is defined by

$$TE(\hat{X}, T) = \frac{h}{T} \sum_{k=1}^{T/h} \left(\sum_{i=1}^{3} \left| \hat{X}^i(t_k; x) - X^i_{exact}(t_k; x) \right|^2 \right)^{1/2}, \tag{3.18}$$

and the RTE for the components of X is given by

$$RTE(\hat{X}^i, T) = \frac{h}{T} \sum_{k=1}^{T/h} \left| \frac{\hat{X}^i(t_k; x) - X^i_{exact}(t_k; x)}{X^i_{exact}(t_k; x)} \right|^2. \tag{3.19}$$

Here $\hat{X}^i(t_k; x)$ denotes the i-th component of the numerical approximation $\hat{X}$, with initial value $\hat{X}(0; x) = x$, at time t_k. Similarly, $X^i_{exact}(t_k; x)$ denotes the i-th component of the exact solution of (3.15), with initial value $X_{exact}(0; x) = x$, at time t_k.

On the other hand, the ELE is defined by

$$ELE(\varphi, \hat{X}) = \left(\sum_{i=1}^{3} \left| \varphi^{erg}(\hat{X}^i) - \varphi^{erg}(X^i_{exact}) \right|^2 \right)^{1/2}, \tag{3.20}$$

and the RELE is given by

$$RELE(\varphi, \hat{X}^i) = \left| \frac{\varphi^{erg}(\hat{X}^i) - \varphi^{erg}(X^i_{exact})}{\varphi^{erg}(X^i_{exact})} \right|^2, \quad i = 1, 2, 3. \tag{3.21}$$

Here $\varphi^{erg}(X)$ is the ergodic limit, defined by

$$\varphi^{erg}(X) = \int \varphi(x) d\mu(x) = \lim_{t \to \infty} E\varphi(X_t),$$

for a smooth function φ, where $\mu(x)$ is the unique invariant measure of the ergodic process

X [67]. This quantity can be approximated via Monte Carlo method by

$$\hat{\varphi}^{erg} = \frac{1}{M}\sum_{m=1}^{M} \varphi(\hat{X}^{(m)}(T;x)), \tag{3.22}$$

where $\hat{X}^{(m)}$ for $m = 1,\dots,M$ are independent simulated trajectories of X. Besides, the ergodic limit $\varphi^{erg}(X)$ also can be approximated based on a single simulated trajectory of X by

$$\check{\varphi}^{erg} = \sum_{k=1}^{T/h} \varphi(\hat{X}(kh;x)) \tag{3.23}$$

for a large value of T, provided that (3.15) is an ergodic system. Here $\varphi^{erg}(X_{exact})$ is computed by (3.23) for a long simulation time T, where the reference exact solution X_{exact} is computed using the Tamed Milstein scheme with a finer stepsize $h_{exact} = 2^{-13}$. We will refer to $ELE(\varphi,\hat{X})$ as Monte Carlo ELE when (3.20) is computed by mean of (3.22) and we will call it trajectorial ELE when (3.20) is computed by means of (3.23). Analogously, We will refer to $RELE(\varphi,\hat{X})$ as Monte Carlo RELE when (3.21) is computed by means of (3.22), and we will refer as trajectorial RELE when (3.21) is computed by means of (3.23).

To make the results of the simulation with each of the numerical methods and stepsizes comparable, the trajectories computed with the methods must be generated from the same Wiener realization. Consequently, the Wiener process paths and the Ornstein-Uhlenbeck processes paths should be simultaneously generated from the same source of randomness. For this, we use results from [22] to simulate each independent component of the Ornstein-Uhlenbeck process (3.3) and the underlying Wiener process by

$$\begin{aligned} U^i_{n+1} &= U^i_n + \begin{bmatrix} 0 & 1 \end{bmatrix}\left(M_{13}\begin{bmatrix} 0 \\ 1 \end{bmatrix}\left(-U^i_n\right) + PD^{1/2}\begin{bmatrix} \mathcal{N}_1^{i,n} & \mathcal{N}_2^{i,n} \end{bmatrix}^\top \right), \\ W^i_{n+1} &= W^i_n + PD^{1/2}\begin{bmatrix} \mathcal{N}_1^{i,n} & \mathcal{N}_2^{i,n} \end{bmatrix}^\top, \end{aligned}$$

for $i = 1,2,3$, where $\mathcal{N}_1^{i,n}$ and $\mathcal{N}_2^{i,n}$ are independent samples from the standard normal

distribution and the matrices P and D are given by $PDP^\top = M_{12}M_{11}^\top$, where M satisfies

$$M = \begin{bmatrix} M_{11} & M_{12} & M_{13} \\ \mathbf{0} & - & - \\ \mathbf{0} & \mathbf{0} & - \end{bmatrix} = \exp(Ch),$$

with

$$C = \begin{bmatrix} B & \Lambda & \mathbb{I} \\ \mathbf{0} & -B^\top & \mathbf{0} \\ \mathbf{0} & \mathbf{0} & \mathbf{0} \end{bmatrix} \in \mathbb{R}^{6\times 6}, \qquad B = \begin{bmatrix} 0 & 0 \\ 0 & -1 \end{bmatrix}, \text{and} \qquad \Lambda = \begin{bmatrix} 1 & \sigma_i \\ \sigma_i & \sigma_i^2. \end{bmatrix}.$$

3.3.2.3 Numerical Experiments

For the numerical tests below, based on example 1 in [99], we use the following parameters for the SVIR system: $\mu = 1$, $\beta = 15$, $\alpha = 15$, $\beta_1 = 10$, $\gamma = 1.5$, $\gamma_1 = 0.4$, and an initial value of $(S_0, I_0, V_0) = (0.4, 0.4, 0.2)$. We then evaluate the performance of the numerical methods for two possible scenarios that depend on the noise intensities σ_k: the free disease case and the endemic one (see Sec. 3.3). For both cases, we calculate the relative trajectory errors (3.19). Additionally, for the first case, we compute the value of $\limsup_{t\to\infty} \log I_t/t$ to evaluate if the diseases free bound (3.16) is reproduced by the numerical integrators. For the second case, we compute the Trajectory RELE (3.21)-(3.23) and MC RELE (3.21)-(3.22). From now on, we say that the simulated trajectory is meaningful when the densities generated by S_t, V_t, and I_t are positive, and $S_t + V_t + I_t \leq 1$ for all simulation time $t \in [0, T]$. Otherwise, we refer to it as a bad trajectory.

Case 1

We take noise magnitudes $\sigma_1 = \sigma_2 = \sigma_3 = 0.825$, so that $\mu = 1 > 0.3403 = \max_{k=1,\dots,3} \sigma_k^2/2$, and

$$R_0^s = \frac{\beta\mu}{(\mu+\alpha)(\mu+\gamma+\sigma_3^2/2)} + \frac{\beta_1\mu\alpha}{(\mu+\gamma_1)(\mu+\alpha)+(\mu+\gamma+\sigma_3^2/2)} = 0.99021.$$

Therefore, the disease will die out in this case. For this disease free scenario, the simulations were carried out in the interval $[0, 10^4]$. The numerical results are presented in Table 3.2 and Table 3.3, as well as in Figure 3.3 and Figure 3.4.

In Figure 3.3, are shown the TEs of the four numerical schemes for different stepsizes.

Scheme	Individuals	$h = 2^{-2}$	$h = 2^{-3}$	$h = 2^{-4}$	$h = 2^{-5}$	$h = 2^{-6}$
Milstein	S	-	-	$1.1599 \cdot 10^{-2}$	$1.6824 \cdot 10^{-3}$	$3.3999 \cdot 10^{-4}$
	V	-	-	$4.2159 \cdot 10^{-3}$	$7.3388 \cdot 10^{-4}$	$1.5996 \cdot 10^{-4}$
	I	-	-	$9.5612 \cdot 10^{-1}$	$8.5973 \cdot 10^{-1}$	$3.5899 \cdot 10^{-1}$
T. Milstein	S	$3.5537 \cdot 10^{-1}$	$3.5537 \cdot 10^{-1}$	$1.1100 \cdot 10^{-2}$	$1.6638 \cdot 10^{-3}$	$3.3855 \cdot 10^{-4}$
	V	4.4040	$9.4655 \cdot 10^{-2}$	$4.0282 \cdot 10^{-3}$	$7.2640 \cdot 10^{-4}$	$1.5934 \cdot 10^{-4}$
	I	1.0024	$9.9720 \cdot 10^{-1}$	$2.5315 \cdot 10^{1}$	$7.3266 \cdot 10^{5}$	$3.7205 \cdot 10^{3}$
Exponential	S	$1.6400 \cdot 10^{-2}$	$5.3065 \cdot 10^{-3}$	$1.5885 \cdot 10^{-3}$	$4.2230 \cdot 10^{-4}$	$1.0728 \cdot 10^{-4}$
	V	$1.0836 \cdot 10^{-2}$	$3.9868 \cdot 10^{-3}$	$1.2641 \cdot 10^{-3}$	$3.5465 \cdot 10^{-4}$	$9.4673 \cdot 10^{-5}$
	I	$9.9806 \cdot 10^{-1}$	$9.9744 \cdot 10^{-1}$	$9.9646 \cdot 10^{-1}$	$9.9490 \cdot 10^{-1}$	$9.9180 \cdot 10^{-1}$
Heun	S	-	-	$2.3738 \cdot 10^{-3}$	$4.3263 \cdot 10^{-4}$	$1.0244 \cdot 10^{-4}$
	V	-	-	$7.9706 \cdot 10^{-4}$	$1.5693 \cdot 10^{-4}$	$3.7338 \cdot 10^{-5}$
	I	-	-	$9.2981 \cdot 10^{-1}$	$7.2606 \cdot 10^{-1}$	$1.9437 \cdot 10^{-1}$

Table 3.2: *RTEs for the four numerical methods with different integration times h. Results have been taken by a single trajectory with reference solution simulated by the Tamed Milstein scheme with step-size $h = 2^{-13}$. The random variables used in the simulation of the numerical methods, for the different step-size h, are taken by the same simulated trajectory of the random process used in the reference solution*

Detailed results can be found in Table 3.2, which provides the RTEs (3.19) for the same simulation. From these results, we observe that all the numerical methods yield meaningful trajectories for the time-steps $h = 2^{-6}$ and $h = 2^{-5}$. Of all of them, the Heun and Exponential schemes exhibit the most accurate results. Despite the small error produced by the numerical methods for the stepsize $h = 2^{-4}$, only the Exponential scheme achieves meaningful trajectories. Additionally, the Exponential scheme also computes meaningful trajectories for the stepsize $h = 2^{-3}$. In contrast, for $h = 2^{-3}, 2^{-2}, 2^{-1}$, the Milstein and Heun schemes exhibit explosive trajectories, while the Tamed Milstein method yields negative densities or violates the condition $S_{t_n} + V_{t_n} + I_{t_n} \leq 1$.

The erroneous results resulting from the Tamed Milstein scheme for the Infected density I_t are produced by the normalization involved in the RTE (3.19). This because the disease does not spread out, and the numerical schemes do not converge at the same rate to zero. This behavior is also shown by the other numerical schemes where different noise magnitudes σ_k are chosen. Besides, for this example, when we compute the trajectory error without normalization, the Tamed Milstein scheme gives similar results to the Milstein scheme.

In Figure 3.4, are presented simulation results of the evolution of the densities S_t, V_t, and I_t for the different numerical methods with stepsize $h = 2^{-3}$. Here, the exponential scheme shows a meaningful trajectory, and the Milstein and Heun schemes show explosive trajectories before $t = 2.5$. In addition, we observe that although the Tamed Milstein scheme provides

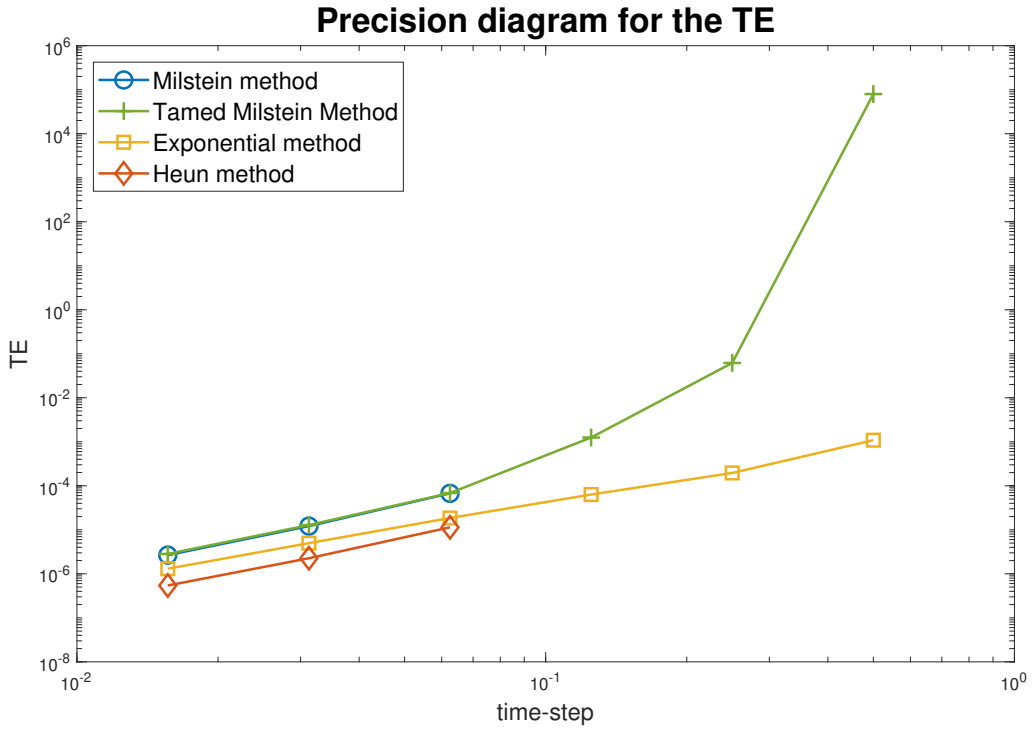

Figure 3.3: *Trajectory errors (TEs) of the numerical methods for Case 1, with* $R_0^s < 1$*, are evaluated using different stepsizes* h*. In the simulations, the Tamed Milstein scheme with a stepsize* $h = 2^{-13}$ *is used as the reference solution.*

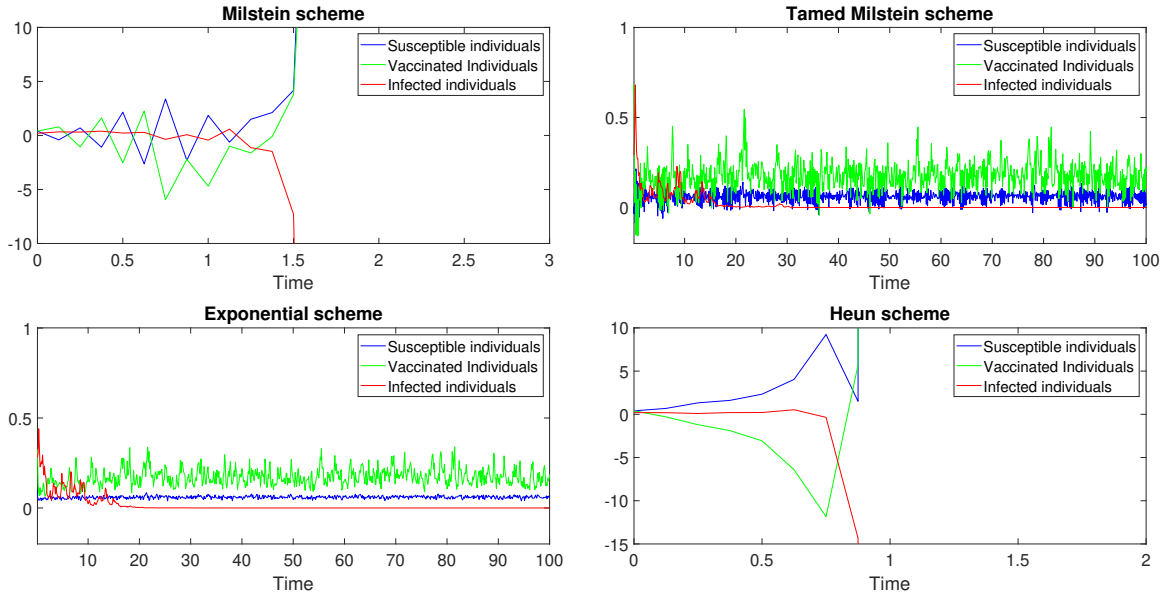

Figure 3.4: *A single trajectory of the evolution of the densities S_t, V_t, and I_t simulated for the Milstein, Tamed Milstein, Exponential, and Heun schemes, using an integration time $h = 2^{-3}$.*

bounded trajectories with regular dynamics, it gets meaningless values several times.

In table 3.3 the reproduction by the numerical schemes of the property (3.16) is tested. To this end were simulated 10^3 trajectories for each of the different numerical methods and computed the trajectory $t \to \log I_t/t$ in the entire simulation interval $[0, 10^4]$. When the upper bound is reached in times $t = 1000, 2500, 5000, 7500, 10000$, we take the average in the 10^3 independent trajectories. Here, all the trajectories were selected so as to ensure that for given simulated random processes W and U, the trajectories obtained from the four numerical methods are meaningful.

From table 3.3, we note that for the stepsize $h = 2^{-6}$ and $h = 2^{-5}$ all the trajectories for the four methods show meaningful densities. However, For the stepsize $h = 2^{-4}$ the Milstein, the Tamed Milstein, and the Heun scheme show $121, 19$ and 10 bad trajectories, respectively. In addition, we observe that for $h = 2^{-3}$ the exponential scheme gives only one bad trajectory and all of the 1000 trajectories match the upper bound. In contrast, for $h = 2^{-3}$, the other numerical methods do not achieve any meaningful trajectory. Even worst, the Milstein scheme and Heun scheme have explosive behavior for all the trajectories.

Scheme	h	$t = 1000$	$t = 2500$	$t = 5000$	$t = 7500$	$t = 10000$
Milstein	2^{-6}	0.709	0.641	0.618	0.604	0.579
	2^{-5}	0.724	0.665	0.632	0.586	0.596
	2^{-4}	0.752	0.701	0.684	0.671	0.686
T. Milstein	2^{-6}	0.700	0.630	0.598	0.580	0.531
	2^{-5}	0.707	0.634	0.571	0.519	0.525
	2^{-4}	0.714	0.636	0.566	0.538	0.535
Exponential	2^{-6}	0.910	0.938	0.976	0.988	0.994
	2^{-5}	0.979	0.997	1.000	1.000	1.000
	2^{-4}	0.999	1.000	1.000	1.000	1.000
Heun	2^{-6}	0.710	0.642	0.620	0.608	0.580
	2^{-5}	0.722	0.670	0.634	0.586	0.597
	2^{-4}	0.754	0.697	0.661	0.650	0.664

Table 3.3: *Proportion of trajectories that fulfill the upper bound* (3.16)*. Results are obtained from the simulation of* 10^3 *independent meaningful trajectories*

Case 2

For the endemic scenario, we take noise magnitudes $\sigma_1 = \sigma_2 = \sigma_3 = 0.625$, so that $\mu = 1 > 0.1953 = \max_{k=1,\dots,3} \sigma_k^2/2$, and

$$\tilde{R}_0^s = \frac{\beta\mu}{(\mu+\alpha+\sigma_1^2/2)(\mu+\gamma+\sigma_3^2/2)} + \frac{\beta_1\mu\alpha}{(\mu+\gamma_1\sigma_1^2/2)(\mu+\alpha+\sigma_2^2/2)+(\mu+\gamma+\sigma_3^2/2)} = 1.0051.$$

Thereby, the disease will spread out in this case. For this scenario, the simulations were carried out in the interval $[0, 10^5]$. The numerical results are summarized in Tables 3.4–3.6, as well as in Figures 3.5–3.8.

In Figure 3.5, are shown the TEs of the four numerical schemes for different stepsizes. Detailed results can be found in Table 3.4, which provides the RTEs (3.19) for the same simulation. From these results, we observe that all the numerical methods yield meaningful trajectories for $h = 2^{-6}$ and $h = 2^{-5}$. Among them, the Heun method exhibits the most accurate results. However, for the slightly larger $h = 2^{-4}$, both the Milstein method and the Tamed Milstein method fail to produce meaningful trajectories. In contrast, the methods proposed in this work demonstrate good performance, with the Heun method yielding the most accurate results. Additionally, we observe that for the stepsize $h = 2^{-3}$, only the exponential scheme computes significant densities. This pattern also occurs for $h = 2^{-2}$ and $h = 2^{-1}$, although for these stepsizes, negative density values are encountered at certain points in the time partition. It is worth noting that this behavior can be expected due to the larger value of h. All the other methods yield adverse results in this case.

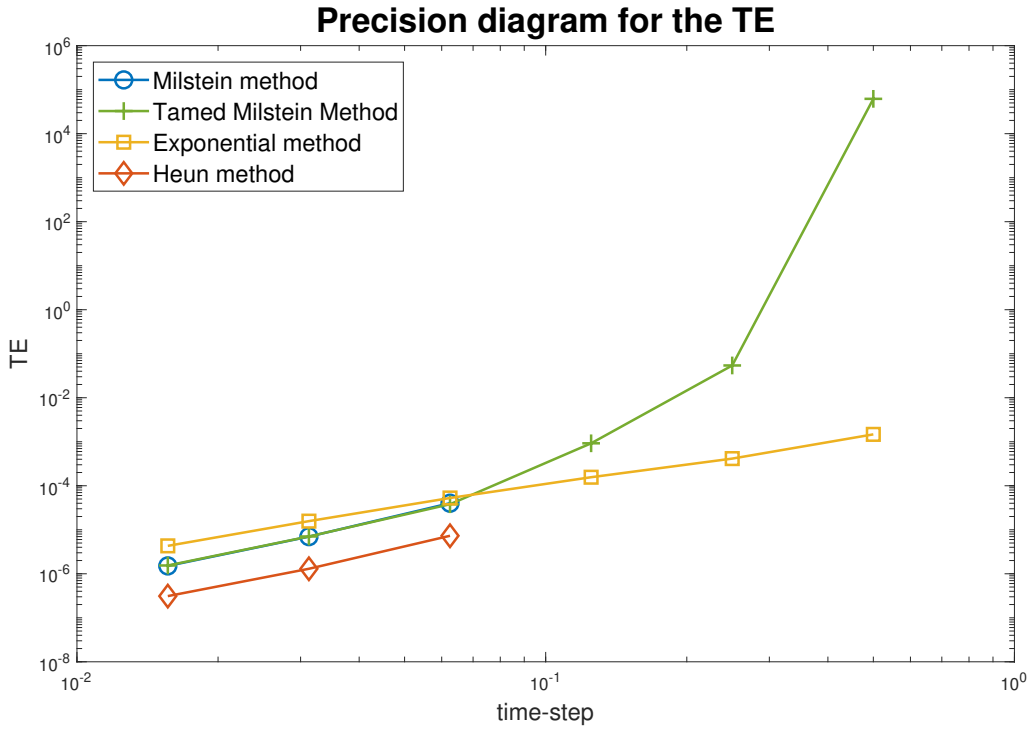

Figure 3.5: *Trajectory errors (TEs) of the numerical methods for Case 2, with $R_0^s > 1$, are evaluated using different stepsizes h. In the simulations, the Tamed Milstein scheme with a stepsize $h = 2^{-13}$ is used as the reference solution.*

Scheme	Individuals	$h = 2^{-2}$	$h = 2^{-3}$	$h = 2^{-4}$	$h = 2^{-5}$	$h = 2^{-6}$
Milstein	S	-	-	$6.5336 \cdot 10^{-3}$	$9.6731 \cdot 10^{-4}$	$1.9643 \cdot 10^{-4}$
	V	-	-	$2.3434 \cdot 10^{-3}$	$4.1112 \cdot 10^{-4}$	$8.9752 \cdot 10^{-5}$
	I	-	-	$1.4412 \cdot 10^{-2}$	$3.7335 \cdot 10^{-3}$	$8.2579 \cdot 10^{-4}$
T. Milstein	S	$1.8073 \cdot 10^{1}$	$2.6998 \cdot 10^{-1}$	$9.5983 \cdot 10^{-3}$	$9.5910 \cdot 10^{-4}$	$1.9593 \cdot 10^{-4}$
	V	3.9202	$7.1679 \cdot 10^{-2}$	$2.2690 \cdot 10^{-3}$	$4.6605 \cdot 10^{-4}$	$9.0099 \cdot 10^{-5}$
	I	1.0026	$1.7401 \cdot 10^{-1}$	$2.1580 \cdot 10^{-2}$	$5.6254 \cdot 10^{-3}$	$1.1117 \cdot 10^{-3}$
Exponential	S	$7.7647 \cdot 10^{-3}$	$3.1076 \cdot 10^{-3}$	$9.8935 \cdot 10^{-4}$	$2.6853 \cdot 10^{-4}$	$6.8702 \cdot 10^{-5}$
	V	$1.6388 \cdot 10^{-2}$	$4.6673 \cdot 10^{-3}$	$1.6460 \cdot 10^{-3}$	$4.6605 \cdot 10^{-4}$	$1.1977 \cdot 10^{-4}$
	I	$9.3508 \cdot 10^{-1}$	$6.6040 \cdot 10^{-1}$	$3.8426 \cdot 10^{-1}$	$1.9443 \cdot 10^{-1}$	$8.3732 \cdot 10^{-2}$
Heun	S	-	-	$1.3698 \cdot 10^{-3}$	$2.5031 \cdot 10^{-4}$	$5.9304 \cdot 10^{-5}$
	V	-	-	$4.5113 \cdot 10^{-4}$	$9.0506 \cdot 10^{-5}$	$2.1682 \cdot 10^{-5}$
	I	-	-	$4.1470 \cdot 10^{-3}$	$8.2586 \cdot 10^{-4}$	$1.8080 \cdot 10^{-4}$

Table 3.4: *RTEs for the four numerical methods with different integration times h. Results have been taken by a single trajectory with reference solution simulated by the Tamed Milstein scheme with step-size $h = 2^{-13}$. The random variables used in the simulation of the numerical methods, for the different step-size h, are taken by the same simulated trajectory of the random process used in the reference solution*

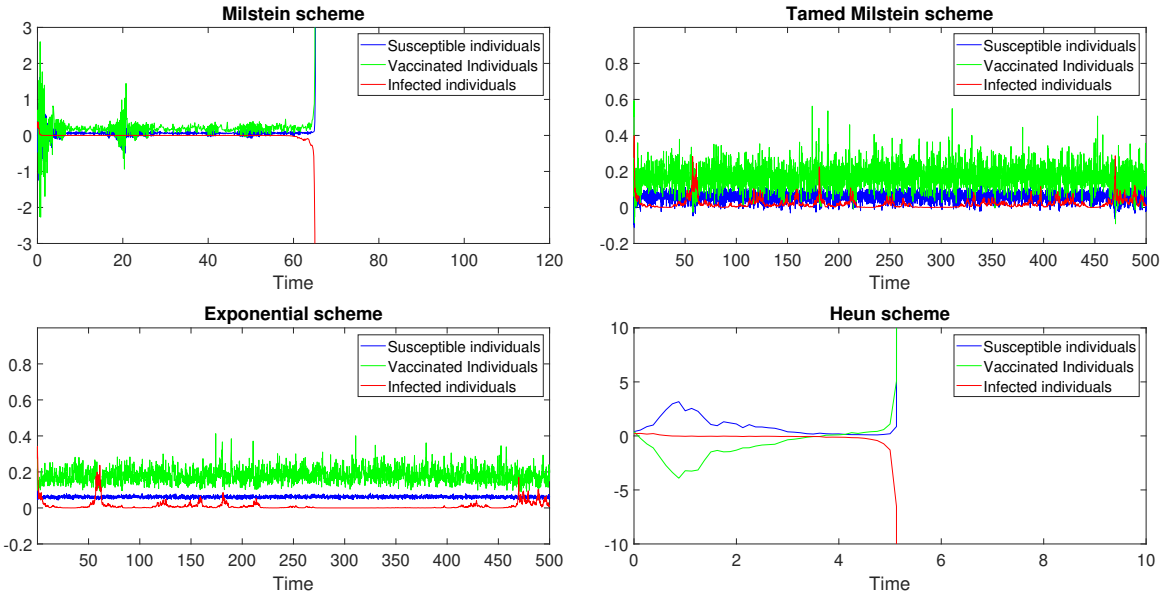

Figure 3.6: *A single trajectory of the evolution of the densities S_t, V_t, and I_t simulated for the Milstein, Tamed Milstein, Exponential, and Heun schemes, using an integration time $h = 2^{-3}$.*

Figure 3.6 shows the simulation results of the evolution of the densities S_t, V_t, and I_t for the different numerical methods with stepsize $h = 2^{-3}$. This clearly shows that the exponential scheme produces a meaningful trajectory, while the Milstein and Heun schemes give explosive trajectories in times $t = 70$ and $t = 6$. We also note that, although the Tamed Milstein scheme provides bounded trajectories with regular dynamics, the involved densities get several meaningless values.

In Figure 3.7, we present the trajectorial ELEs for the functional $\varphi(x) = x^2$ of the four numerical schemes using different stepsizes. Detailed results can be found in Table 3.5, which provides the trajectorial RELEs (3.21) for the same simulation. From these results, we observe that for the stepsizes $h = 2^{-6}$, 2^{-5}, 2^{-4}, the most accurate results are obtained by the Heun scheme and the exponential scheme. In addition, we note that the exponential scheme has a good performance even for $h = 2^{-3}, 2^{-2}, 2^{-1}$.

In Figure 3.8, are shown the MC ELEs for the functional $\varphi(x) = x^2$ of the four numerical schemes using different stepsizes. Detailed results can be found in Table 3.6, which provides the MC RELEs (3.21) Here, the Monte Carlo simulations for the time steps $h = 2^{-6}$, 2^{-5}, 2^{-4}, were performed with 10^4 independent trajectories simulated on the interval $[0, 500]$. All the trajectories in the Monte Carlo simulations were selected ensuring that for the simulated

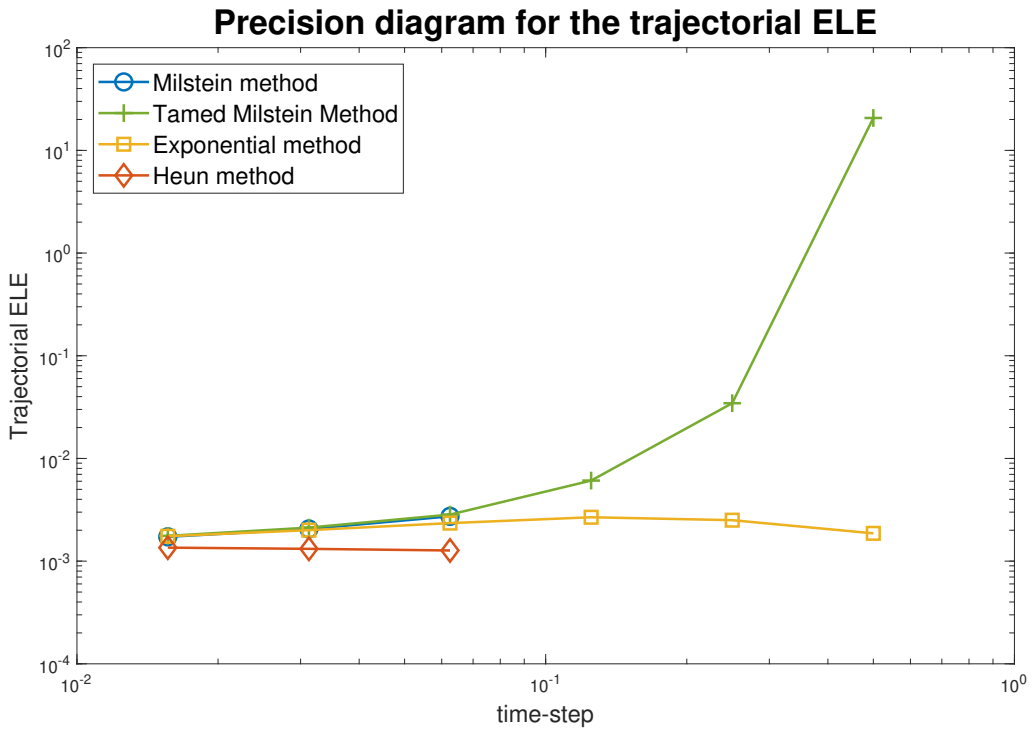

Figure 3.7: *Trajectorial ergodic limit errors (ELEs) of the four numerical methods with different time-steps h. Results have been taken by a single trajectory with reference solution simulated by the Tamed Milstein scheme with stepsize $h = 2^{-13}$. The random variables used in the simulation of the numerical methods, for the different time-steps h, are taken by the same simulated trajectory of the random process used in the reference solution.*

Scheme	Individuals	$h = 2^{-2}$	$h = 2^{-3}$	$h = 2^{-4}$	$h = 2^{-5}$	$h = 2^{-6}$
Milstein	S_t	-	-	$1.4025 \cdot 10^{-2}$	$4.6483 \cdot 10^{-3}$	$1.9770 \cdot 10^{-3}$
	V_t	-	-	$1.3367 \cdot 10^{-2}$	$5.5448 \cdot 10^{-3}$	$2.5653 \cdot 10^{-3}$
	I_t	-	-	$3.5185 \cdot 10^{-2}$	$1.3905 \cdot 10^{-2}$	$6.1128 \cdot 10^{-3}$
T. Milstein	S_t	$1.5902 \cdot 10^{1}$	$2.4997 \cdot 10^{-1}$	$1.3994 \cdot 10^{-2}$	$4.6867 \cdot 10^{-3}$	$1.9880 \cdot 10^{-3}$
	V_t	3.0811	$8.7237 \cdot 10^{-2}$	$1.4787 \cdot 10^{-2}$	$6.1537 \cdot 10^{-3}$	$2.8484 \cdot 10^{-3}$
	I_t	$9.8497 \cdot 10^{-1}$	$1.8823 \cdot 10^{-1}$	$1.0262 \cdot 10^{-2}$	$3.0001 \cdot 10^{-3}$	$1.1339 \cdot 10^{-3}$
Exponential	S_t	$3.8741 \cdot 10^{-2}$	$1.0224 \cdot 10^{-2}$	$8.9471 \cdot 10^{-4}$	$9.3803 \cdot 10^{-4}$	$8.5324 \cdot 10^{-4}$
	V_t	$1.0678 \cdot 10^{-2}$	$1.2786 \cdot 10^{-2}$	$9.5170 \cdot 10^{-3}$	$5.8052 \cdot 10^{-3}$	$3.2129 \cdot 10^{-3}$
	I_t	$9.4910 \cdot 10^{-1}$	$6.9907 \cdot 10^{-1}$	$4.5736 \cdot 10^{-1}$	$2.0988 \cdot 10^{-1}$	$1.4380 \cdot 10^{-1}$
Heun	S_t	-	-	$3.3744 \cdot 10^{-3}$	$8.3828 \cdot 10^{-4}$	$1.9850 \cdot 10^{-4}$
	V_t	-	-	$2.7725 \cdot 10^{-5}$	$4.9906 \cdot 10^{-5}$	$1.6254 \cdot 10^{-5}$
	I_t	-	-	$1.1056 \cdot 10^{-2}$	$2.8941 \cdot 10^{-3}$	$4.4879 \cdot 10^{-4}$

Table 3.5: *Trajectory RELE with $\phi(x) = x^2$, for the four numerical method and different integration times. Results have been taken by the same simulations of Table 3.4.*

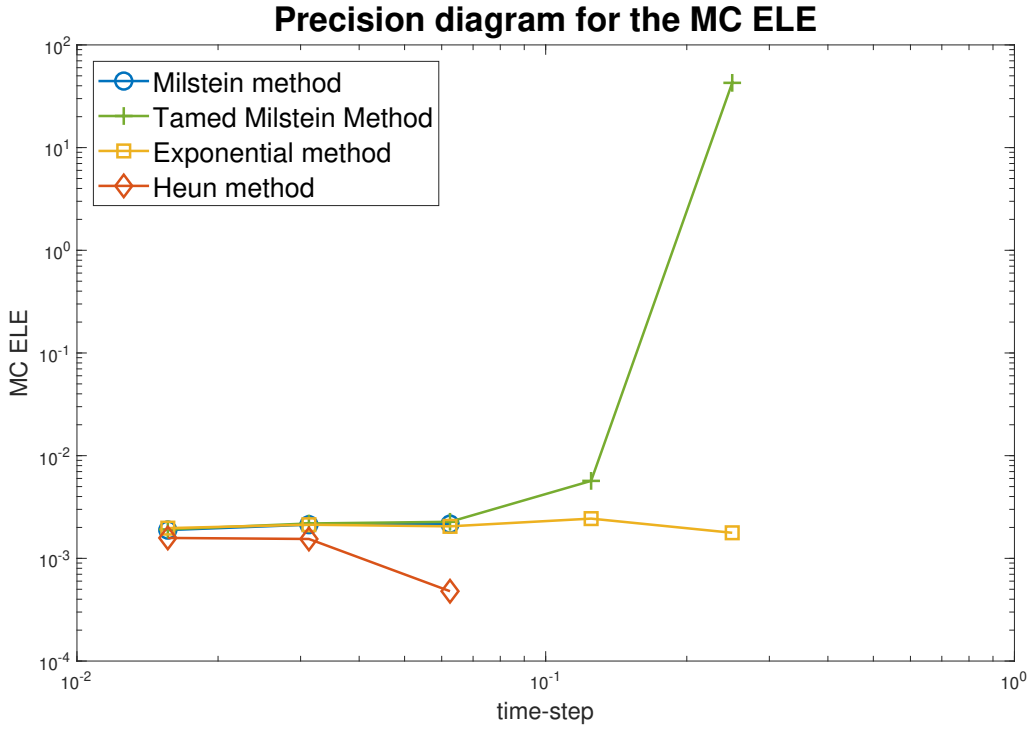

Figure 3.8: *Monte Carlo ergodic limit errors (MC ELEs) of the four numerical methods with different time-steps h. Results have been taken by a single trajectory with reference solution simulated by the Tamed Milstein scheme with stepsize $h = 2^{-13}$. The random variables used in the simulation of the numerical methods, for the different time-steps h, are taken by the same simulated trajectory of the random process used in the reference solution.*

random processes, W and U, the four numerical methods produce meaningful densities. The Monte Carlo simulations for the stepsize $h = 2^{-3}$ and $h = 2^{-2}$ were also performed with 10^4 independent trajectories.

In the results presented in Figure 3.8 and Table 3.6, no wrong trajectories were observed for the stepsize $h = 2^{-6}$ and $h = 2^{-5}$ for all numerical methods. Of all these methods, the Heun method yields the most accurate results. However, for the slightly larger stepsize $h = 2^{-4}$, Milstein, Tamed Milstein, and Heun methods produce 352, 31, and 47 bad trajectories, respectively. When the stepsize is $h = 2^{-3}$, the Tamed Milstein method fails to produce any significant trajectory, all them having negative densities. On the other hand, the Milstein method exhibits explosive behavior in most of the trajectories. Notably, the exponential scheme stands out from the other methods producing a few wrong trajectories. Furthermore, for the stepsize $h = 2^{-2}$, the exponential scheme also demonstrates a very good performance.

Scheme	Individuals	$h = 2^{-2}$	$h = 2^{-3}$	$h = 2^{-4}$	$h = 2^{-5}$	$h = 2^{-6}$
Milstein	S	-	-	$1.4924 \cdot 10^{-2}$	$4.9064 \cdot 10^{-3}$	$2.3249 \cdot 10^{-3}$
	V	-	-	$1.2605 \cdot 10^{-2}$	$1.2371 \cdot 10^{-2}$	$9.7841 \cdot 10^{-3}$
	I	-	-	$1.7056 \cdot 10^{-2}$	$4.6864 \cdot 10^{-2}$	$8.7476 \cdot 10^{-3}$
T. Milstein	S	$2.4437 \cdot 10^{8}$	$2.5659 \cdot 10^{-1}$	$1.4788 \cdot 10^{-2}$	$4.9344 \cdot 10^{-3}$	$2.3447 \cdot 10^{-3}$
	V	$1.6442 \cdot 10^{6}$	$8.5393 \cdot 10^{-2}$	$1.4023 \cdot 10^{-2}$	$1.3080 \cdot 10^{-2}$	$1.0093 \cdot 10^{-2}$
	I	$7.6586 \cdot 10^{7}$	$2.4083 \cdot 10^{-1}$	$1.2905 \cdot 10^{-2}$	$3.6488 \cdot 10^{-2}$	$3.8245 \cdot 10^{-3}$
Exponential	S	$4.1337 \cdot 10^{-2}$	$6.3373 \cdot 10^{-3}$	$1.0503 \cdot 10^{-3}$	$1.0777 \cdot 10^{-3}$	$1.2327 \cdot 10^{-3}$
	V	$6.6725 \cdot 10^{-3}$	$1.5180 \cdot 10^{-2}$	$1.0831 \cdot 10^{-2}$	$1.2003 \cdot 10^{-2}$	$1.0476 \cdot 10^{-2}$
	I	$9.0361 \cdot 10^{-1}$	$7.1401 \cdot 10^{-1}$	$4.7201 \cdot 10^{-1}$	$2.9110 \cdot 10^{-1}$	$1.4207 \cdot 10^{-1}$
Heun	S	-	-	$4.0355 \cdot 10^{-3}$	$5.9218 \cdot 10^{-4}$	$1.3320 \cdot 10^{-4}$
	V	-	-	$5.7697 \cdot 10^{-4}$	$6.5261 \cdot 10^{-3}$	$6.8951 \cdot 10^{-3}$
	I	-	-	$1.3498 \cdot 10^{-3}$	$3.5550 \cdot 10^{-2}$	$3.5347 \cdot 10^{-3}$

Table 3.6: *MC RELE with $\phi(x) = x^2$, for the four numerical method and different integration times. Results have been taken by 10^4 trajectories in the time interval $[0, 500]$ and reference solution simulated by Tamed Milstein scheme with step-size $h = 2^{-13}$*

Chapter 4

Conclusions

4.1 Conclusions and future work

This thesis has addressed two investigations on the numerical approximation of stochastic differential equations with non-global Lipschitz continuous coefficients.

Firstly, we have successfully solved the non-linear stochastic Schrödinger equation with finite state space by using the Talay-Tubaro extrapolation procedure. We provided theoretical support for this method by obtaining the first-order asymptotic expansion of the weak error produced when applying the Euler-Exponential scheme to the non-linear stochastic Schrödinger equation. To achieve this, we derived a new short-time asymptotic expansion with respect to the step-size and utilized a localization procedure. We demonstrated that the Euler-Exponential scheme converges with weak-order 1 and strong-order 1/2. Furthermore, we employed the Multilevel Monte Carlo method in combination with the Euler-Exponential scheme to numerically solve the non-linear stochastic Schrödinger equation. A numerical experiment involving a quantized electromagnetic field interacting with a reservoir showcased the effectiveness of the weak second-order method and the satisfactory results achieved by the Multilevel Monte Carlo method acting on the Euler-Exponential scheme.

Secondly, we focused on constructing an explicit conjugacy between the non globally Lipschitz SDE with linear multiplicative noise and a suitable auxiliary RDE. This approach allowed us to systematically devise numerical integrators for analyzing the original SDE without relying on the global Lipschitz condition assumption. We successfully constructed two new integrators: one based on an exponential method and the other on the Heun method. To assess the performance of these new numerical methods, we apply the proposed approach to a

stochastic SVIR model. Thereafter, the numerical approximations were tested and compared with existing methods in the literature through various numerical simulations. Our analysis revealed that the methods devised using this approach outperformed commonly used methods such as the Milstein and Tamed Milstein methods. Specifically, the exponential-based method proved to be suitable for integrating the SVIR model over large time intervals. In contrast, the Heun method exhibited higher accuracy when a small step-size could be utilized. It is worth noting the potential application of this framework to other epidemiological models with similar noise structures in the diffusion coefficient of the equation.

In summary, our investigations have developed effective numerical methods for solving SDEs with non-globally Lipschitz coefficients. Specifically, the numerical analysis was performed on the non-linear stochastic Schrödinger equation and the stochastic SVIR model. The proposed methods offer improved convergence and stability compared to existing approaches. Furthermore, the conducted numerical analysis holds significant potential for studying other SDEs.

The methods developed and the results obtained in this thesis have motivated several ongoing and future projects. Next, we described some of them.

In the first investigation, the numerical analysis presented in Chapter 2 establishes the mathematical foundation for implementing scalable Euler-Exponential methods. These scalable methods emerge from approximations, such as the use of Padé approximants of orders 1 and 2, for the exponential matrix involved in Scheme 1. Furthermore, we are exploring the extension of the numerical analysis from Chapter 2 to investigate SDEs evolving on compact manifolds.

Regarding the second investigation, we are currently working on various generalizations and numerical improvements for conjugate methods. Firstly, we may consider alternative mappings to (3.2) that define the conjugacy between SDEs and RDEs. Second, we are exploring potential numerical improvements for the presented conjugated LL and Heun methods. Specifically, we are considering the exploration of their averaged versions. Next, various numerical methods for RDEs and ODEs can be explored to develop potential conjugated versions and assess their practical applicability. Finally, we are investigating several generalizations for the linear noise present in (3.1).

4.2 Conclusiones y trabajo futuro

Esta tesis ha abordado dos investigaciones sobre la aproximación numérica de ecuaciones diferenciales estocásticas con coeficientes no globalmente Lipchitz continuos.

En primer lugar, hemos resuelto con éxito la ecuación estocástica no lineal de Schrödinger con espacio de estados finito mediante el procedimiento de extrapolación de Talay-Tubaro. Hemos proporcionado apoyo teórico a este método obteniendo la expansión asintótica de primer orden del error débil producido al aplicar el esquema Euler-Exponencial a la ecuación estocástica no lineal de Schrödinger. Para lograrlo, derivamos una nueva expansión asintótica de corto plazo con respecto al tamaño del paso y utilizamos un procedimiento de localización. Demostramos que el esquema Euler-Exponential converge con un orden débil de 1 y un orden fuerte de 1/2. Además, empleamos el método de Monte Carlo multinivel en combinación con el esquema Euler-Exponencial para resolver numéricamente la ecuación estocástica no lineal de Schrödinger. Un experimento numérico en el que interviene un campo electromagnético cuantizado que interactúa con un depósito mostró la eficacia del método de segundo orden débil y los resultados satisfactorios obtenidos por el método de Monte Carlo multinivel actuando sobre el esquema Euler-Exponencial.

En segundo lugar, nos centramos en construir una conjugación explícita entre la SDE no globalmente Lipschitz con ruido multiplicativo lineal y una RDE auxiliar adecuada. Este enfoque nos permitió idear sistemáticamente integradores numéricos para analizar la SDE original sin depender del supuesto de la condición de Lipschitz global. Construimos con éxito dos nuevos integradores: uno basado en un método exponencial y otro en el método de Heun. Para evaluar el rendimiento de estos nuevos métodos numéricos, aplicamos la aproximación propuesta a un modelo SVIR estocástico. Posteriormente, las aproximaciones numéricas se probaron y compararon con los métodos existentes en la literatura mediante diversas simulaciones numéricas. Nuestro análisis reveló que los métodos ideados utilizando este enfoque superaron a los métodos comúnmente utilizados, como los métodos Milstein y Tamed Milstein. En concreto, el método basado en la exponencial demostró ser adecuado para integrar el modelo SVIR a lo largo de grandes intervalos de tiempo. En cambio, el método de Heun mostró una mayor precisión cuando se pudo utilizar un tamaño de paso pequeño. Cabe destacar la posible aplicación de este marco a otros modelos epidemiológicos con estructuras de ruido similares en el coeficiente de difusión de la ecuación.

En conclusión, en esta investigación se desarrolló dos métodos numéricos eficaces para

resolver EDEs con coeficientes no globalmente Lipschitz. En concreto, el análisis numérico se ha realizado sobre la ecuación estocástica no lineal de Schrödinger y un modelo estocástico SVIR. Los métodos propuestos ofrecen una convergencia y estabilidad mejoradas en comparación con los enfoques existentes. Además, el análisis numérico realizado encierra un importante potencial para el estudio de otras EDE.

Los métodos desarrollados y los resultados obtenidos en esta tesis han motivado varios proyectos en curso y futuros. A continuación, describimos algunos de ellos.

En la primera investigación, el análisis numérico presentado en el Capítulo 2 establece las bases matemáticas para la implementación de métodos escalables Euler-Exponencial. Estos métodos escalables surgen de aproximaciones, como el uso de aproximantes de Padé de órdenes 1 y 2, para la matriz exponencial involucrada en el Esquema 1. Además, estamos explorando la extensión del análisis numérico del Capítulo 2 para investigar SDEs que evolucionan en variedades compactas.

En cuanto a la segunda investigación, actualmente estamos trabajando en varias generalizaciones y mejoras numéricas para los métodos conjugados. En primer lugar, podemos considerar transformaciones alternativas a (3.2) que definan la conjugación entre EDEs y EDAs. En segundo lugar, estamos explorando posibles mejoras numéricas para los métodos conjugados LL y Heun presentados. En concreto, estamos considerando sus versiones promediadas. Además, podemos desarrollar y evaluar la aplicación práctica de nuevos métodos conjugados, basado en métodos numéricos para EDA y EDO. Por último, estamos estudiando varias generalizaciones al ruido lineal presente en (3.1).

Bibliography

[1] A. Abdulle and S. Cirilli, *S-ROCK: Chebyshev methods for stiff stochastic differential equations*, SIAM J. Sci. Comput., 30 (2008), pp. 997–1014.

[2] J. Alcock and K. Burrage, *A note on the Balanced method*, BIT, 46 (2006), pp. 689–710.

[3] E. Allen, *Modeling with Itô Stochastic Differential Equations*, vol. 22, Springer Netherlands, 2007.

[4] L. J. S. Allen, *An Introduction to Stochastic Epidemic Models*, Springer Berlin Heidelberg, Berlin, Heidelberg, 2008, pp. 81–130.

[5] A. J. Arenas, G. González-Parra, and J.-A. Moraño, *Stochastic modeling of the transmission of respiratory syncytial virus (rsv) in the region of valencia, spain*, Biosystems, 96 (2009), pp. 206–212.

[6] L. Arnold, *Stochastic differential equations: Theory and applications*, Wiley, New York, 1974.

[7] A. Barchielli and M. Gregoratti, *Quantum trajectories and measurements in continuous time: the diffusive case*, vol. 782 of Lecture Notes in Physics, Springer, Berlin, 2009.

[8] R. Biscay, J. C. Jimenez, J. J. Riera, and P. A. Valdes, *Local linearization method for the numerical solution of stochastic differential equations*, Ann. Inst. Statist. Math., 48 (1996), pp. 631–644.

[9] M. Bossy, J. F. Jabir, and K. Martinez, *On the weak convergence rate of an exponential euler scheme for sdes governed by coefficients with superlinear growth*, Bernoulli, 27 (2021), pp. 312–347.

[10] H. P. Breuer, U. Dorner, and F. Petruccione, *Numerical integration methods for stochastic wave function equations*, Comp. Phys. Commun., 132 (2000), pp. 30–43.

[11] H. P. Breuer and F. Petruccione, *The theory of open quantum systems*, Oxford University Press, 2002.

[12] H.-P. Breuer, F. Petruccione, et al., *The theory of open quantum systems*, Oxford University Press on Demand, 2002.

[13] K. Burrage and P. Burrage, *High strong order explicit runge-kutta methods for stochastic ordinary differential equations*, Applied Numerical Mathematics, 22 (1996), pp. 81–101.

[14] K. Burrage, P. Burrage, and T. Mitsui, *Numerical solutions of stochastic differential equations – implementation and stability issues*, Journal of Computational and Applied Mathematics, 125 (2000), pp. 171–182.

[15] K. Burrage and T. Tian, *A note on the stability properties of the euler methods for solving stochastic differential equations*, New Zealand J. Math., 29 (1999).

[16] K. Burrage and T. Tian, *The composite euler method for stiff stochastic differential equations*, Journal of Computational and Applied Mathematics, 131 (2001), pp. 407–426.

[17] B. Cao, M. Shan, Q. Zhang, and W. Wang, *A stochastic sis epidemic model with vaccination*, Physica A: Statistical Mechanics and its Applications, 486 (2017), pp. 127–143.

[18] T. Caraballo, J. López-de-la Cruz, and A. Rapaport, *Modeling bounded random fluctuations in biological systems: application to the chemostat model with two species*, IFAC-PapersOnLine, 52 (2019), pp. 187–192.

[19] F. Carbonell, J. C. Jimenez, R. J. Biscay, and H. de la Cruz, *The local linearization method for numerical integration of random differential equations*, BIT Numerical Mathematics, 45 (2005), pp. 1–14.

[20] H. J. Carmichael, *Statistical Methods in Quantum Optics 2: Non-Classical Fields*, Springer, 2008.

[21] A. Cottet, Z. Leghtas, and T. Kontos, *Theory of interactions between cavity photons induced by a mesoscopic circuit*, Phys. Rev. B, 102 (2020), p. 155105.

[22] H. de la Cruz and J. C. Jimenez, *Exact pathwise simulation of multi-dimensional ornstein–uhlenbeck processes*, Applied Mathematics and Computation, 366 (2020), p. 124734.

[23] B. Donvil and P. Muratore-Ginanneschi, *Quantum trajectory framework for general time-local master equations*, Nat Commun, 13 (2022), p. 4140.

[24] P. Drummond and I. Mortimer, *Computer simulations of multiplicative stochastic differential equations*, Journal of Computational Physics, 93 (1991), pp. 144–170.

[25] F. Fagnola and C. M. Mora, *Stochastic Schrödinger equations and applications to Ehrenfest-type theorems*, ALEA, Lat. Am. J. Probab. Math. Stat., 10 (2013), pp. 191–223.

[26] M. Fan, M. Y. Li, and K. Wang, *Global stability of an seis epidemic model with recruitment and a varying total population size*, Mathematical Biosciences, 170 (2001), pp. 199–208.

[27] R. Farnoosh, P. Nabati, R. Rezaeyan, and M. Ebrahimi, *A stochastic perspective of rl electrical circuit using different noise terms*, COMPEL - The international journal for computation and mathematics in electrical and electronic engineering, 30 (2011), pp. 812–822.

[28] M. Giles, *Multilevel Monte Carlo methods*, Acta Numerica, 24 (2015), pp. 259–328.

[29] ——, *An introduction to multilevel Monte Carlo methods*, in Proceedings of the International Congress of Mathematicians, vol. IV, World Sci. Publ, 2018, pp. 3571–3590.

[30] E. Gobet, *Monte-Carlo methods and stochastic processes. From linear to non-linear.*, CRC Press, Boca Raton, FL, 2016.

[31] C. Graham and D. Talay, *Stochastic simulation and Monte Carlo methods. Mathematical foundations of stochastic simulation*, vol. 68, Springer, Heidelberg, 2013.

[32] L. Grüne and P. E. Kloeden, *Pathwise approximation of random ordinary differential equations*, Bit Numerical Mathematics, 41 (2001), pp. 711–721.

[33] Q. Guo, W. Liu, X. Mao, and R. Yue, *The partially truncated euler–maruyama method and its stability and boundedness*, Applied Numerical Mathematics, 115 (2017), pp. 235–251.

[34] ——, *The truncated milstein method for stochastic differential equations with commutative noise*, Journal of Computational and Applied Mathematics, 338 (2018), pp. 298–310.

[35] M. Hairer, M. Hutzenthaler, and A. Jentzen, *Loss of regularity for Kolmogorov equations*, Ann. Probab., 43 (2015), pp. 468–527.

[36] S. Haroche and J. M. Raimond, *Exploring the Quantum: Atoms, Cavities, and Photons*, Oxford University Press, 2006.

[37] D. J. Higham, *Mean-square and asymptotic stability of the stochastic theta method*, SIAM J. Numer. Anal., 38 (2000), pp. 753–769.

[38] D. J. Higham, X. Mao, and C. Yuan, *Almost sure and moment exponential stability in the numerical simulation of stochastic differential equations*, SIAM Journal on Numerical Analysis, 45 (2007), pp. 592–609.

[39] M. Hutzenthaler and A. Jentzen, *On a perturbation theory and on strong convergence rates for stochastic ordinary and partial differential equations with nonglobally monotone coefficients*, Ann. Probab., 48 (2020), pp. 53–93.

[40] M. Hutzenthaler, A. Jentzen, and P. E. Kloeden, *Strong and weak divergence in finite time of Euler's method for stochastic differential equations with non-globally Lipschitz continuous coefficients*, Proc. R. Soc. Lond. Ser. A, 467 (2011), pp. 1563–1576.

[41] M. Hutzenthaler, A. Jentzen, and P. E. Kloeden, *Strong convergence of an explicit numerical method for SDEs with nonglobally Lipschitz continuous coefficients*, The Annals of Applied Probability, 22 (2012), pp. 1611 – 1641.

[42] D. Jiang, J. Yu, C. Ji, and N. Shi, *Asymptotic behavior of global positive solution to a stochastic sir model*, Mathematical and Computer Modelling, 54 (2011), pp. 221–232.

[43] L. Jianquan and M. Zhien, *Global analysis of sis epidemic models with variable total population size*, Mathematical and Computer Modelling, 39 (2004), pp. 1231–1242.

[44] J. Jimenez, C. Mora, and M. Selva, *A weak local linearization scheme for stochastic differential equations with multiplicative noise*, Journal of Computational and Applied Mathematics, 313 (2017), pp. 202–217.

[45] J. C. Jimenez, R. Biscay, C. Mora, and L. M. Rodriguez, *Dynamic properties of the local linearization method for initial-value problems*, Appl. Math. Comput., 126 (2002), pp. 63–81.

[46] J. C. Jimenez, I. Shoji, and T. Ozaki, *Simulation of stochastic differential equations through the local linearization method. a comparative study*, Journal of Statistical Physics, 94 (1999), pp. 587–602.

[47] J. Johansson, P. Nation, and F. Nori, *Qutip 2: A python framework for the dynamics of open quantum systems*, Computer Physics Communications, 184 (2013), pp. 1234–1240.

[48] L. Kaup and B. Kaup, *Holomorphic functions of several variables*, Walter de Gruyter, Berlin - New York, 1983.

[49] C. Kelly and G. J. Lord, *Adaptive euler methods for stochastic systems with non-globally lipschitz coefficients*, Numerical Algorithms, 89 (2022), pp. 721–747.

[50] W. O. Kermack and A. G. McKendrick, *A contribution to the mathematical theory of epidemics*, Proceedings of the Royal Society of London. Series A, Containing Papers of a Mathematical and Physical Character, 115 (1927), pp. 700–721.

[51] A. Khan, G. Hussain, M. Zahri, G. Zaman, and U. W. Humphries, *A stochastic sacr epidemic model for hbv transmission*, Journal of Biological Dynamics, 14 (2020), pp. 788–801.

[52] R. Khasminskii, *Stochastic Stability of Differential Equations*, vol. 66, Springer Berlin Heidelberg, 2012.

[53] P. Kloeden and E. Platen, *Numerical Solution of Stochastic Differential Equations*, Stochastic Modelling and Applied Probability, Springer Berlin Heidelberg, 2011.

[54] P. E. Kloeden and A. Jentzen, *Pathwise convergent higher order numerical schemes for random ordinary differential equations*, Proceedings of the Royal Society A: Mathematical, Physical and Engineering Sciences, 463 (2007), pp. 2929–2944.

[55] P. E. Kloeden and E. Platen, *Higher-order implicit strong numerical schemes for stochastic differential equations*, Journal of Statistical Physics, 66 (1992), pp. 283–314.

[56] P. E. Kloeden and E. Platen, *Numerical solution of stochastic differential equations*, Springer, Berlin, 1992.

[57] N. Krylov, *Introduction to the theory of diffusion processes.*, American Mathematical Society, 1996.

[58] J. Li and X. Li, *Exponential integrators for stochastic Schrödinger equation*, Phys. Rev. E, 101 (2020), p. 013312.

[59] X. Liu, Y. Takeuchi, and S. Iwami, *Svir epidemic models with vaccination strategies*, Journal of Theoretical Biology, 253 (2008), pp. 1–11.

[60] Y. LIU and J.-A. CUI, *The impact of media coverage on the dynamics of infectious disease*, International Journal of Biomathematics, 01 (2008), pp. 65–74.

[61] Q. Lu, *Stability of sirs system with random perturbations*, Physica A: Statistical Mechanics and its Applications, 388 (2009), pp. 3677–3686.

[62] Q. Lv and J. W. Pitchford, *Stochastic von bertalanffy models, with applications to fish recruitment*, Journal of Theoretical Biology, 244 (2007), pp. 640–655.

[63] X. Mao, *The truncated euler-maruyama method for stochastic differential equations*, J. Comput. Appl. Math., 290 (2015), pp. 370–384.

[64] H. A. Mardones and C. M. Mora, *First-order weak balanced schemes for stochastic differential equations*, Methodology and Computing in Applied Probability, 22 (2020), pp. 833–852.

[65] G. Maruyama, *Continuous markov processes and stochastic equations*, Rendiconti del Circolo Matematico di Palermo, 4 (1955), pp. 48–90.

[66] J. Mattingly, A. Stuart, and D. Higham, *Ergodicity for sdes and approximations: locally lipschitz vector fields and degenerate noise*, Stochastic Processes and their Applications, 101 (2002), pp. 185–232.

[67] G. Milstein and M. Tretyakov, *Computing ergodic limits for langevin equations*, Physica D: Nonlinear Phenomena, 229 (2007), pp. 81–95.

[68] G. N. Milstein, *Approximate integration of stochastic differential equations*, Theory of Probability & Its Applications, 19 (1975), pp. 557–562.

[69] G. N. Milstein, E. Platen, and H. Schurz, *Balanced implicit methods for stiff stochastic systems*, SIAM J. Numer. Anal., 35 (1998), pp. 1010–1019.

[70] G. N. Milstein and M. V. Tretyakov, *Stochastic numerics for mathematical physics*, Springer-Verlag, Berlin, 2004.

[71] C. Mode and C. Sleeman, *Stochastic Processes in Epidemiology: HIV/AIDS, Other Infectious Diseases, and Computers*, World Scientific, 2000.

[72] C. B. Moler and C. F. Van Loan, *Nineteen dubious ways to compute the exponential of a matrix, twenty-five years later*, SIAM Rev., 45 (2003), pp. 3–49.

[73] C. Mora, *Numerical solution of conservative finite-dimensional stochastic Schrödinger equations*, Ann. Appl. Probab., 15 (2005), pp. 2144–2171.

[74] ——, *Weak exponential schemes for stochastic differential equations with additive noise*, IMA J. Numer. Anal., 25 (2005), pp. 486–506.

[75] C. M. Mora, *Numerical simulation of stochastic evolution equations associated to quantum Markov semigroups*, Math. Comp., 73 (2004), pp. 1393–1415.

[76] ——, *Regularity of solutions to quantum master equations: a stochastic approach*, Ann. Probab., 41 (2013), pp. 1978–2012.

[77] C. M. Mora, J. Fernández, and R. Biscay, *Numerical solution of stochastic master equations by exponential schemes*, J. Comput. Phys., (2018), pp. 28–48.

[78] C. M. Mora, H. A. Mardones, J. C. Jimenez, M. Selva, and R. Biscay, *A stable numerical scheme for stochastic differential equations with multiplicative noise*, SIAM J. Numer. Anal., 55 (2017), pp. 1614–1649.

[79] C. M. Mora and M. Muñoz, *On the rate of convergence of an exponential scheme for the non-linear stochastic schrödinger equation with finite-dimensional state space*, Physica Scripta, 98 (2023), p. 065226.

[80] C. M. Mora and R. Rebolledo, *Basic properties of non-linear stochastic Schrödinger equations driven by Brownian motions*, Ann. Appl. Probab., 18 (2008), pp. 591–619.

[81] M. Muñoz, H. de la Cruz, and C. Mora, *Pathwise methods for the integration of a stochastic svir model*, Mathematical Methods in the Applied Sciences, (2023), pp. 1–15.

[82] I. C. Percival, *Quantum state diffusion*, Cambridge University Press, 1998.

[83] P. E. Protter, *Stochastic integration and differential equations*, Springer, Berlin, 2005.

[84] R. Remmert, *Theory of Complex Functions*, Springer, New York, 1991.

[85] D. Revuz and M. Yor, *Continuous Martingales and Brownian Motion*, Springer, 1999.

[86] Y. SAITO and T. MITSUI, *T-stability of Numerial Scheme for Stochastic Differential Equations*, vol. 2 of World Scientific Series in Applicable Analysis, Worls Scientific, 1993, pp. 333–344.

[87] R. Schack, T. A. Brun, and I. C. Percival, *Quantum state diffusion, localization and computation*, J. Phys. A: Math. Gen., 28 (1995), pp. 5401–5413.

[88] M. Shinozuka and G. Deodatis, *Stochastic process models for earthquake ground motion*, Probabilistic Engineering Mechanics, 3 (1988), pp. 114–123.

[89] A. Soheili, *Stochastic runge-kutta method with weak and strong convergency*, International Journal of Contemporary Mathematical Sciences, 3 (2008).

[90] D. Talay, *Probabilistic numerical methods for partial differential equations: elements of analysis*, in Probabilistic models for nonlinear partial differential equations (Montecatini Terme, 1995), D. Talay and L. Tubaro, eds., vol. 1627 of Lecture Notes in Mathematics, Berlin, 1996, Springer-Verlag, pp. 148–196.

[91] ——, *Stochastic Hamiltonian systems: exponential convergence to the invariant measure, and discretization by the implicit Euler scheme*, Markov Process. Related Fields, 8 (2002), pp. 163–198.

[92] D. Talay and L. Tubaro, *Expansion of global error for numerical schemes solving stochastic differential equations*, Stoch. Anal. Appl., 8 (1990), pp. 483–509.

[93] E. Tornatore, S. Maria Buccellato, and P. Vetro, *Stability of a stochastic sir system*, Physica A: Statistical Mechanics and its Applications, 354 (2005), pp. 111–126.

[94] J. M. Torres and T. H. Seligman, *Protecting coherence by environmental decoherence: a solvable paradigmatic model*, New J. Phys., 19 (2017), p. 113016.

[95] M. V. Tretyakov and Z. Zhang, *A fundamental mean-square convergence theorem for SDEs with locally Lipschitz coefficients and its applications*, SIAM J. Numer. Anal., 51 (2013), pp. 3135–3162.

[96] X. Wang and S. Gan, *The tamed milstein method for commutative stochastic differential equations with non-globally lipschitz continuous coefficients*, Journal of Difference Equations and Applications, 19 (2013), pp. 466–490.

[97] H. M. Wiseman and G. J. Milburn, *Quantum measurement and control*, Cambridge University Press,, 2009.

[98] G. Zaman, Y. H. Kang, and I. H. Jung, *Stability analysis and optimal vaccination of an sir epidemic model*, Biosystems, 93 (2008), pp. 240–249.

[99] X. Zhang, D. Jiang, T. Hayat, and B. Ahmad, *Dynamical behavior of a stochastic svir epidemic model with vaccination*, Physica A: Statistical Mechanics and its Applications, 483 (2017), pp. 94–108.

[100] X. Zhang, Z. Shi, and H. Peng, *Transmission dynamics of stochastic svir influenza models with media coverage*, Journal of Applied Analysis & Computation, 11 (2021), pp. 2792–2814.

[101] Z. Zhang, A. Zeb, S. Hussain, and E. Alzahrani, *Dynamics of covid-19 mathematical model with stochastic perturbation*, Advances in Difference Equations, 2020 (2020), p. 451.

[102] M. Zhao and H. Zhao, *Asymptotic behavior of global positive solution to a stochastic sir model incorporating media coverage*, Advances in Difference Equations, 2016 (2016), p. 149.

[103] Y. Zhou, W. Zhang, and S. Yuan, *Survival and stationary distribution of a sir epidemic model with stochastic perturbations*, Applied Mathematics and Computation, 244 (2014), pp. 118–131.

[104] B. Øksendal, *Stochastic Differential Equations*, Springer Berlin Heidelberg, 2003.